

FINAL REPORT ON

CHARACTERISTICS OF THE MID-WATER AND NEAR-BOTTOM
CURRENTS IN THE VICINITY OF THE ENCINA OUTFALL
AND THE HEAD OF CARLSBAD CANYON

SUBMITTED TO

ENCINA WATER POLLUTION CONTROL FACILITY

BY

DR. TAREAH J. HENDRICKS

SOUTHERN CALIFORNIA COASTAL WATER RESEARCH PROJECT
646 WEST PACIFIC COAST HIGHWAY
LONG BEACH, CALIFORNIA 90806

February, 1987

TABLE OF CONTENTS

	<u>Page</u>
Executive Summary.....	1
Background.....	4
 I. Ocean Currents	
A. Summary.....	9
B. Moorings.....	10
C. Deployment Periods.....	11
D. Current Speeds	
1. Mid-Water Currents.....	11
2. Near-Bottom Currents.....	13
E. Direction of Flow.....	13
F. Variability.....	14
G. Temporal Characteristics.....	15
H. Correlations Between Moorings.....	17
 II. Sedimentation and Accumulation of Effluent Particles	
A. Summary.....	19
B. Background.....	20
C. Outfall-Related Sedimentation and Accumulation	
1. EPA-Suggested Technique.....	21
2. SEDF2D Simulations.....	24
3. Actual Accumulations of Organic Material...	25
a. Sediment Resuspension.....	26
 III. Initial Dilution	
A. Summary.....	29
B. Background.....	29
C. 10-Percentile "Worst Case" Initial Dilutions....	30
1. 10-Percentile "Lowest" Current Speeds.....	31
2. 10-Percentile "Strongest" Density	
Gradients.....	31
3. Initial Dilution Simulation Models.....	32
4. Computed 10-Percentile Initial Dilutions...	33
D. Actual Initial Dilutions for "Typical"	
Conditions.....	34
 IV. Cross-shore Transport	
A. Summary.....	35
B. Background	
1. Cross-shore Transport.....	37
2. Vertical Exchange.....	37
C. The Transport Model "PXYT2D".....	39

EXECUTIVE SUMMARY

Four basic tasks were addressed during this study: (1) measurements of the properties of the currents in the discharge area, (2) simulation of the critical initial dilutions achieved by the outfall, (3) calculation of the sedimentation rates of effluent particulates and the associated accumulation of organic material and, (4) estimation of cross-shore transport of wastewater constituents.

Currents were measured at two depths ("mid-water" and "near-bottom") during both winter (January-March) and summer (July-September) oceanographic seasons at a mooring near the outfall diffuser and near the head of Carlsbad Canyon. During portions of these measurement periods, an additional mooring (also with two meters) was positioned either inshore from the outfall mooring, or upcoast from Carlsbad Canyon. The mid-water currents were measured below the thermocline (some density stratification was observed throughout the study period) at depths of 15m (summer) to 20m (winter). The near-bottom meters were located 2 meters above the bottom.

The predominant motion of the mid-water currents is along the contours of constant water depth. Typical speeds are on the order of 9-10 cm/sec, but they are highly variable. Most of the variations occur over time periods of days to weeks, but tidal fluctuations are also evident. The longshore components of the slowly varying fluctuations are highly correlated over distances of at least 5 kilometers. Cross-shore motions are generally uncorrelated over distances of less than 1 kilometer. The net motion was

weak during the winter season, and upcoast during the summer season.

Near-bottom (2m elevation) currents are about two-thirds as strong as the mid-water currents and are dominated by tidal and shorter period fluctuations. The net movement is upcoast and offshore.

Initial dilutions achieved by the outfall were measured during a cooperative EPA-SCCWRP study on June 13, 1986 and ranged (near the outfall) from a low of 390:1 to a high of 1470:1, with a "typical" value of about 650:1. The effluent discharge rate during the study varied from about 12 to 29 MGD, and ocean current speeds ranged from about 6 to 14 cm/sec--both representative of "typical" values.

The computed "worst-case" initial dilutions are based on the 10-percentile slowest current speeds and 10-percentile "strongest" density stratifications of the water column. From the current observations, it was determined that the 10-percentile current speed would correspond to a (mid-water) current speed of 4-4.5 cm/sec. "Worst case" density profiles were selected from 38 observations collected as part of the normal Encina monitoring program and during the SCCWRP special studies. Simulations were carried out using the EPA initial dilution models "PLUME" and "MERGE", for the flows permitted under the NPDES permit. For "winter" conditions, the "minimum" (10-percentile) initial dilution was estimated to be 206:1; for "summer" conditions, 224:1.

The current meter record collected from the vicinity of the outfall diffuser was used to estimate, on a statistical basis, the distribution of the wastefield in the outfall area for various elapsed times following discharge. Figure ES1 shows the estimated probability distribution

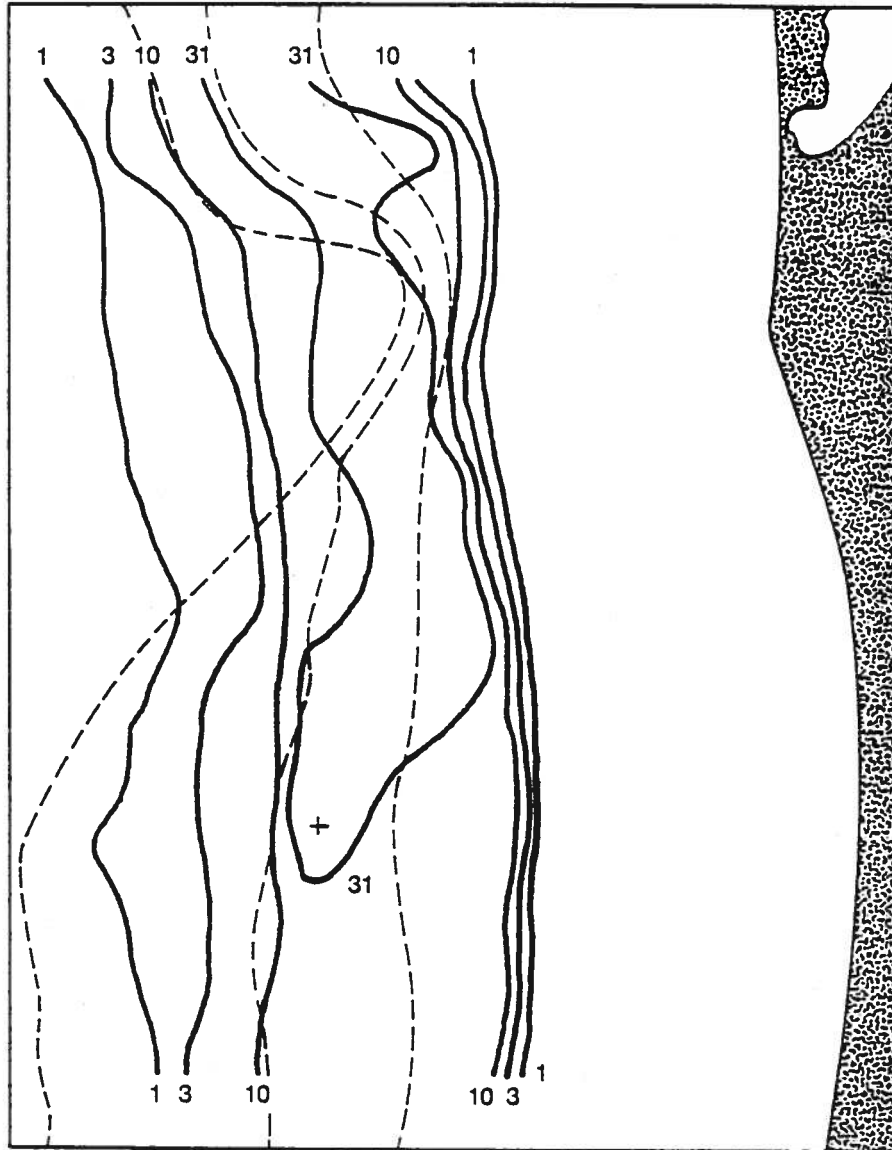


**Fig ES1 . Probabilities from PXYT2D after 48 hours
for 25m wastefield for August 15 to
September 18, 1986**

describing the presence of wastewater. In this figure, "presence" refers to the probability of detecting any wastewater that has been discharged within the previous 48 hours, as averaged over an approximately one month long period. This estimation procedure assumes that the waste-field forms at a depth of 25 meters, and the isopycnal surfaces are horizontal (constant depth).

The rate of sedimentation and accumulation of effluent-related particulates on the ocean bottom was estimated using both the SCCWRP-EPA sedimentation model "SEDF2D", and the estimation procedure outlined in the EPA 301(h) Technical Support Document. The SEDF2D simulations (which have the greatest spatial resolution) indicate that for the "worst-case" conditions observed during the current measurements, the maximum sedimentation rate would be about 28-29 mg/cm²/yr (over a 0.03 square kilometer area), and sedimentation rates equal to, or in excess of, natural sedimentation rates (10 mg/cm²/yr) would occur over an area of about 0.19 square kilometers.

Following the initial sedimentation of this material, it may be transformed by "decay" or by the resuspension and redistribution of the deposited material. Estimates of the "steady-state" accumulation of organic material (using the method in the EPA 301(h) Tech. Support Doc.), and measurements of the resuspension rate of particulates by SCCWRP (using sediment traps) indicate that the accumulation of organic material around the outfall will be essentially undetectable. This conclusion is supported by measurements of the change in volatile solids in the sediments over a period of time (no change), and comparison with adjacent natural sediments (undetectable difference).

BACKGROUND

Effluent from the Encina treatment plant is discharged through a series of "ports" near the terminus of the outfall. The "shear" associated with these "jets" of effluent emerging into the receiving water causes entrainment of ocean water into the effluent stream--diluting the concentration of effluent and reducing the velocity of the stream. At the same time, the low density of the effluent (warm, nearly fresh, water), relative to sea water, causes the effluent jet to rise in the water column and form a "plume". The buoyancy-induced velocity of the rising flow within this plume of effluent produces additional shear and mixing with the surrounding sea water. If ocean currents are present, they can augment this mixing and dilution as a result of the additional shear and the density-driven mixing associated with current-induced "bending over" of the plume.

In general, the density of ocean waters will increase with depth. In the upper 50 meters of the water column (i.e. the portion of the water column receiving the discharge from the Encina plant), nearly all of this stratification is associated with temperature changes. As the effluent plume emerges from the diffuser and mixes with the surrounding ocean water, cold, dense sea water is entrained into the plume. If sufficient density stratification of the water column exists, the density of the combination of effluent and cold sea water in the plume will be equal to the density of the surrounding sea water at some higher (shallower) position in the water column.

When the plume reaches this elevation, further vertical motion is inhibited by the adverse density gradient,

and a wastefield is formed (some "overshoot" of the plume, followed by a descent back to the equilibrium depth, may occur, however because of the momentum of the rising plume). The thickness and width of the wastefield will be determined by a variety of factors, including the shape of the density profile describing the ambient (receiving) water, the strength and direction of the ocean currents, and the shape, extent, and orientation of the outfall diffuser. Generally the thickness will be roughly between 30-percent (unstratified water, or a strong thermocline) and 100-percent (constant density gradient) of the height of rise.

Immediately following the formation of the wastefield, the thickness and width may change in time as the result of density-driven "readjustments" that minimize the total energy associated with the formation of the wastefield. After this initial "adjustment" period, the transport and dispersion of the wastefield is primarily determined by the properties of the ocean currents. In the southern California coastal area, ocean currents can be roughly classified into three categories according to depth or density stratification of the water column. "Surface" currents refer to the layer of water lying above the thermocline. In general, this layer is relatively well mixed through the action of wind and waves. Typical mixed layer depths may range from a few meters to roughly 15 meters. "Near-bottom" currents are confined to a layer near the bottom of the ocean where the frictional interaction of the flow with the bottom modifies the properties of the currents from the properties of the overlying water. The thickness of this layer is related to the density stratification of the water column, however, for operational purposes, a typical

thickness can be considered to be on the order of 2-5 meters. The "mid-water" currents occupy the region between the near-bottom currents and the thermocline. Since a sub-surface wastefield is formed throughout most (and perhaps sometimes, all) of the year, the mid-water and near-bottom currents determine the transport and dispersion of dissolved and settleable components of the effluent.

Energy is required to generate flows across, or promote mixing between, layers of different density. Therefore mixing and flow tends to occur within "layers" of constant density (i.e. along "isopycnal surfaces"). These layers are roughly horizontal, but a variety of factors can modify this configuration. In the southern California coastal area, the net (long-term) surface flow is downcoast, while the net mid-water flow is upcoast. This flow reversal is accompanied by an (average) "shoaling" of the isopycnal surfaces with proximity to the coast. On shorter time scales, upwelling and downwelling represent "adjustments" of the density structure of the water column in response to a variety of factors, such as surface winds or atmospheric pressure differences, or flow over changing topography. Often these adjustments only occur over a restricted portion of the water column because of the changing energy requirements associated with increasing density stratification of the water column.

"Internal tides" (changes in the depth of a isopycnal surface analogous to sea surface elevation changes associated with surface tides) and "internal waves" can produce shorter-term changes in the position of isopycnal surfaces within the water column.

The movement of a wastefield away from the outfall is governed by the ambient ocean currents along the isopycnal

surface corresponding to the depth of the wastefield, and the slow vertical motions associated with readjustments of the local isopycnal surfaces (i.e. internal tides, upwelling/downwelling, etc.). The movement along the isopycnal surfaces can be sub-divided into two types: (1) an overall (bulk) motion associated with the large-scale properties of the currents and, (2) a random, dispersive-type, motion associated with smaller-scale fluctuations in the currents (associated with the turbulent nature of the flow).

The longshore movement of the wastefield is generally dominated by the first type of transport and can often be predicted with reasonable accuracy since the characteristics of the motion tend to be nearly the same over a fairly large area. Cross-shore motions are, however, generally characterized by shorter-time scales and substantial changes over relatively short distances. Thus the transport characteristics in this direction often appear to be more of a dispersive nature. This lack of predictability, combined with the dependence on the slope of isopycnal surfaces (see below), introduces great difficulties into estimating cross-shore transport. Under these conditions, direct measurements of wastewater constituents (e.g. through appropriate "monitoring") may provide the most accurate estimations of transport.

A further complicating factor is the presence of the coastal boundary. Increased "shoaling" of the isopycnal surfaces will permit water of a particular density to be advected closer to the shore; conversely, downwelling will restrict the same water to regions further from the coast. In general, it is difficult to relate these density distribution changes (and associated changes in the "boundary"

for cross-shore flow) to the flow field on a synoptic basis. In general, however, changes in the slope of the isopycnal surfaces can be expected to be enhanced by strong winds, but suppressed by strong density stratification of the water column.

These characteristics of the ocean flow field and of the ocean disposal process tend to introduce a considerable degree of uncertainty into the prediction or estimation of the occurrence(s) of "rare" (low probability) events, such as the onshore transport of wastewater materials into shallow water. In many cases, however, events with a "high" probability of occurrence (e.g. sedimentation of particulates in the main portion of the "sediment field") can be treated with a greater level of confidence using appropriate statistical techniques.

Four basic tasks were addressed during this study: (1) measurements of the properties of the currents in the discharge area, (2) simulation of the critical initial dilutions achieved by the outfall, (3) calculation of the sedimentation rates of effluent particulates and the associated accumulation of organic material and, (4) estimation of cross-shore transport of wastewater constituents.

I. OCEAN CURRENTS

I.A. Summary

Three moorings containing current meters have been used to collect seasonal information on the properties of the mid-water and near-bottom currents in the vicinity of the Encina outfall.

Most of the time, the Encina discharge creates a subsurface wastefield that is trapped below the thermocline. Our measurements indicate that currents at this depth have typical speeds of 9-10 cm/sec, but are highly variable. The dominant mid-water motion is along contours of constant water depth. Most of the variability in these motions is associated with changes that occur over time periods of days to weeks. A weak onshore flow (0.5-0.6 cm/sec) was observed at the outfall site, but such low speeds are statistically indistinguishable from a speed of zero with the accuracy of the present meters (~1 cm/sec).

Near-bottom currents are about two-thirds the strength (6-7 cm/sec) of the mid-water flows, and are dominated by tidal and shorter period fluctuations. The net movement of near-bottom water is upcoast and offshore (velocities on the order of 1-4 cm/sec).

The dominant long-period mid-water motions are highly correlated over distances of at least 5 kilometers. Tidal and short-period fluctuations in both the longshore and cross-shore direction are uncorrelated, or only weakly correlated, over distances of 1-3 kilometers. These features indicate that it is relatively simple to estimate

the longshore advection of wastewater constituents, but cross-shore exchange may be regulated by dispersive rather than advective processes.

I.B. Moorings

Two moorings were placed in the vicinity of the Encina outfall for two seasonal measurement periods. One mooring was positioned 250 meters downcoast from the outfall diffuser in 46 meters of water (Figure 1). The second mooring was positioned approximately 2500 meters (2.5 km) upcoast, on the 46 meter isobath, adjacent to the head of Carlsbad Canyon.

Two meters were used on each mooring. The upper ("mid-water") meter was at a depth of 20m during the "winter" measurement period, and at a depth of 16 meters during the "summer" deployment. The "winter" measurement period began on January 9 and extended to April 4, 1986. The "summer" period ran from July 13 to September 18, 1986. The lower ("near-bottom") meter was positioned 2 meters above the bottom. The function of the mid-water meters was to provide information on the transport of dissolved and suspended solids components of the wastefield; the function of the lower meter was to provide information on the transport of resuspended sediments.

A third mooring was deployed in the area by the Southern California Coastal Water Research Project during the two measurement periods as part of an ongoing program of studies. This mooring was positioned inshore from the "outfall mooring" station (in 25m of water) during the winter and half of the summer period; during the remainder

of the summer study, it was located approximately 5 kilometers upcoast from the outfall in the same depth of water as the outfall and canyon stations (see Figure 1). The mooring included a mid-water meter (12.5m-inshore station, 16m-upcoast station) and a near-bottom meter (see Table 1).

Tiltmeter-type current meters, of SCCWRP design, were used at all the moorings. The construction details and performance characteristics of these meters are described in Hendricks (1985) and Boylls and Hendricks (1985).

I.C. Deployment Periods

Table 1 summarizes the deployment periods, mooring locations, meter depths, and days of data recovery for the two measurement periods. At least 43 days of mid-water current measurements and 33 days of near-bottom measurements were obtained at both the "outfall" and the "canyon" moorings.

I.D. Current Speeds

I.D.1. Mid-Water Currents

Figure 2 shows the cumulative distribution of current speeds observed at each depth and mooring during the winter measurement period. The mid-water current speeds were nearly identical at each of the three moorings, with median (50-percentile) speeds of 8-9 cm/second. At the outfall mooring, 10 percent of the speeds were less than 4 cm/sec, or greater than 16 cm/second.

Figure 3 contains the cumulative speed distribution for the summer measurement period. In contrast to the winter period, some differences appeared in the mid-water speed distributions among the three moorings. In general the range of speeds at the outfall mooring was more restricted than at the canyon station. The speeds observed at the inshore mooring were weaker than at either offshore mooring. The median mid-water speed at the outfall was 9.5 cm/sec, with 10-percentile speeds of 4.5 and 16 cm/sec. These are virtually identical to those observed during the winter period.

Physical model studies (Roberts, 1977) indicate that there is a threshold speed that must be attained before current-induced increases in the initial dilution become significant. For the Encina outfall, this threshold speed is on the order of 4 cm/sec for flow across the outfall, and substantially higher for flow parallel to the diffuser. Thus the "critical" initial dilutions (based on the 10-percentile lowest current speeds) for the Encina discharge will be essentially independent of the currents--although "typical" initial dilutions generated by the discharge can be expected to be enhanced by the ambient flows.

When either upcoast or downcoast flows occur, the average long-shore component of the velocity is 8-9 cm/sec. For the cross-shore flows, the average speeds are on the order of 3-4 cm/sec. However, as will be shown later, the temporal properties of the cross-shore flow are substantially different from those of the longshore motions.

I.D.2. Near-Bottom Currents

Figures 2 and 3 also show the distribution of current speeds for the near-bottom flows for the winter and summer periods respectively. During the winter, the near-bottom speeds near the head of the canyon were noticeably weaker than in the vicinity of the outfall. There was very little difference between the distributions of near-bottom speeds near the outfall in 46 meters of water, and inshore from the outfall in 25 meters of water. Median speeds in the vicinity of the outfall were about 6.5 cm/sec, with 10-percentile speeds of about 3 and 13.5 cm/sec.

During the summer, the near-bottom speeds observed near the outfall mooring were substantially less than observed at the canyon, inshore from the outfall, or upcoast from the canyon. The median speed was 3.5 cm/sec, or almost half the median speed during the winter period. Ten-percentile speeds were approximately 1.5-2 cm/sec and 6 cm/sec.

These are about one-half the winter values. It should be noted, however, that some of these differences might reflect that not all the records were collected simultaneously.

I.E. Direction of Flow

The probability of flow in ten degree sectors for each mooring and meter depth are listed in Appendix A. In general, the mid-water flows tend to have bi-modal distributions aligned with the local contours of constant water depth (isobaths). The near-bottom currents have a much

less pronounced tendency toward a bimodal distribution, and the major principal axis of the fluctuations is frequently not parallel to the local isobaths.

As was noted earlier, the temporal properties of the currents are substantially different between the longshore and cross-shore components. Since transport represents the combined effects of the direction of flow, its strength, and its duration, longshore and cross-shore transport cannot be simply estimated from the speed and direction probability matrices.

I.F. Variability

Table 2 summarizes the mean flows, and the variability about the mean, for each season, depth, and mooring. The seasonal values represent the average over all the deployments during that season. It is immediately evident that the variations in the flow (root-mean-square speeds) are greater than the mean flows for both the mid-water and near-bottom measurements.

Mid-water mean currents during the winter season were generally weak (< 1 cm/sec), although an onshore flow of 1.5 cm/sec was measured inshore from the outfall, and an offshore flow of 1.2 cm/sec was observed at the canyon mooring. Speeds on the order of 1 cm/sec, or less, are comparable with the accuracy of the meters and hence are statistically indistinguishable from zero.

Near the bottom (2m elev.), there was a net upcoast flow (0.9 \rightarrow 3.2 cm/sec), combined with an offshore movement (0.9 \rightarrow 2.4 cm/sec). Similar weak upcoast and offshore movements in the near-bottom currents are often observed in other southern California coastal waters, and

suggest that the net transport of resuspended sediments will have an offshore component.

RMS speeds are relatively independent of sampling period and season. Typical mid-water longshore rms speeds are on the order of 10-11 cm/sec; cross-shore rms speeds are on the order of 3-4 cm/sec. The principal axis of variation is approximately parallel to the local contours of constant water depth. For the near-bottom currents, the rms-speeds are generally less, and the principal axis of variation generally is rotated 10 -> 50 degrees relative to the local isobaths.

I.G. Temporal Characteristics

Figure 4a illustrates the temporal variability in the longshore component of the currents at Stations 1 (inshore), 2 (outfall) and 3 (canyon) for the period from July 13 to August 15, 1986. Figure 4b contains the corresponding plots for the cross-shore components. Plots for the other major periods of record are contained in Appendix B.

Examination of Figure 4 suggests that variations in the flow can be roughly broken down into three types: (1) fluctuations characterized by variations similar to tidal variations, (2) changes occurring more rapidly than tidal fluctuations and, (3) flows persisting longer than tidal flows. For operational purposes, we define "long-period" fluctuations as those characterized by "durations" longer than 24.75 hours; "tidal-period" flows by "durations" in the range of 3 -> 24.75 hours; and "short-period"

variations as those associated with "durations" of less than 3 hours.

Figure 5 shows the mid-water currents for this same time period after removing the tidal (and shorter) period fluctuations from both the longshore and cross-shore components. Several features are evident in the remaining "long-period" flows. First of all, the longshore components are substantially more "energetic" than the corresponding cross-shore components. Secondly, there is a high degree of correlation between the changes that occur in the longshore flows at one mooring and those that are observed at the other two moorings.

Figure 6a and 6b show the "variance" of the fluctuations (square of the rms speeds about the net motion) for the longshore and cross-shore components of the flow respectively. To illustrate the temporal properties of each component, each figure shows the cumulative variance as a function of increasing "duration" of the fluctuations. The "durations" are estimated by representing the time series of velocity measurements as a Fourier series (of sine and cosine functions). The "duration" of each component in the Fourier series is defined as its "periodicity" (inverse of the angular frequency).

The cumulative variance is obtained by first calculating the variance associated with the most rapidly fluctuating term in the series. Additional terms, in the order of increasing periodicity, are sequentially included in the sum of the variances to obtain the "cumulative variance" plotted in Figure 6a,b.

Examination of Figures 6a,b substantiates our earlier observation that slowly varying components of the longshore and cross-shore motions differ substantially from each

other. In general, tidal and higher frequency fluctuations account for about 10 (cm/sec)^2 of the variance, while the slowly varying components contribute an additional 50-80 (cm/sec)^2 (Figure 6a). In the cross-shore direction, virtually all of the variance ($\sim 10 \text{ (cm/sec)}^2$) is contributed by tidal or shorter period fluctuations (Figure 6b). Thus the principal difference between the longshore and cross-shore flows is the presence, or absence, of these long-period fluctuations (although some differences in the tidal contributions are also evident).

Corresponding plots for the near-bottom currents are shown in Figures 7a,b. A comparison of the longshore components of the flow near the bottom (Fig. 7a) with those at mid-water depth (Fig. 6a) shows that the long-period fluctuations are substantially diminished near the bottom. This is in agreement with the frictional effects predicted by simple boundary layer theory. Two other differences are evident: (1) the variance associated with tidal and shorter period fluctuations is generally substantially greater than at mid-water depths and, (2) the energy of the cross-shore components of the near-bottom flow can be comparable with, or exceed, the energy of the longshore component.

Plots of the cumulative variance, as a function of "periodicity" for other periods of record are contained in Appendix C.

I.H. Correlations Between Moorings

As might be expected, the correlation between the currents observed at pairs of moorings depends on both the

component (longshore vs. cross-shore) and the temporal characteristics.

Table 3 summarizes the values of the square of the correlation coefficient (i.e. the fraction of the variance in common between the two moorings) for various pairs of meters as a function of "frequency band", longshore or cross-shore component, and deployment period. The long-period, longshore components are highly correlated, with an average r^2 of 0.88. This correlation holds even over a separation of 5 kilometers (Stations 2,5; $r^2 = 0.88$).

The short-period fluctuations are virtually uncorrelated along both the longshore and cross-shore directions ($r^2 < 0.03$). Cross-shore fluctuations are relatively uncorrelated in both the tidal and long-period bands ($r^2 = .09 \rightarrow 0.16$), and the long-shore component of the flow in the tidal band is only weakly correlated ($r^2 = 0.28$).

This combination of "duration" and direction dependent correlations and the variances associated with the various "frequencies" suggests that only longshore transport can be computed as a simple advective flow. This component can, however, be estimated with good accuracy over spatial scales of at least 5 kilometers. Cross-shore transport appears to occur more as a dispersive process than as an advective one--therefore, statistical techniques may be more appropriate for the transport of effluent constituents in this direction.

II. SEDIMENTATION AND ACCUMULATION OF EFFLUENT PARTICLES

II.A. Summary

The maximum outfall-related sedimentation estimated by the technique suggested in the EPA 301h Technical Support document is estimated to be about $36 \text{ gm/m}^2/\text{yr}$ of organic material over an area of 1.25 square kilometers. The maximum total (organic and inorganic) sedimentation rate estimated with the numerical simulation model SEDF2D and the current meter data collected during the study is about $290 \text{ gm/m}^2/\text{yr}$ over an area of 0.03 square kilometers. The corresponding sedimentation rate for organic material would be $230 \text{ gm/m}^2/\text{yr}$. Outfall-related sedimentation rates comparable with natural rates ($100\text{--}300 \text{ gm/m}^2/\text{yr}$) are predicted in SEDF2D simulations to be limited to an area of less than 0.2 square kilometers.

Steady-state accumulations of organic material, estimated using the technique described in the EPA Technical Support document, are predicted to range from about 9.7 gm/m^2 (EPA sedimentation method, 1.25 km^2) to about 63 gm/m^2 (SEDF2D, 0.03 km^2). At a density of $0.5 \text{ dry-gm/wet cm}^3$, this would result in a deposit (before bioturbation) with a thickness of less than $1/8$ of a millimeter.

Sedimentation trap studies indicated that the Encina site is an active area of resuspension during both the summer and winter. Therefore, settling effluent particles are likely to be resuspended and dispersed over a larger area.

The low estimated sedimentation rates, small predicted steady-state accumulated masses, and sedimentation trap studies all suggest that any outfall generated changes in

the organic content of the sediments should be minor or undetectable. This conclusion is supported by direct measurements of organic material (as measured by volatile solids) in the upper 2 cm of the sediments over a 4 year period. Concentrations have ranged from 2.0 to 3.0 percent over the four year period, with the lowest values observed in the latest samples (April 1986). Concentrations of organic material in the surface sediments at distances of 4 km from the outfall range from 2.7 to 3.0 percent. Concentrations increase to about 3.2 to 3.3 percent at a depth of 10-15 cm near the outfall and at the distant stations.

II.B. Background

The Encina effluent contains organically enriched particles that can settle to the ocean bottom. The rate and areal pattern of sedimentation of these particles will depend on the properties of the ocean currents, the elevation of the wastefield above the ocean bottom, the mass emission rate of particles from the outfall, and the particle settling speeds.

After reaching the bottom, some of the organic material may be lost to bacterial "decay". In addition, the particles may be transformed by ingestion by benthic biota, or resuspended and redistributed by the near-bottom ocean currents.

We have used several computational techniques to estimate the sedimentation rates of the effluent particles, and the area "affected" by this sedimentation. These include: (1) the estimation techniques outlined in the EPA 301h Technical Support Document, (2) a recently developed

and more sophisticated model (SEDF2D Ver. 5.2.01) of particle sedimentation and, (3) observations from sediment traps and cores collected from the ocean bottom.

II.C. Outfall-Related Sedimentation and Accumulation

II.C.1. EPA-Suggested Technique

The computational procedure suggested by the EPA for estimating the sedimentation of effluent particulates is described in their 301h Technical Support Document (1982).

Input information required for a simulation includes:

1. Average current velocities in each of four quadrant directions (upcoast, downcoast, onshore, offshore).
2. Mass distribution of particle settling speeds.
3. Annual mass emission rate of suspended solids.
4. Elevation of the wastefield above the ocean bottom.
5. Bathymetry of the area.

The average current velocities were computed from the current meter records collected near the outfall diffuser and are summarized in Table 4. These velocities are relatively independent of season, hence there is no "critical" period associated with weak currents. The average values for each of the component directions were used for the simulation.

The mass distribution of particle settling speeds listed in the Technical Support document for "Primary and Advanced Primary" effluent were used (although the actual effluent includes some contribution of secondary treated effluent).

Calculations were carried out for wastefield elevations of 11 meters (wastefield depth = 35m) and 21 meters (wastefield depth = 25m) above the ocean bottom. Typical density profiles suggest that the wastefield would generally form at an elevation of more than 11m above the bottom. However, since median current speeds are substantially in excess of those required to enhance the initial dilutions achieved by the discharge, the wastefield can be expected to form deeper in the water column than suggested by calculations assuming zero current.

During a joint EPA-SCCWRP study of initial dilution at this outfall on June 13, 1986, it was found that the wastefield generally occupied the region between a depth of 30-40 meters. The currents during this study ranged from 6 to 14 cm/sec. Approximately 50-60 percent of all the current speeds measured during the current study fell within this range, suggesting that this study was carried out during "typical" conditions (assuming that the June water column density stratification was representative of the "usual" conditions). Therefore, we assumed that a "typical" depth for the middle of the wastefield was on the order of 35 meters. This assumption should be "conservative" in the sense that if there is any error, it should overestimate the predicted sedimentation rate. A separate calculation was carried out for a wastefield depth of 25m to provide an indication of the sensitivity of the results to the assumed wastefield depth.

An examination of the bathymetry of the discharge area indicates that the bottom slope in the range of depths from 30 meters to 46 meters is approximately 3.2 percent. The technical support document indicates that no "variable depth" correction to the sedimentation patterns is

necessary if the slope is less than 5 percent, and no correction was made in our simulations.

The annual mass emission rate of suspended solids was estimated to be 1070 metric-tons. For the 35m wastefield depth, this resulted in a maximum sedimentation rate of organic material (assumed = 80% of the total mass--as per the EPA guidelines) of $36 \text{ gm/m}^2/\text{yr}$ ($3.6 \text{ mg/cm}^2/\text{yr}$)--see Figure 8. This average sedimentation rate occurred over an area of about 1.25 square kilometers. A sedimentation rate of $1.3 \text{ gm/m}^2/\text{yr}$ (of organic material) was predicted to occur over an area of 125 square kilometers. For comparison purposes, the sedimentation rate of natural particles (after decay) has been estimated to be in the range of 100 to $300 \text{ gm/m}^2/\text{yr}$ (e.g. Emery, 1960).

For a wastefield depth of 25m, the maximum sedimentation rate is estimated to drop to about $9.5 \text{ gm/m}^2/\text{yr}$, but the affected area has increased to 4.5 square kilometers (Figure 9).

Figures 10 and 11 show the corresponding "steady-state" accumulations of organic material. These estimates were made using the technique suggested in the Technical Support Document (a mass balance between decay and sedimentation in the absence of resuspension). The maximum accumulation (31m deep wastefield) is estimated to be about $10 \text{ gm/m}^2/\text{yr}$ over the 1.25 square kilometer area. With the shallower (25m) wastefield, the corresponding accumulation and area of coverage are $2.7 \text{ gm/m}^2/\text{yr}$ and 4.5 square kilometers.

3. The influence of the coastal boundary can be approximated by assuming that flows must be parallel to the boundary immediately adjacent to the boundary, and the "influence" of the boundary on the flow diminishes in a linear fashion until at some offshore position, it no longer has any influence on the flow.

Descriptions of two versions of the model, including comparisons of the model predicted and observed sedimentation rates for the White Point outfall area, are contained in Hendricks (1983).

The sedimentation rates and pattern predicted with the model for an annual mass emission rate of 1070 m-tons of suspended solids and a wastefield depth of 35m (elevation above the bottom of 11m) are shown in Figure 12. The peak sedimentation rate is $285 \text{ gm/m}^2/\text{yr}$ ($28.5 \text{ mg/cm}^2/\text{yr}$) over an area of 0.03 km^2 (the area of a simulation grid "cell"). Assuming natural sedimentation rates on the order of $100\text{--}300 \text{ gm/m}^2/\text{yr}$, outfall-related sedimentation rates comparable with natural rates (e.g. $100 \text{ gm/m}^2/\text{yr}$) occur over an area of approximately 0.19 square kilometers.

The corresponding peak accumulation of organic material (using the sedimentation rate - decay balance suggested in the EPA document) will be 63 gm/m^2 (6.3 mg/cm^2)--See Figure 13.

II.C.3. Actual Accumulations of Organic Material

The low predicted accumulations would be expected to produce only minor increases in the organic content of the sediments. Assuming a sediment particle density of 0.5

dry-gm/wet cm^2 , an accumulation of 63 gm/m^2 would correspond to a layer thickness of about one-eighth of a millimeter. This layer would be mixed with natural sediments to a depth of about 5 cm as a result of mixing by benthic biota (bioturbation). Neglecting the inorganic component of the effluent particulates, the increase in concentration of organic material in the sediments as a result of effluent deposition can be estimated to be less than 0.7 percent (i.e. an increase from about 3.0 percent volatile solids to 3.7 percent in the immediate vicinity of the outfall).

There are some other factors to be considered in estimating these outfall-induced changes in sediment volatile solids concentrations. The EPA technique described in the Technical Support document for estimating "steady-state accumulation" neglects the effects of sediment resuspension and also assumes that all of the organic material is subject to decay.

II.C.3.a. Sediment Resuspension

The EPA guidelines suggest that resuspension effects can be qualitatively estimated from measured near-bottom current speeds. The qualitative threshold resuspension speeds listed in the document are in general agreement with "threshold resuspension speeds" measured during in-situ studies of the resuspension of "permanent" sediments carried out by SCCWRP (Hendricks, 1978).

Subsequent sediment transport and dispersion modeling efforts, combined with near-bottom sediment trap studies at a variety of locations along the southern California coast

suggest that a "thin" layer of surficial sediment may exist on top of the "permanent" sediments. These surficial sediments appear to be easily resuspended and undergo a large number of resuspensions and depositions before they become incorporated into the "permanent" sediments. This resuspension, transport, and deposition sequence can result in substantial dispersion of the effluent particulates after they settle to the ocean bottom.

Measurements of near-bottom "apparent sedimentation rates" in the vicinity of the Encina outfall diffuser indicate that resuspension is an active process in this location. Sediments collected in near-bottom sediment traps over four to five week periods corresponded to "apparent" sedimentation rates ranging from 1100 to 3400 $\text{mg}/\text{cm}^2/\text{yr}$ (11,000 to 34,000 $\text{gm}/\text{m}^2/\text{yr}$). These rates are more than two orders of magnitude (e.g. > 100 times) greater than typical net accumulation rates of natural sediments, and more than 45-120 times greater than the estimated maximum sedimentation rate of effluent particulates. This suggests that resuspension processes could substantially limit the accumulation of effluent-related particles around the outfall.

On the other hand, laboratory studies (Myers, 1974) indicate that only about one-half of the organic material in the effluent particulates is subject to decay. This refractory fraction of the organic material might continue to accumulate around the outfall--resulting in increased, but steady-state, concentrations of organic material in the sediments, but not steady-state accumulations.

In order to examine the possible effects of the two processes of resuspension and resistance to decay on the accumulation of organic material, we examined the changes

in volatile solids concentrations in the surface sediments over a four year period. The concentrations in the outfall area were compared the values observed in areas in which the effects of the discharge on the sediments can be expected to be minor, to obtain an estimate of possible outfall-induced changes.

Surface sediments (0-2 cm depth) collected with a Van Veen grab sampler in the immediate vicinity of the Encina outfall in 1982 (prior to the conversion to secondary treatment) had organic contents (as measured by volatile solids) of about 2.6-3.0 percent. For comparison, the surface sediments near Carlsbad Canyon had a concentration of about 1.9 percent, and surface sediments near the Oceanside outfall (secondary treatment) had a concentration of 3.7-6.5 percent.

Two years later, in July, 1984, the area was resampled. Surface sediments around the Encina outfall had a concentration of 2.9 percent; around the Oceanside outfall, the concentrations had fallen off to 2.3 to 2.6 percent. Four kilometers downcoast from the Encina outfall, the surface sediment concentration was 3.0 percent, while 4 km upcoast from the Oceanside outfall, the surface sediment concentration of volatile solids was 2.7 percent. Subsurface samples collected from the bottom of the grab (10-15 cm deep) had concentrations of 3.1 to 3.3 percent 4 kilometers away from the two outfalls, and concentrations ranging from 2.8 to 3.3 percent near the outfalls.

Grab samples were again collected in the vicinity of the Encina outfall in April, 1986 (approx. 11 months after reversion to advanced primary treatment). The concentration of volatile solids in the surface sediments was 2.0 percent.

This combination of sediment trap measurements, low predicted accumulation rates, and the history of volatile solids in the surface and subsurface sediments suggests, that the area around the outfall diffuser is a dynamic region with frequent resuspension, dispersion, and redeposition of surficial sediments with little, if any, detectable accumulation of outfall-related organic material.

III. INITIAL DILUTION

III.A. Summary

Thirty-eight density profiles collected from July, 1985 to October, 1986 were combined with information on the currents and effluent discharge rates to estimate "10-percentile" "worst case" initial dilutions using the EPA simulation models PLUME and MERGE. For the 5-year flows permitted under the NPDES permit, the corresponding 10-percentile dilutions for "winter" and "summer" were 206:1 and 224:1 respectively.

Direct measurements carried out on June 13, 1986 suggest that "typical" dilutions (including the effects of the ocean currents) are likely to be on the order of 650:1.

III.B. Background

Effluent from the Encina treatment plant is discharged through a series of "ports" near the terminus of the outfall. The shear associated with these "jets" of

effluent emerging into the receiving water causes the entrainment of ocean water into the effluent stream, diluting the concentration of effluent, and reducing the velocity of the jet. At the same time, the low density of the effluent relative to the receiving water (resulting from its lower salinity and higher temperature) causes the effluent jet to rise in the water column forming an effluent plume. The shear associated with the buoyancy generated flow causes additional entrainment of ocean water and further dilution. Ocean currents can generate additional shear, as well as additional buoyancy induced mixing (associated with "bending" of the plume), enhancing the entrainment of ocean water into the plume.

If there is sufficient density stratification of the water column, at some point the density of the plume will match that of the surrounding receiving water, the upward movement of the plume will be halted, and a wastefield forms at the equilibrium depth.

The dilution of the effluent achieved during this process between discharge and wastefield formation is termed the "initial dilution". Its magnitude depends on a variety of factors, including the physical characteristics of the outfall diffuser (e.g. port diameter, shape, discharge direction, and spacing), the effluent discharge rate and density, the density structure of the receiving water, and the strength of the ocean currents and their direction of flow relative to the orientation of the outfall diffuser.

III.C. 10-Percentile "Worst Case" Initial Dilutions

Obviously it is difficult to measure all these quanti-

ties simultaneously over an extended period of time. Therefore, "minimum" initial dilutions (for a given discharge rate) are generally defined as the initial dilutions that would be produced if the 10-percentile "worst" receiving water conditions occurred simultaneously. This is equivalent to using both the 10-percentile "slowest" currents with the 10-percentile "strongest" density stratification. Since the latter depends not only on the magnitude of the density stratification, but also on the "shape" of the profile, the "strongest" stratification can generally only be determined by "trial-and-error" from a selected set of "candidate" profiles.

III.C.1. 10-Percentile "Lowest" Current Speeds

Strictly speaking, the 10-percentile currents should be determined by considering both the flow speed and direction (relative to the diffuser alignment). For simplicity, we assumed that the 10-percentile current speeds, independent of direction, could be used for the "critical" simulations. From Figures 2 and 3 (in the "CURRENTS" section), it can be seen that the 10-percentile lowest speeds are approximately 4.0 and 4.5 cm/sec for the summer and winter seasons, respectively. A speed of 4 cm/sec was used for the simulations with the EPA initial dilution model MERGE (PLUME neglects the effects of ocean currents)--see Section III.C.3.

III.C.2. 10-Percentile "Strongest" Density Gradients

Densities were calculated from temperature information collected as part of the normal Encina monitoring program

for the period from July, 1985 to October, 1986. This was supplemented by salinity and temperature information collected by SCCWRP during deployment and servicing of the current meters (February, April, August, September, 1986), and during the joint EPA-SCCWRP study of initial dilution (June, 1986).

Salinity information collected during the regular monitoring studies was not used since it showed more variation than was observed during CTD (conductivity-temperature-depth) casts with a Niel Brown "Smart" CTD by SCCWRP, in discrete samples analyzed by PCODF (Scripps Institute of Oceanography), or in historical records collected by the CalCOFI program. The latter measurements indicate that there is generally no, or very little (< 0.2 ppm), salinity gradient over the upper 46m of the water column in this area. The computed density profiles, expressed in sigma-t units, are listed in Appendix D.

After the densities were computed, the density differences between water depths of 23m and 46m (diffuser depth), and 33m and 46m were calculated. These differences were used to make an initial "cull" of the candidate profiles to minimize the number of initial dilution simulations that needed to be carried out.

III.C.3. Initial Dilution Simulation Models

A number of initial dilution programs exist that could be used to estimate the magnitude of the initial dilution achieved at the Encina outfall. The EPA numerical simulation models of PLUME and MERGE, were selected to compute the 10-percentile "worst" cases from the selected density

profiles since they generally yield the most conservative (lowest) estimates of the initial dilution.

PLUME assumes the speed of the ocean currents is zero, eliminating the dilution enhancing effects of the ocean currents. On the other hand, it does not take into account possible merging of the individual plumes. If merging occurs, their neglect could lead to overestimation of the dilution.

MERGE, on the other hand allows for ocean currents and includes their effect on the initial dilution process. It also takes into account dilution reductions associated with merging of the plumes. A port spacing of 12 ft (3.65m) was used for the MERGE simulations.

Initial dilutions were computed for each selected density profile and each of the effluent flow rates listed in Table 4 using both models.

III.C.4. Computed 10-Percentile Initial Dilutions

The 10-percentile current speeds obtained from the mid-water current measurements were nearly independent of season. The "worst case" density profiles (in terms of lowest initial dilutions) were associated with the months of February, September, and October. Differences in initial dilutions calculated for different months were frequently less than those calculated for density profiles collected on the same day, but on opposite sides of the diffuser, or using profiles collected only a few days apart.

This variability suggests that the 10-percentile initial dilution will be nearly independent of season. Nevertheless, the 38 available density sections were

subdivided into winter (Nov.->April, 15 profiles) and summer (May->Oct., 23 profiles), and initial dilutions calculated for each season. The 10-percentile "worst case" initial dilutions were selected to be the second lowest initial dilutions computed from the density profiles for each season.

The resulting 10-percentile "worst case" initial dilutions are listed in Table 5 for each flow and "season". These initial dilutions were all computed with MERGE--estimates using the program PLUME were generally higher. The corresponding density profiles are shown in Figures 14 and 15. For the discharge presently permitted under the NPDES permit (22.5 MGD), the 10-percentile "summer" initial dilution is 224:1. For "winter" (32.1 MGD), the 10-percentile value is 206:1. If all the density profiles are combined, without regard to season (38 profiles), the 10-percentile I.D. (fourth lowest value) would be 224:1.

III.D. Actual Initial Dilutions for "Typical" Conditions

The EPA and SCCWRP participated in a joint study of initial dilution at the Encina ocean outfall on June 11-13, 1986. A dye (Rhodamine-WT) was injected at the treatment plant at a constant concentration (0.5 ppm "active" component) over a 14 hour period. Samples were collected as a function of depth and position downstream from the outfall diffuser. During the study period, the speed of the ocean currents varied from a low of 6 cm/sec to a high of 14 cm/sec. The discharge rate varied from 12.5 to 28.5 MGD.

The data from this study is still undergoing analysis. Tentative average initial dilutions, and the corresponding distances downstream from the outfall, are listed in Table 6. The dilutions range from 390:1 to 1470:1 near the outfall, with a "typical" value of about 650:1. These values are probably more representative of the initial dilutions frequently achieved by the outfall.

It is interesting to note that the depth of the mid-point of the wastefield observed during this study was on the order of 35m. The wastefield depths estimated in the 10-percentile "worst case" simulations were all on the order of 30 meters (see Figures 14 and 15). The fact that higher initial dilutions were achieved for a deeper wastefield (i.e. shorter entrainment elevation between the discharge port and the wastefield) illustrates the effect of the ambient currents on the initial dilution process. In the absence of currents, higher initial dilutions would be associated with a greater entrainment length and a shallower wastefield.

IV. CROSS-SHORE TRANSPORT

IV.A. Summary

It is virtually impossible to quantitatively predict the likelihood of the transport of wastewater materials contained in a subsurface wastefield into the surface waters at the coast from limited current meter records and the present understanding of the dynamics of the physical processes.

The sedimentation model SEDF2D was, however, modified to provide an upper bound on the likelihood of transport from the outfall diffuser to the 25m isobath for a wastefield initially formed at a depth of about 25 meters. This probability is obviously a function of the range of "ages" permitted for the wastewater. For example, if the wastewater is allowed to be between 0 and 24 hours of "age" (elapsed time since discharge), the probability will generally be greater than if the age is required to be less than 6 hours.

For the three periods of current meter data from the mooring near the outfall diffuser, the period from JD 227 (August 15, 1986) to 261 (Sept. 18, 1986) was found to have the highest probability of onshore transport. The likelihood of wastewater constituents with an "age" of 24 hours, or less, reaching the 25m isobath was estimated to be about 10 percent along most of an eight kilometer section of the coastline. This probability increases to approximately 30 percent for about half of this length after an additional 24 hours (48 hours total).

The probability of wastewater reaching the surface waters at the coast is much less because water column density stratification conditions permitting the cross-shore transport to the coastal surface waters are uncommon. In addition, the advective transport probability for carrying wastewater into the shore will be reduced below 10 percent because of the additional distance involved.

IV.B. Background

IV.B.1. Cross-shore Transport

It is exceedingly difficult to estimate the cross-shore transport of wastewater discharged from an ocean outfall into a density stratified receiving water. As was noted in the section on currents, there is generally little correlation between the cross-shore flows at moorings spatially separated in either the longshore or cross-shore direction. This lack of correlation is a general feature of the coastal flow patterns and is not specific to the Encina area.

The end result of this lack of correlation is that it is impossible to deterministically predict the advective transport from a "sparse" array of current meters. It is not unlikely that data collected from current meter arrays are neither the most accurate nor the most efficient method of estimating cross-shore transport.

IV.B.2. Vertical Exchange

There are other significant impediments to making these cross-shore transport estimates. Density stratification of the water column suppresses vertical exchange or movement of "parcels" of water. As a result, transport and mixing tends to occur along surfaces of constant water density (isopycnal surfaces).

The general trend of the surface currents in this area is down-coast, while the sub-thermocline currents tend to flow upcoast. As a result, the isopycnal surfaces generally tend to slope upward toward the coast. However, this

"shoaling" of the isopycnal surfaces is reduced as the local stratification of the water column increases due to the increased energy requirements associated with "lifting" the isopycnal surfaces. As a result, during periods of onshore transport, the wastefield will generally be located at a shallower depth than near the outfall, but its appearance at the surface can be expected to be a relatively rare event. This conclusion is consistent with the observations from the intensive bacterial sampling carried out in the vicinity of the Point Loma outfall (operated by the City of San Diego), where elevated concentrations of bacteria at depths of 40-60 feet were observed, but elevated concentrations in the upper 10 feet of water were rare. The sampling was carried out twice a week for more than one and one-half years.

The inhibitory effects of the thermocline (large temperature gradient) on vertical exchange were also evident during the June initial dilution study. Water temperatures in the lower 15 meters of the water column (30-46m depths) were in the range of 10-11 degrees Celsius. These are substantially lower temperatures than observed in the other profiles used to compute the initial dilutions, suggesting that a period of upwelling of deeper, colder water into this depth range had occurred prior to the study. Nevertheless, surface water temperatures were on the order of 20 degrees Celsius, or comparable with the highest surface temperatures recorded among the set of density profiles.

Transport to the surface waters of the coast therefore requires that two simultaneous conditions exist: (1) onshore transport of the wastewater and, (2) sufficient "shoaling" of the isopycnal surfaces so that the surface corresponding to the depth of the wastefield (offshore)

"surfaces" at the coast ("upwelling" can be considered as a special case of the latter process).

Thus it is not only necessary to be able to estimate the cross-shore transport, but one must simultaneously estimate the cross-shore slope of the isopycnal surfaces. At the present time, the methods for adequately making these estimates are not feasible considering the existing constraints of time, money, and equipment. Perhaps the most reliable method of estimating the crossshore transport of wastewaters is through monitoring programs designed to detect and quantify the presence of effluent constituents.

IV.C. The Transport Model "PXYT2D"

In spite of these severe problems, some insight into the likelihood of the cross-shore transport of wastewaters might be obtained from an admittedly highly simplified simulation model based on ocean current measurements.

To pursue this approach, we used the basic framework and conceptual approach applied to the sedimentation model SEDF2D, which appears to adequately reproduce the sedimentation field around the White Point outfall. Instead of predicting sedimentation rates, however, the goal in the transport model will be to estimate the probability that wastewater with an "age" less than some selected value (e.g. 6, 12, 24, or 48 hours) would be observed at some particular location in the outfall area.

The sedimentation model SEDF2D was modified to provide an estimate of these probabilities, and the resulting model has been named PXYT2D. Figures 16a,b,c,d show the areal distribution of probabilities for elapsed times (since

discharge) of 6, 12, 24, and 48 hours, respectively for a wastefield formed at a depth of 25 meters under the flow conditions existing between Julian Days 227 to 261.

Note that the probability for a particular elapsed time (e.g. 24 hours) does not refer to the probability that 24 hour "old" effluent will be found in the area, but rather the probability that effluent with an "age" of 24 hours, or less, will be present. Thus the probabilities at any given location in the area for the 24 hour elapsed time simulation will include, and hence be at least as large as, the corresponding probabilities for any shorter period of time (e.g. 6 or 12 hours). Similar plots are presented for two other current meter record periods (JD 58 -> 94, and 194 -> 227) in Appendix E.

Since the model formulation assumes that transport will only occur along horizontal isopycnal surfaces, constituents of a wastefield at a depth of 25m in the water column (at the outfall diffuser) can never be transported inshore of the 25m isobath (the "effective" coastline for the wastefield). Thus the probability of these effluent components reaching the surface waters at the coast is also determined by the probability that sufficient "slope" exists in the isopycnal surfaces to produce the required shoaling.

For example, to lowest order, the probability of "dissolved" components of the effluent reaching the surface at the offshore location of the 25m isobath could be estimated by multiplying the probability of wastewater of a particular "age" reaching the vicinity of the isobath (i.e. the probabilities estimated in Figure 16) times the probability that sufficient "shoaling" of the isopycnal surfaces will simultaneously occur with the transport. Since the latter

will always be less than unity (and evidence from the Point Loma study indicates it is probably much, much less than unity), the transport calculation greatly overestimates the likelihood of onshore transport to the surface waters.

It can be anticipated that the "shoaling" probabilities are likely to substantially increase toward unity as the water column density stratification declines. This reduction in stratification has two effects: (1) the isopycnal surfaces corresponding to the wastefield depth are more likely to surface at the coast and, (2) a surfacing wastefield will be generated if the density gradient is too "weak" to "trap" the wastefield below the surface.

It can be expected that even with the "correct" amount of shoaling of the isopycnal surfaces to permit the cross-shore transport of wastewater from the submerged wastefield to the surface waters at the beach, the transport probabilities will be less than indicated in Figure 16a -> 16d because of the greater transport distances involved.

In principal, it is possible to estimate the transport probabilities for the case of a surfacing wastefield, or in the event that the isopycnal surfaces surface at the coast by "telling" the model that the wastefield was formed at the surface.

For the shoaling isopycnal surfaces, the current meter records collected below the thermocline could be used to provide a rough estimate of the cross-shore transport. For the case of a density stratified water column, but of insufficient "strength" to prevent the formation of a surface wastefield, current meter data collected above the thermocline would be required. In any case, the procedure requires the creation of a new simulation grid, or

substantial alterations to the sedimentation model. These changes could not be carried out in the available time, and their validity would be highly questionable.

REFERENCES

- Boylls, J.C. and T.J. Hendricks, 1985. A Tilting Current Meter for Low Velocity Currents. In: Conference Record. Oceans 85 - Ocean Engineering and the Environment. Marine Technology Society, IEEE Ocean Engineering Society. Vol. 2. Nov. 12-14, 1985. San Diego, CA. p 749-751.
- Emery, K.O. 1960. The Sea Off Southern California. A Modern Habitat of Petroleum. Wiley, New York, NY, 366 pp.
- EPA, 1982. Revised Section 301(h) Technical Support Document. United States Environmental Protection Agency, Office of Water Program Operations (WH546). Washington, D.C. 20460.
- Hendricks, T.J. 1976. Current velocities required to move sediments. Coastal Water Research Project-1976 Annual Report. Southern California Coastal Water Research Project, Long Beach, CA. 1976.
- Hendricks, T.J. 1983. Final Report - Numerical Model of Sediment Quality near an Ocean Outfall. Submitted to: National Oceanographic and Atmospheric Administration (NOAA), ERL/PMEL, Seattle, WA. Oct., 1983.
- Hendricks, T.J. 1985. Use of Inclinator Current Meters in Weak Currents. In: Conference Record. Oceans 85 - Ocean Engineering and the Environment. Marine Technology Society, IEEE Ocean Engineering Society. Vol. 2. Nov. 12-14, 1985. San Diego, CA. p 742-748.
- Myers, E.P. 1974. The Concentration and Isotopic Composition of Carbon in Marine Sediments Affected by a Marine Discharge. Ph.D. dissertation. Calif. Inst. of Tech., Pasadena, CA. February, 1974.
- Roberts, P.J.W., 1977. Dispersion of buoyant waste water discharged from outfall diffusers of finite length. W.M. Keck Laboratory, California Institute of Technology Report No. KH-R- 35, March, 1977.

Table 1
Current Meter Deployment

Period *****	Station *****	Water Depth *****	Meter Depth *****	Days of Record *****
009 -> 041	1-Inshore	25	12.5	31.8
			23.0	31.8
	2-Outfall	46	20.0	6.8*
			44.0	31.9
	4-Canyon	46	20.0	4.3*
			44.0	31.8
041 -> 058	1-Inshore	25	12.5	16.9
			23.0	16.9
	2-Outfall	46	20.0	0.0*
			44.0	16.9
	4-Canyon	46	20.0	4.9
			44.0	17.0
058 ->	1-Inshore	25	12.5	36.0
			23.0	--
	2-Outfall	46	20.0	35.9
			44.0	35.9
	4-Canyon	46	20.0	35.1
			44.0	35.8
194 -> 227	2-Outfall	46	16.0	32.9
			44.0	32.7
	4-Canyon	46	16.0	32.8
			44.0	32.9
194 -> 230	1-Inshore	25	12.5	35.9
			23.0	35.9
227 -> 261	2-Outfall	46	16.0	33.8
			44.0	0.0*
	5-Upcoast	46	16.0	33.9
			44.0	33.9
230 -> 261	4-Canyon	46	16.0	29.2
			44.0	30.9

009 -> January 9, 1986
041 -> February 10, 1986
058 -> February 27, 1986

194 -> July 13, 1986
227 -> August 15, 1986

Table 2

Mean and Root-Mean-Square Speeds

Season	Sta.	Meter Depth	Axis	Mean Speed		RMS Speeds		Princ. Axis
				Vx	Vy	Vx	Vy	
Mid-Water Flows:								
Winter	1	12.5	320	0.1	1.5	11.8	4.4	323
	2	20	320	(-.8)	(.5)	(10.6)	(3.9)	(318)
	4	20	310	(0.6)	(1.6)	(10.0)	(3.9)	(309)
Summer	1	12.5	320	(2.1)	(.8)	(7.1)	(3.4)	(318)
	2	16	320	4.6	0.6	10.7	3.3	319
	4	16	310	5.1	-1.2	10.0	3.9	309
	5	16	290	(7.0)	(-.5)	(10.4)	(3.6)	(292)
Near-Bottom Flows:								
Winter	1	23	320	2.6	-2.4	7.3	5.0	300
	2	44	320	3.2	-1.7	7.6	4.7	270
	4	44	320	0.9	-0.9	5.7	4.0	298
Summer	1	33	320	(1.9)	(-1.5)	(6.0)	(4.6)	(277)
	2	44	320	(1.0)	(-0.4)	(3.9)	(3.1)	(211)
	4	44	310	2.1	-0.7	5.0	4.2	270
	5	44	290	3.8	-0.1	5.3	4.2	280

Speeds in cm/sec; + -> upcoast / onshore
 - -> downcoast / offshore

Heading in degrees(mag.); depth in meters

Principal axis -> Principal major axis of
 variation (e.g. 300 -> 120-300 degrees)

Values in () indicate an approximately 37 day
 long period; values without () are
 averaged over an approximately 74 day
 period.

TABLE 3

Correlation Coefficients

	Sample Period (Julian Days)	Stations	R and (Lag - hrs) 2 Longshore Cross-shore	
			Longshore	Cross-shore
Long Period (>24.75 hr)	058 - 094	4 - 2	0.87 (**)	0.33 (**)
		1 - 2	0.90 (1.5)	0.09 (-3)
	194 - 227	4 - 2	0.79 (4.5)	0.01 (4.5)
		1 - 2	0.88 (-1.5)	0.00 (-1.5)
	227 - XXX	4 - 2	0.89 (2.3)	0.03 (0.8)
		5 - 2	0.88 (-2.3)	0.16 (0.8)
		4 - 5	0.95 (2.3)	0.53 (-3.8)
	Average:		.879 + .047	.163 + .199
	058 - 094	4 - 2	0.27 (**)	0.01 (**)
		1 - 2	0.53 (0)	0.09 (0)
Tidal Per. (3.0 to 24.75 hr)	194 - 227	4 - 2	0.26 (-.8)	0.12 (-.8)
		1 - 2	0.20 (0.8)	0.08 (3.0)
	227 - XXX	4 - 2	0.29 (-1.5)	0.12 (-1.5)
		5 - 2	0.24 (-2.3)	0.10 (-0.8)
		4 - 5	0.18 (0)	0.14 (-1.5)
	Average:		.281 + .116	.094 + .043
Short Per. (< 3 hr)	058 - 094	4 - 2	0.02 (**)	0.00 (**)
		1 - 2	0.03 (0.8)	0.00 (0.8)
	194 - 277	4 - 2	0.01 (-.8)	0.01 (-.8)
		1 - 2	0.01 (0)	0.00 (0)
	227 - XXX	4 - 2	0.00 (0)	0.00 (0)
		5 - 2	0.01 (0)	0.00 (0)
		4 - 5	0.01 (0)	0.00 (0)
	Average:		.015 + .009	.003 + .001

Table 4

Average Mid-Water Current Velocities
(by direction)

Beginning Day *****	Avg. Velocity (cm/sec)		Onshore *****	Offshore *****
	Upcoast *****	Downcoast *****		
01/09/86 (009)	8.9	9.2	4.0	3.2
04/04/86 (058)	8.5	9.6	4.0	3.6
07/13/86 (194)	9.6	9.4	3.5	3.1
08/15/85 (227)	10.8 ****	8.2 ***	4.0 ***	3.1 ***
Average:	9.4	9.1	3.9	3.2

Table 5

Flow Rates and 10-Percentile "Worst-Case" Initial Dilutions

Season	Flow Condition	MGD	I.D. (10%)	Profile	I.D. (Worst)	Profile
*****	*****	***	*****	*****	*****	*****
Winter	Rated PWWF	54.0	165:1	4/86(Z2)	130:1	2/10/86
	5-yr PWWF	32.1	206:1	4/86(Z2)	157:1	2/10/86
	Current PWWF	28.0	267:1	4/86(Z2)	199:1	2/10/86
Summer	Rated PDWF	34.8	182:1	10/85(Z1)	173:1	9/85(Z1)
	5-yr PDWF	22.5	224:1	10/85(Z1)	199:1	9/85(Z1)
	Current ADWF	18.5	205:1	10/85(Z1)	205:1	9/85(Z1)

Simulation Conditions:

# Ports	88
Port Dia. (for simulation)	0.0762 meters
Port Angle (rel. to horiz)*	0.0 degrees
Discharge Depth	43.3 meters
Port Spacing	3.65 meters
Eff. Density	0.997 gm/cm**3

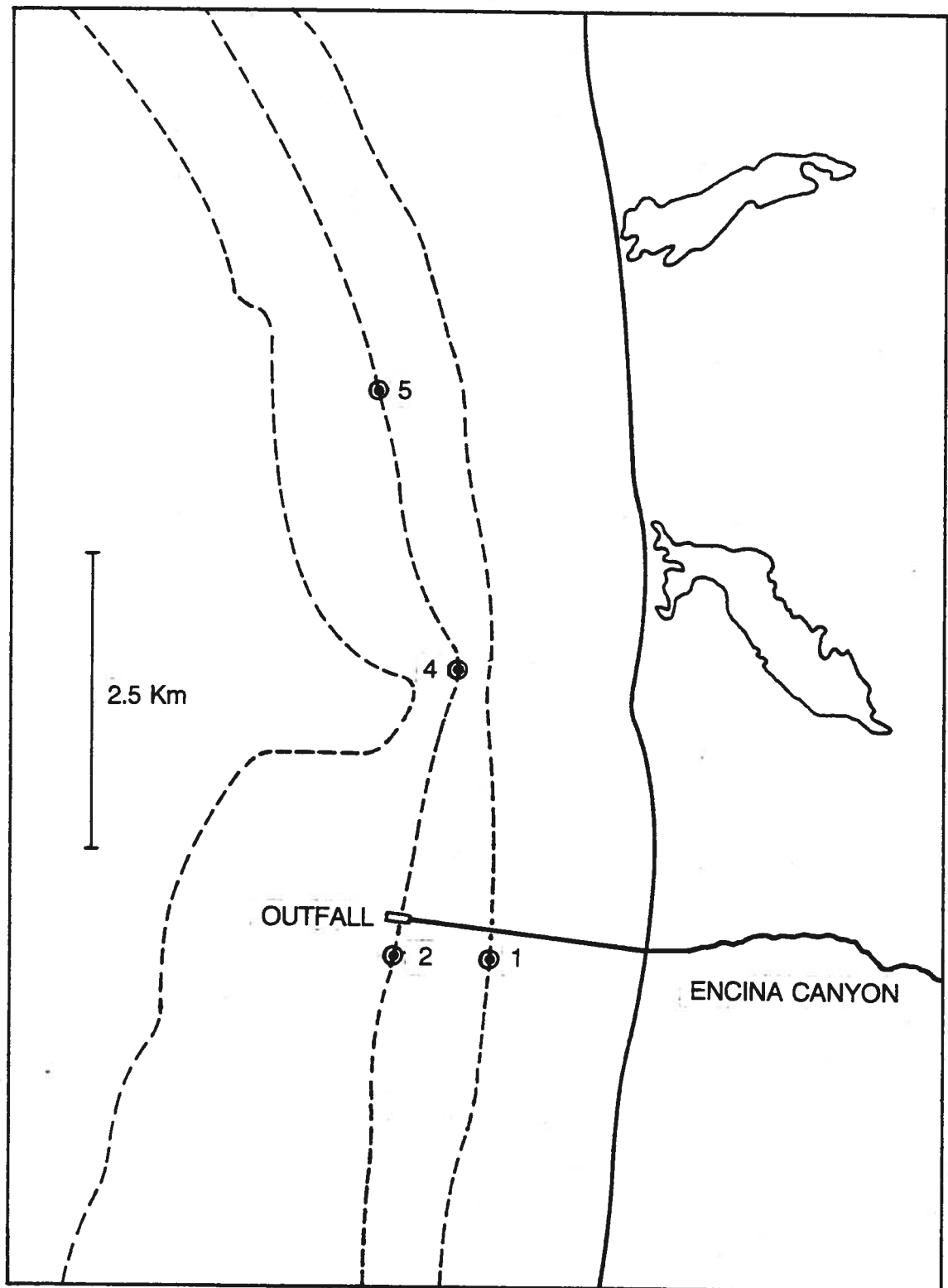
(* Actual port angle is -5 degrees. The initial dilution program would not execute with an angle less than 0.)

Table 6

Measured Average Initial Dilutions
(June 13, 1986)

1	2	3	4	5	6
Sta	Distance	MGD	Vx	Dilution	Location
***	*****	*****	**	*****	*****
1	30	12.5	14	480	Side
2	61	17.7	10	1470	Edge
3	119	25.4	13	885	Mid
4	90	28.5	10	595	Mid
5	101	26.6	10	815	Edge->Mid
6	31	26.3	8	740	Mid
7	116	(25.7)	8	640	Mid
8	41	(24.2)	6	390	Side
9	453	(26.0)	9	736	Mid->Side

- 1 - Station Number
- 2 - Downstream distance (meters) to sampling point (avg).
- 3 - Discharge rate at time of "release"
- 4 - Velocity perpendicular to outfall diffuser at time of "release" (cm/sec)
- 5 - Time and space (wastefield) averaged initial dilutions (e.g. 480:1)
- 6 - Samples collected downstream from diffuser. "Location" refers to the across wastefield location.



**Fig 1. Location of Current
meter moorings.**

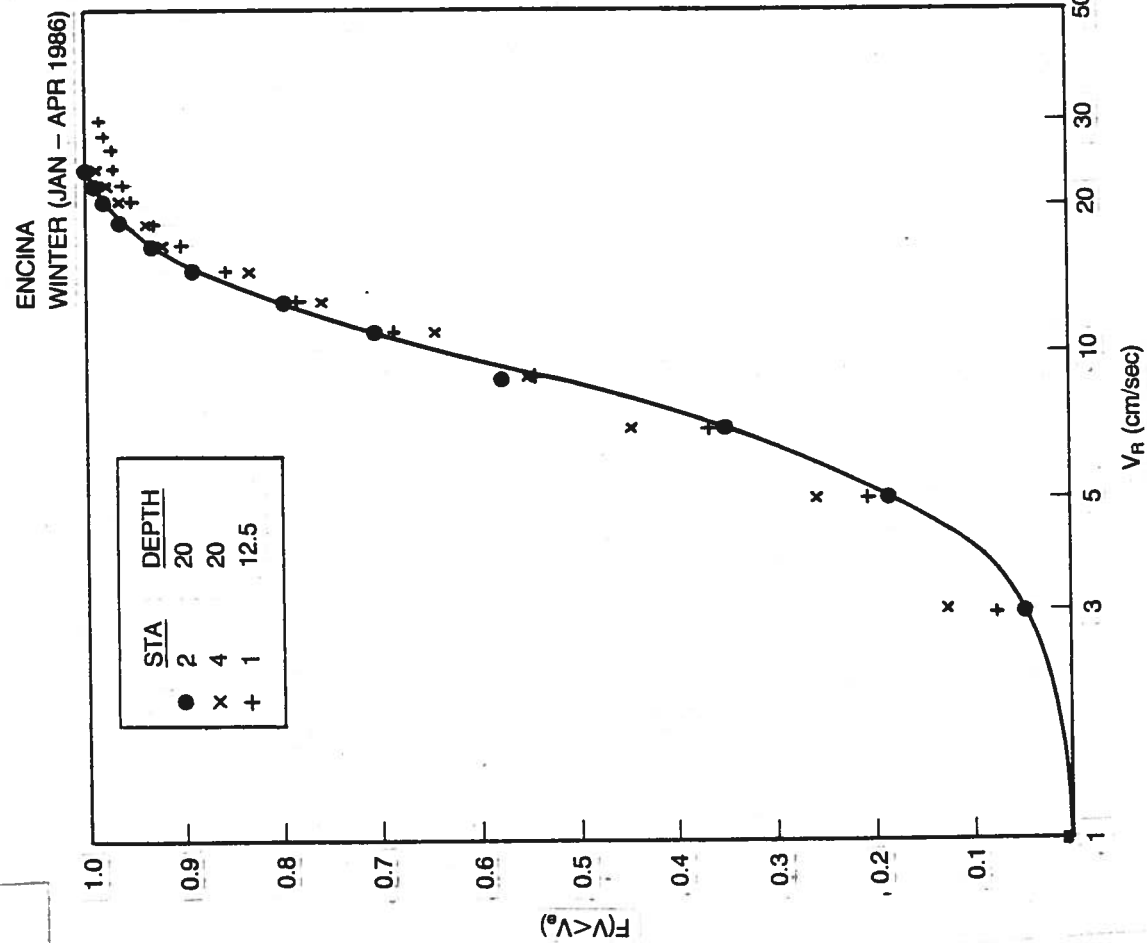


Fig 2a. Cumulative description
of winter currents.

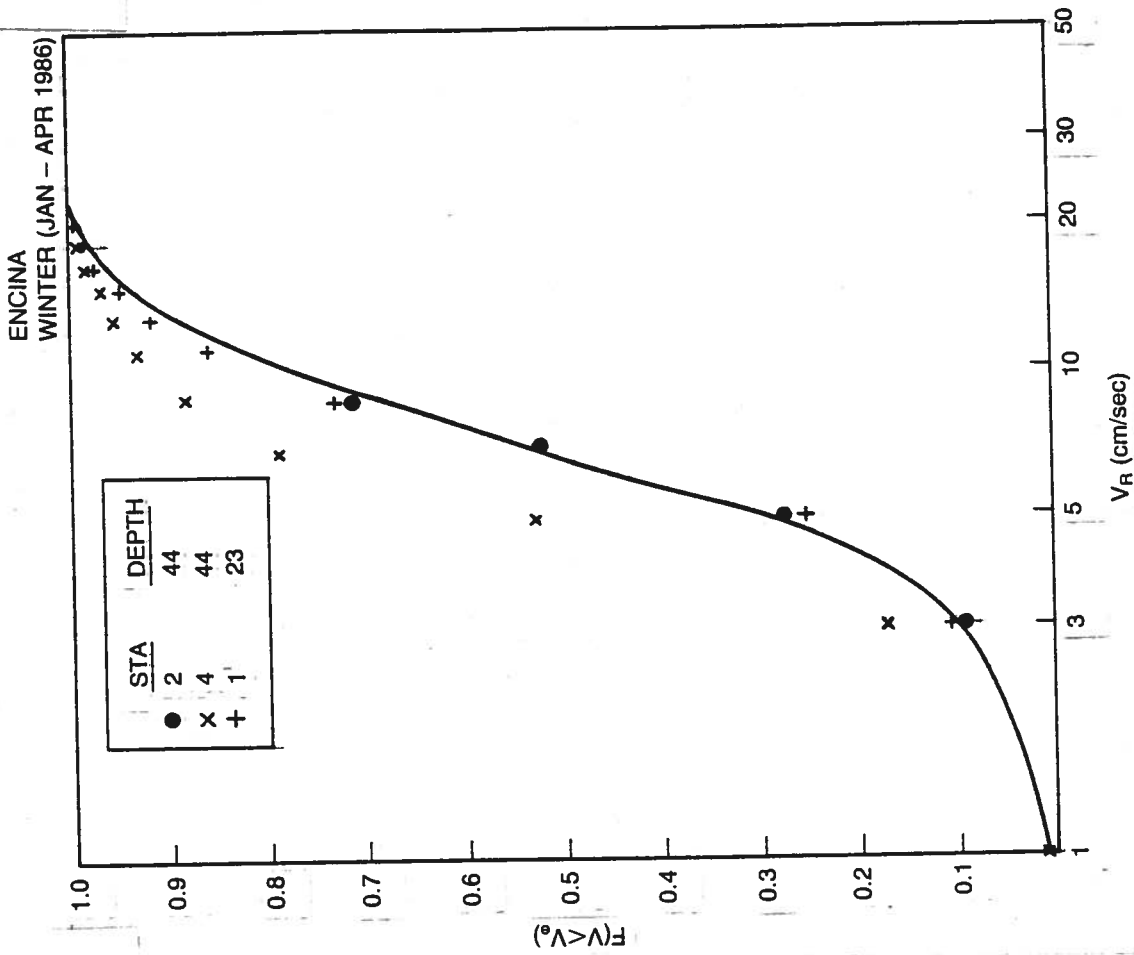


Fig 2b. Cumulative description
of winter currents.

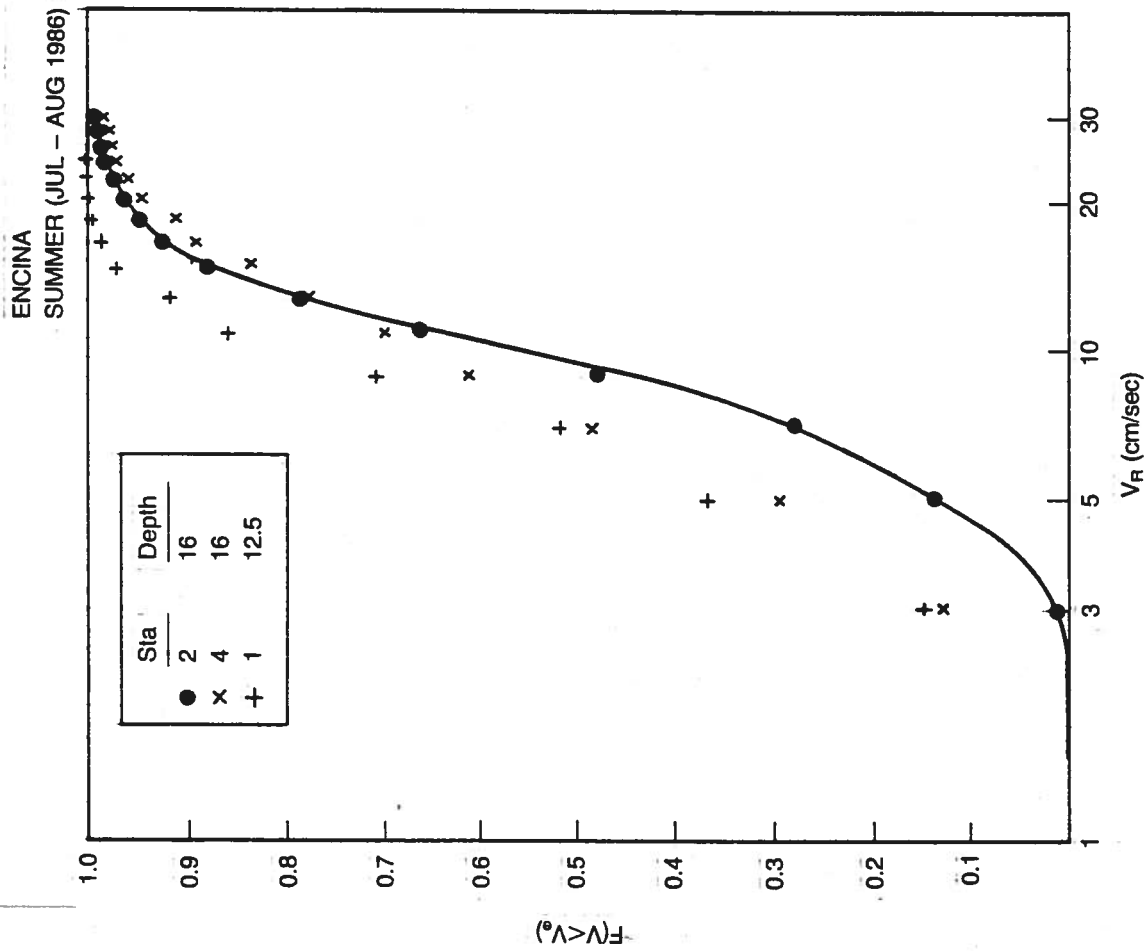


Fig 3a. Cumulative description of summer currents.

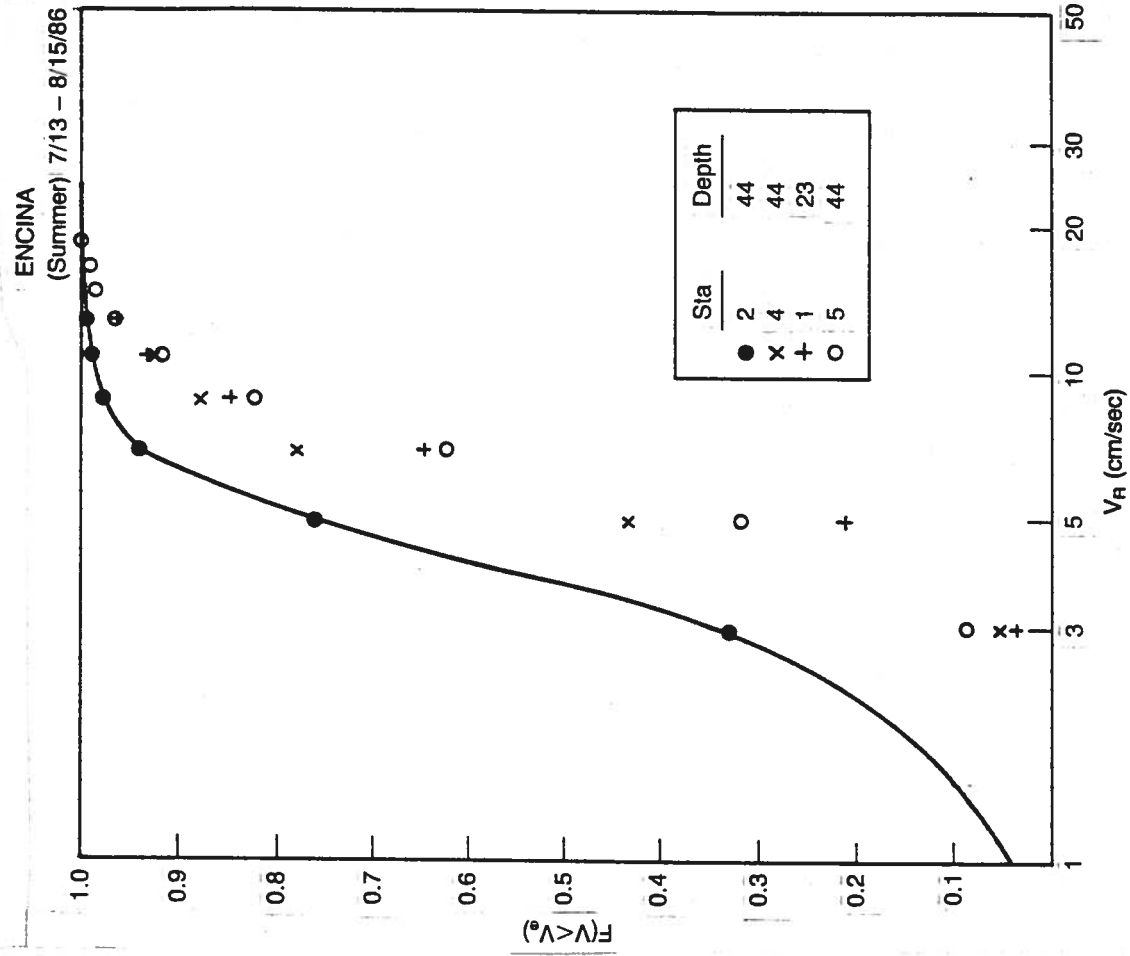


Fig 3b. Cumulative description of summer currents.

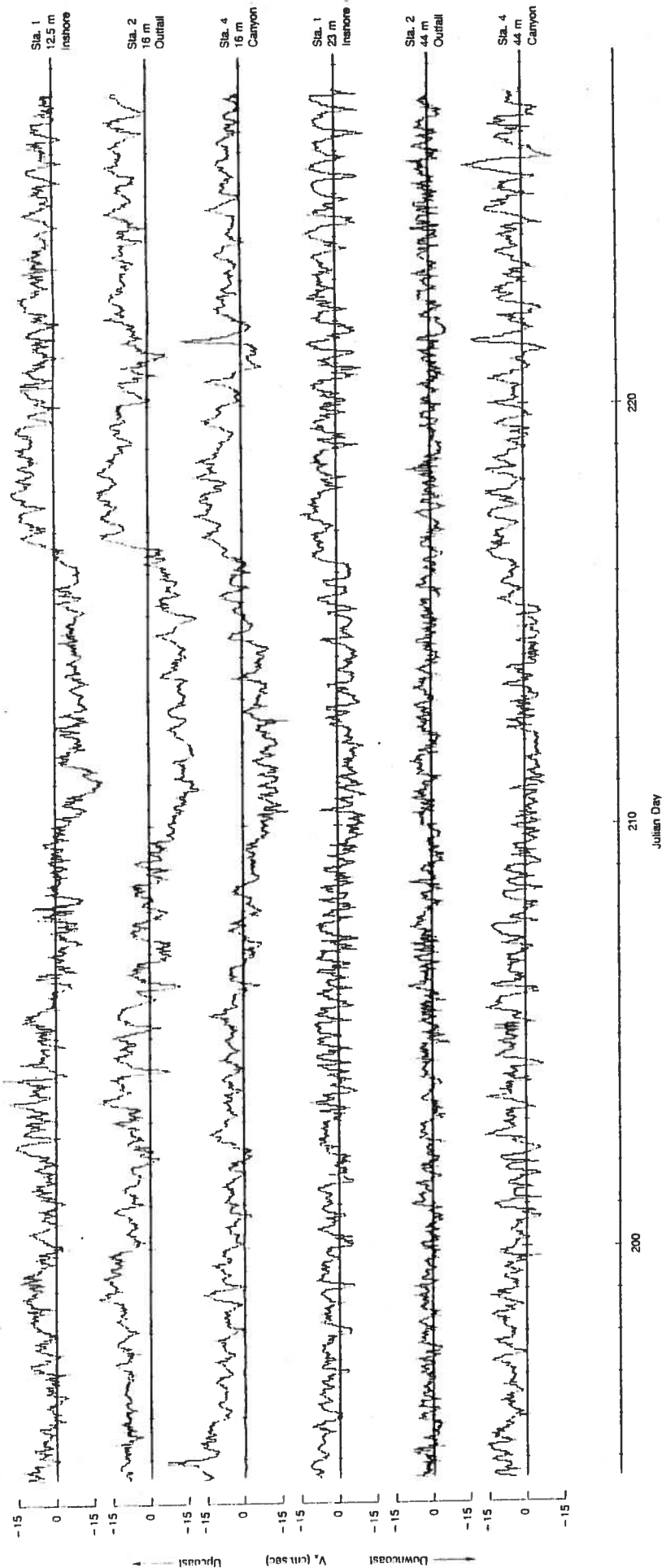


Fig 4a - Longshore Component of the Currents, Encina, 7/13 - 8/15/86
(+ = Upcoast, - = Downcoast)

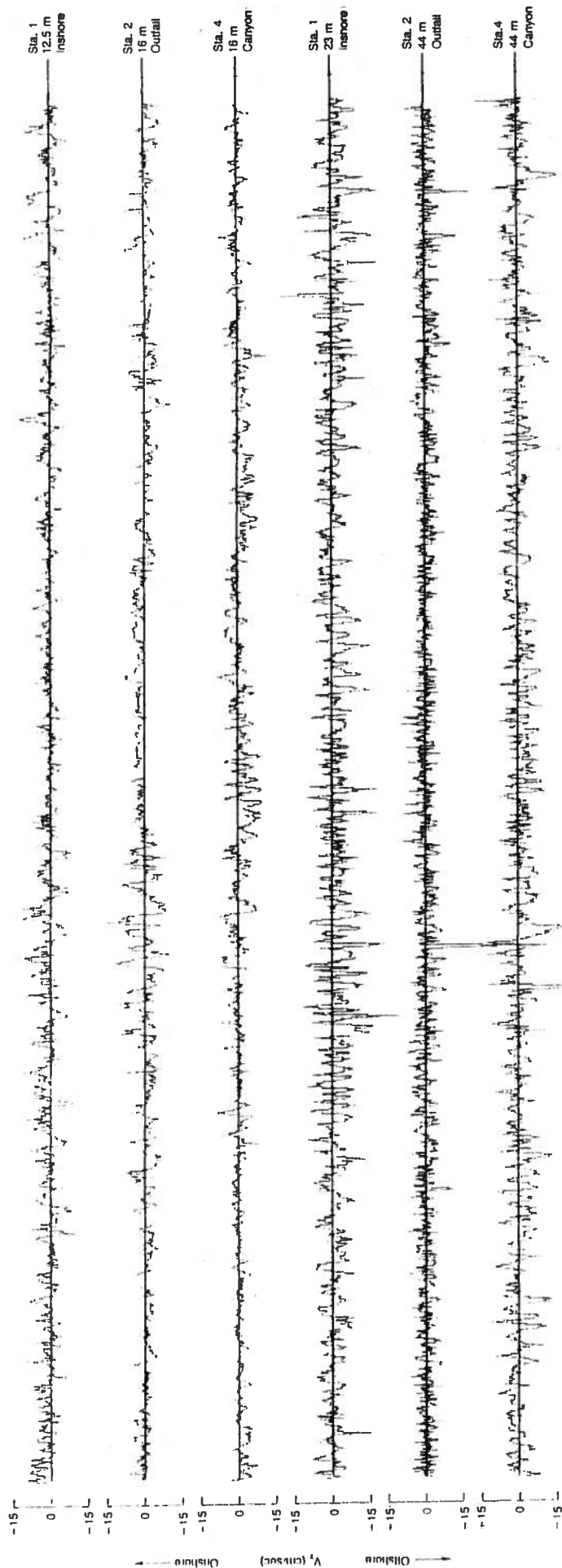


Fig 4b - Cross-shore Component of the Currents, Encina, 7/13 - 8/15/86
($+$ = Onshore, $-$ = Offshore)

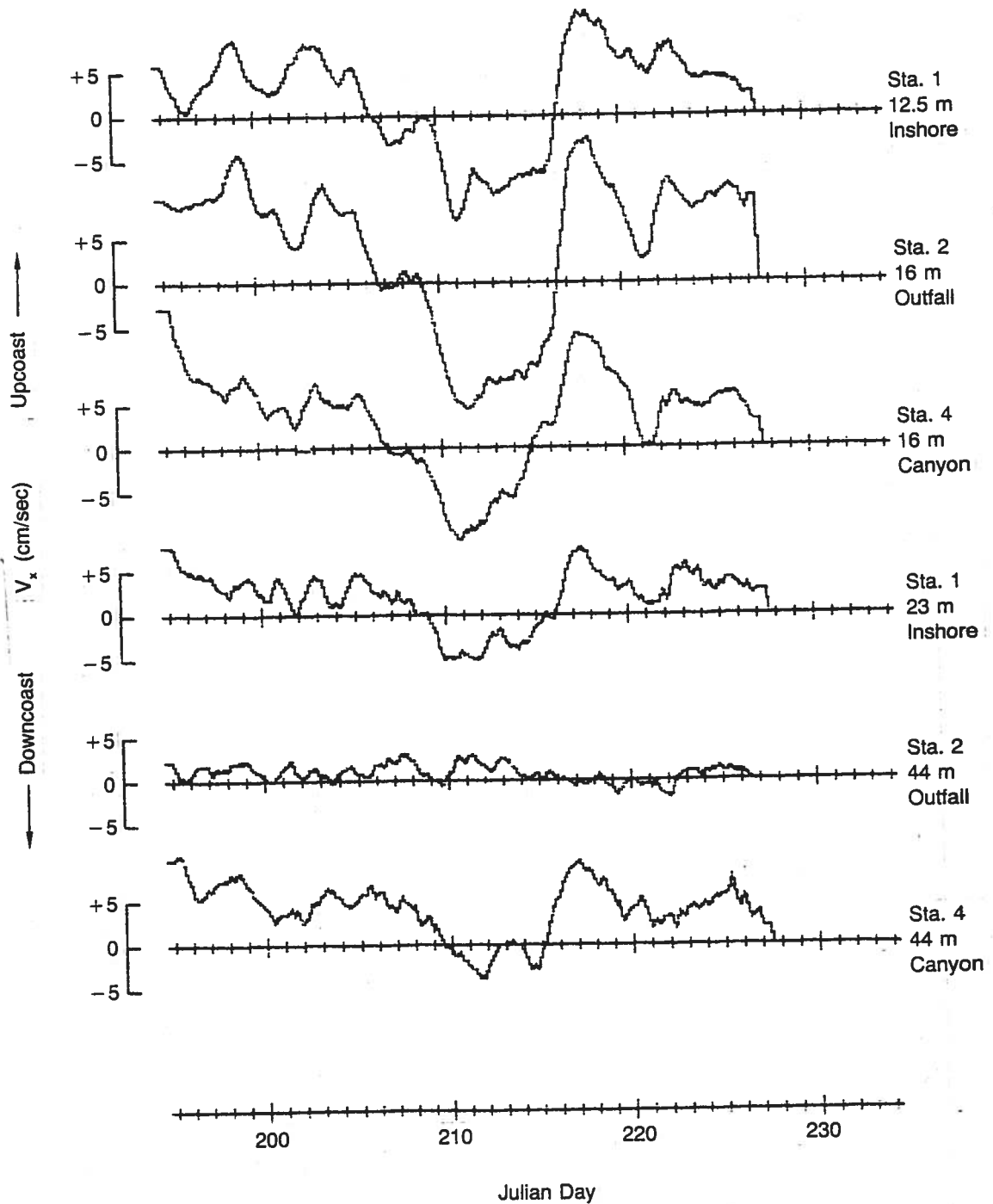


Fig 5a - Midwater Long-shore Currents, Encina, 7/13 - 8/15/86
 (24.75 hr. low-pass filter)
 (+ = Upcoast, - = Downcoast)

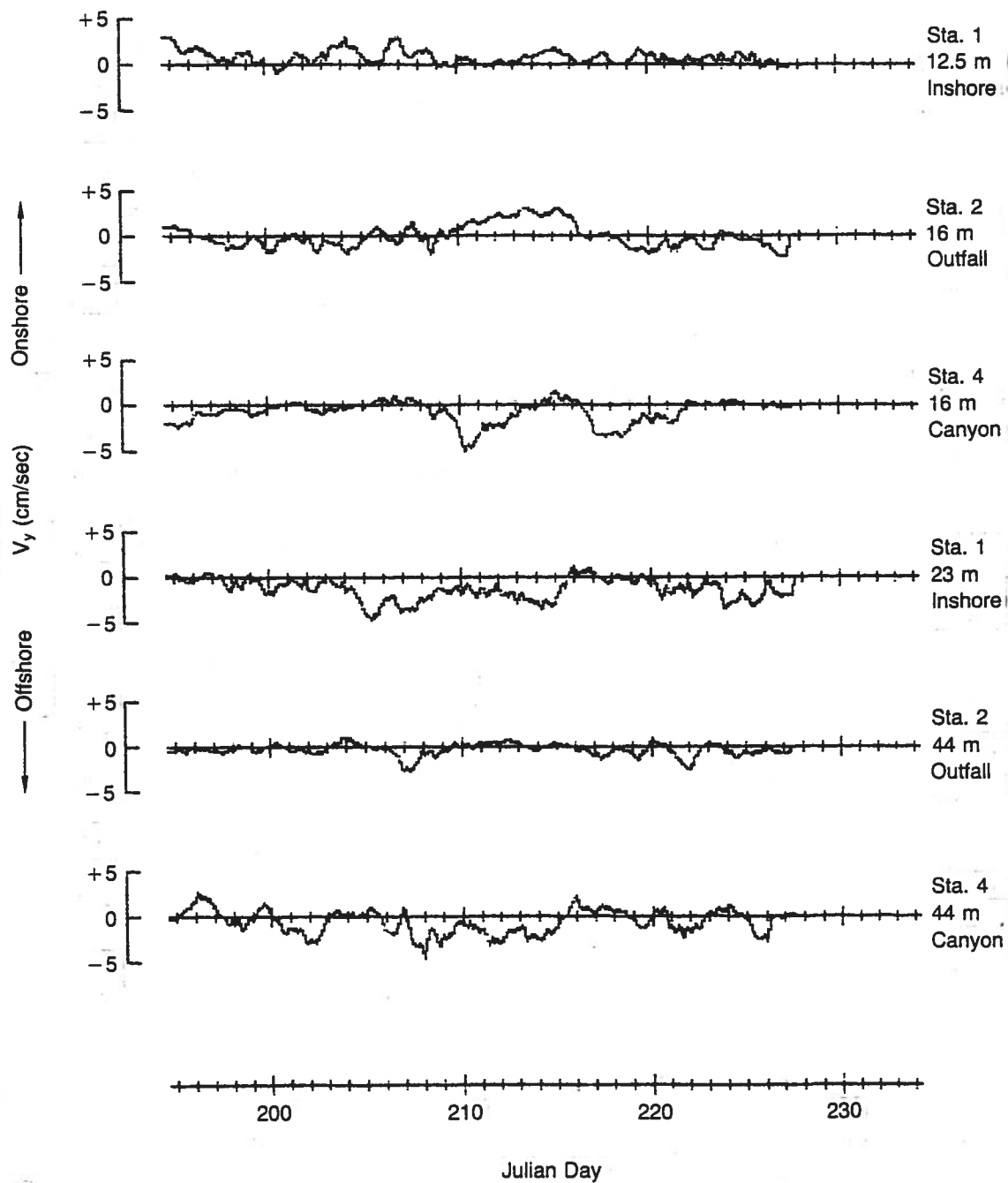


Fig 5b – Cross-shore Component of the Currents, Encina, 7/13 – 8/15/86
 (+ = Onshore, - = Offshore)

LONGSHORE
MIDWATER
7/13 - 8/15/86

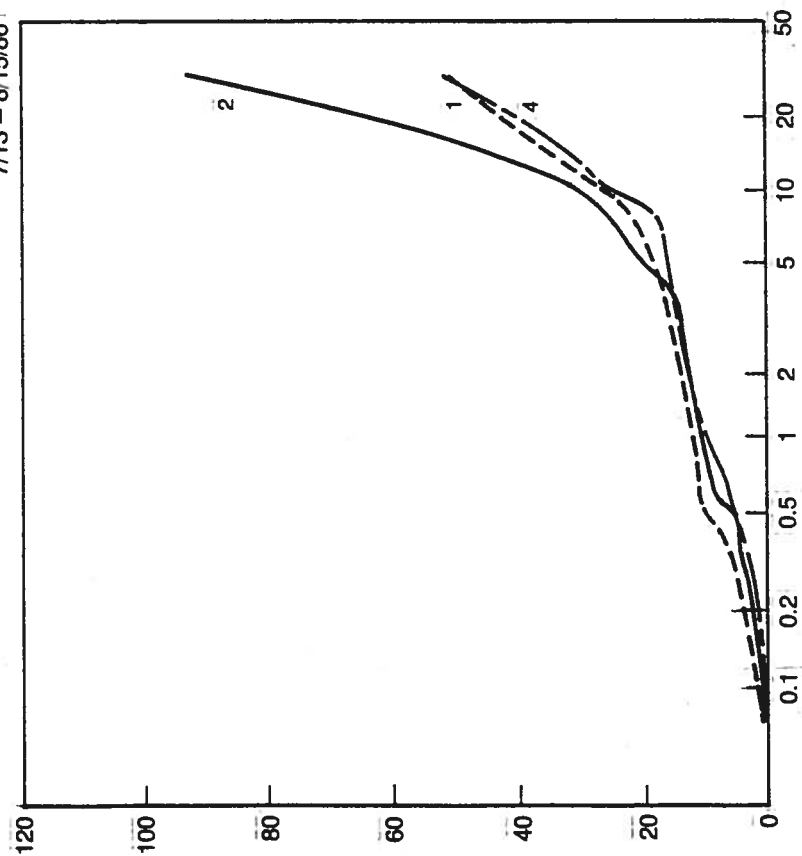


Fig 6(a). Cumulative variance for
longshore mid-water currents
7/13 - 8/15/86.

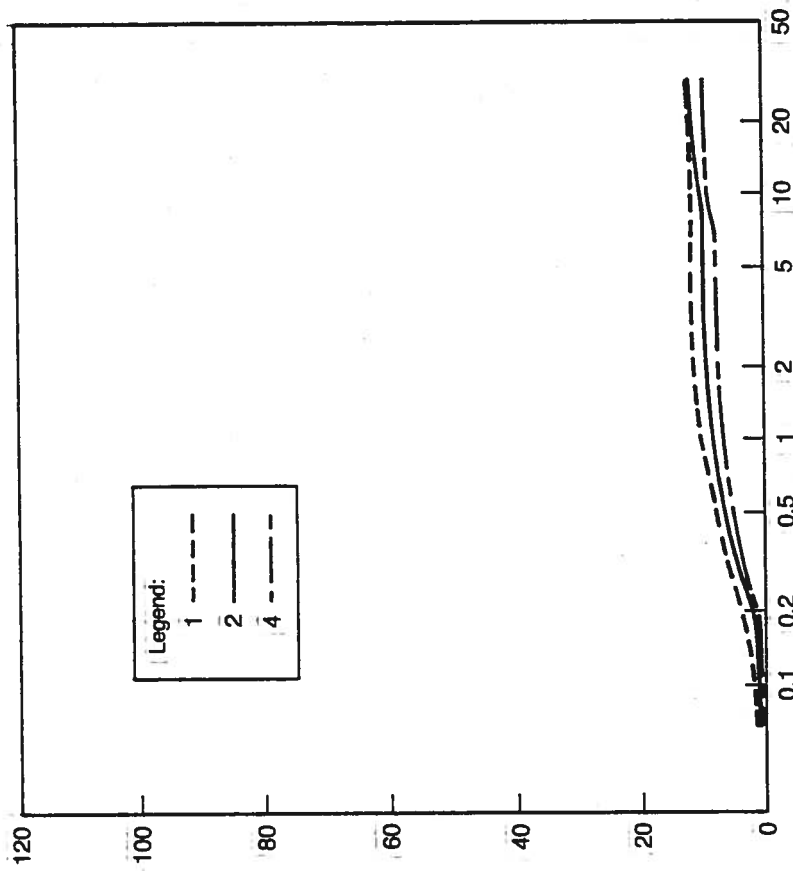


Fig 6(b). Cumulative variance for
cross-shore mid-water currents
7/13 - 8/15/86.

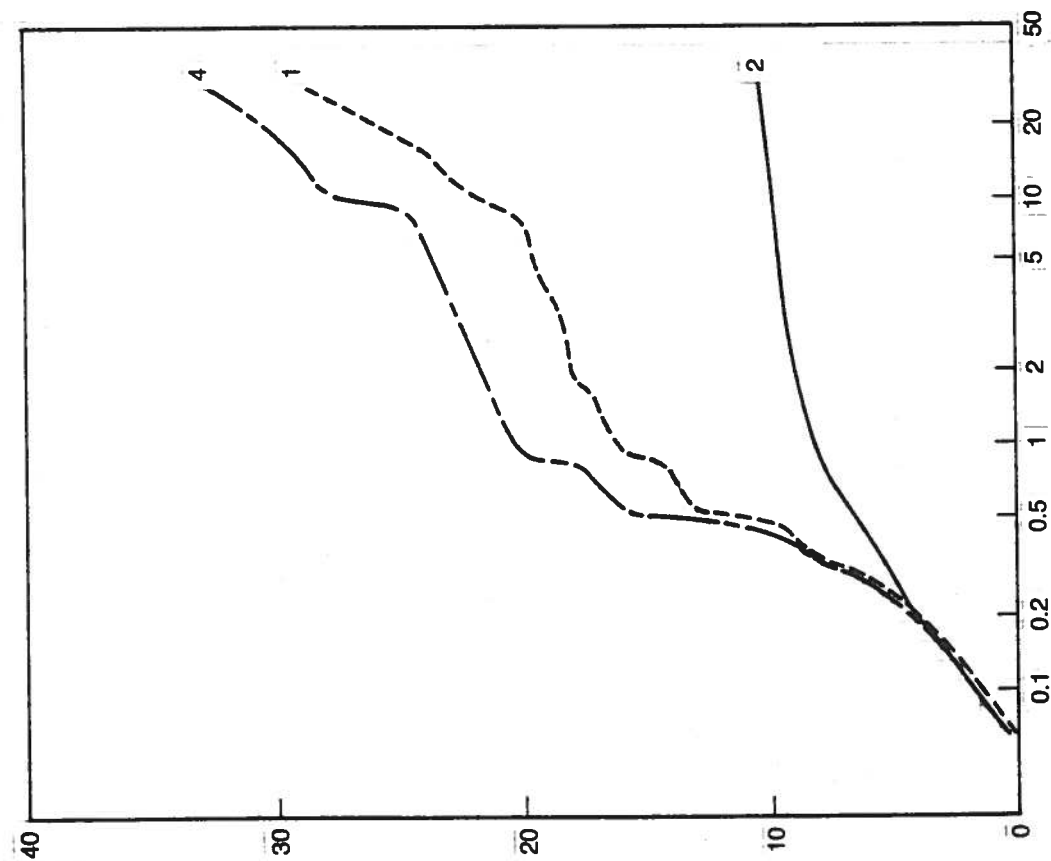


Fig 7(a). Cumulative variance for longshore near bottom currents 7/13 - 8/15/86.

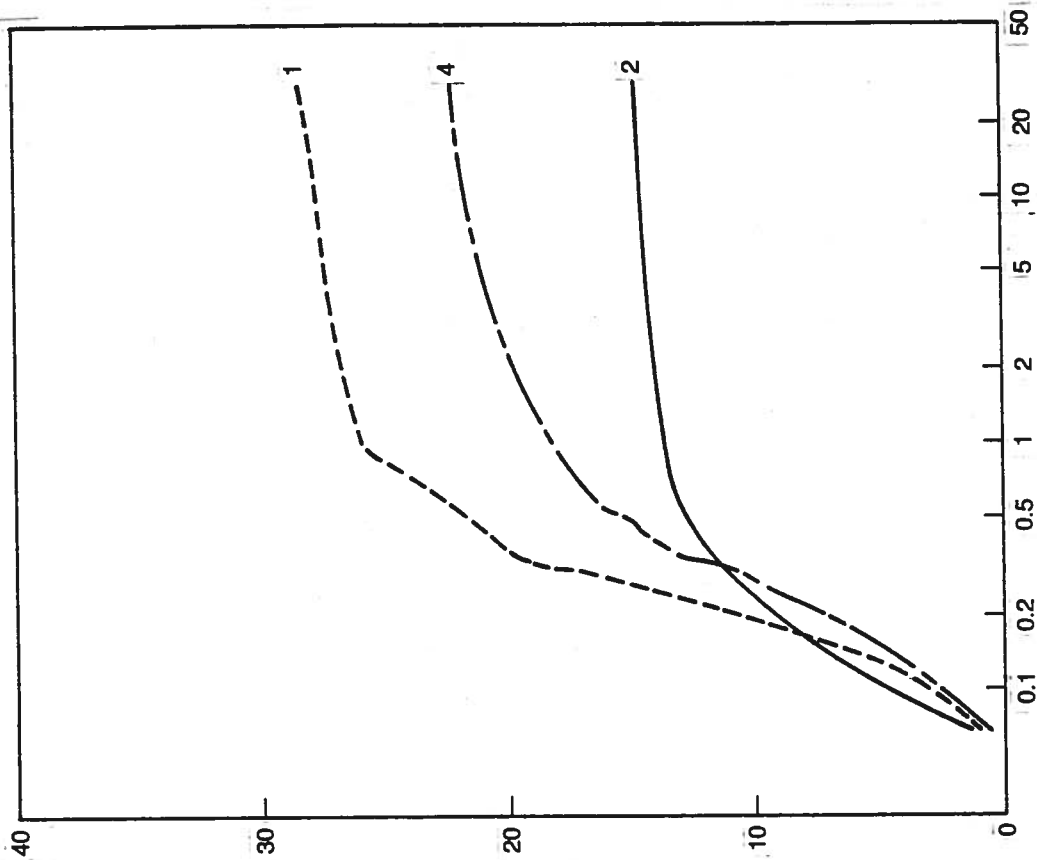


Fig 7(b). Cumulative variance cross-shore near bottom currents 7/13 - 8/15/86.

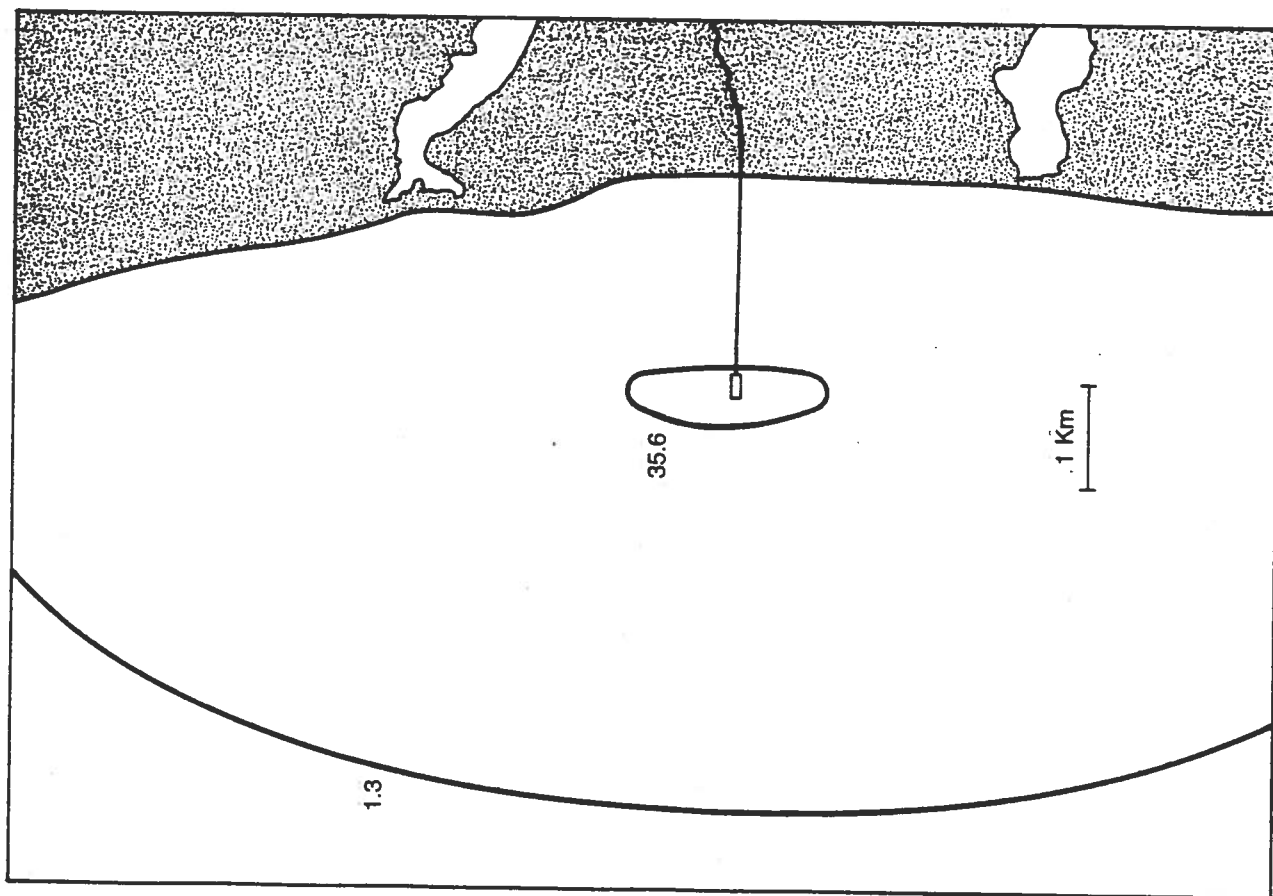


Fig 8. Sedimentation flux for 35m waste field using EPA model.

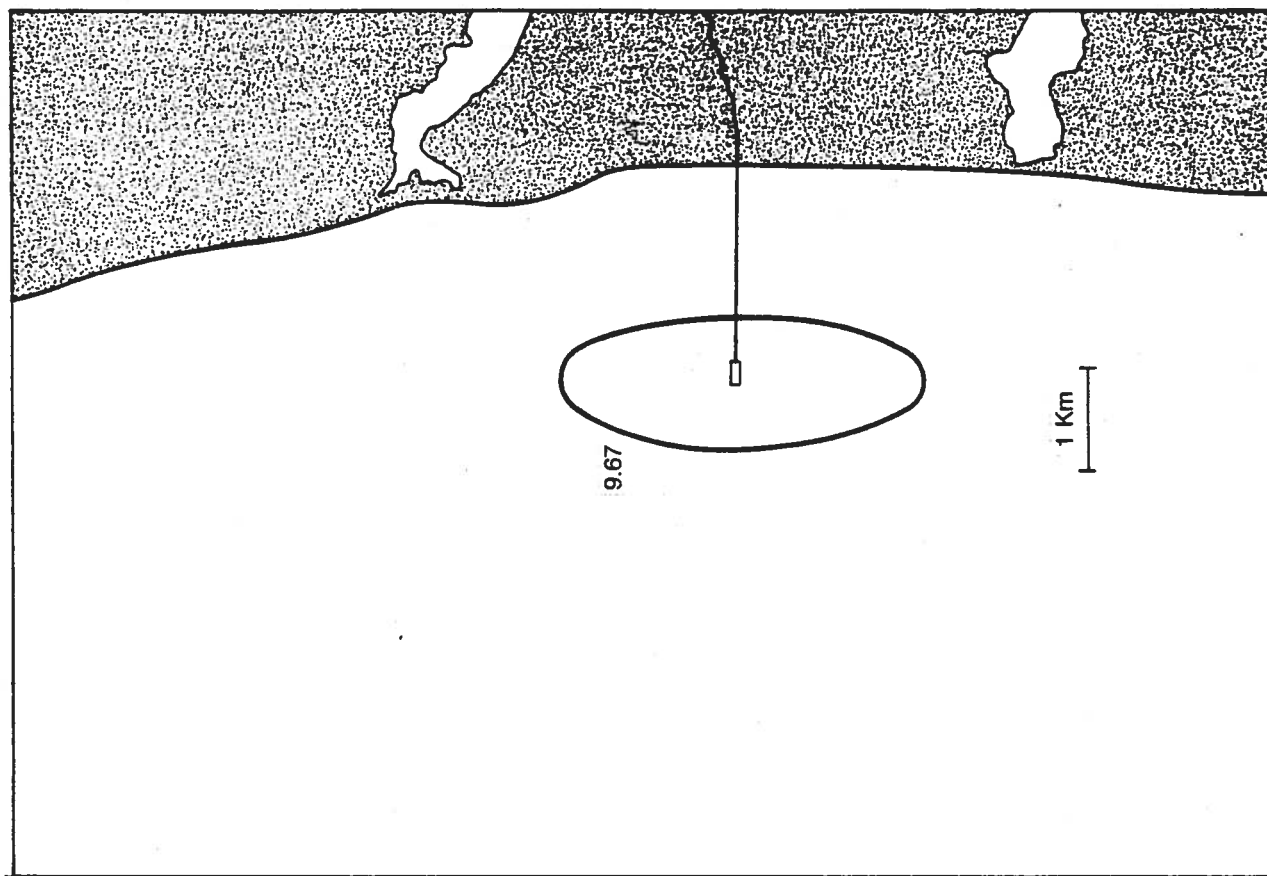


Fig 9. Sedimentation flux for 25m waste field using EPA model.

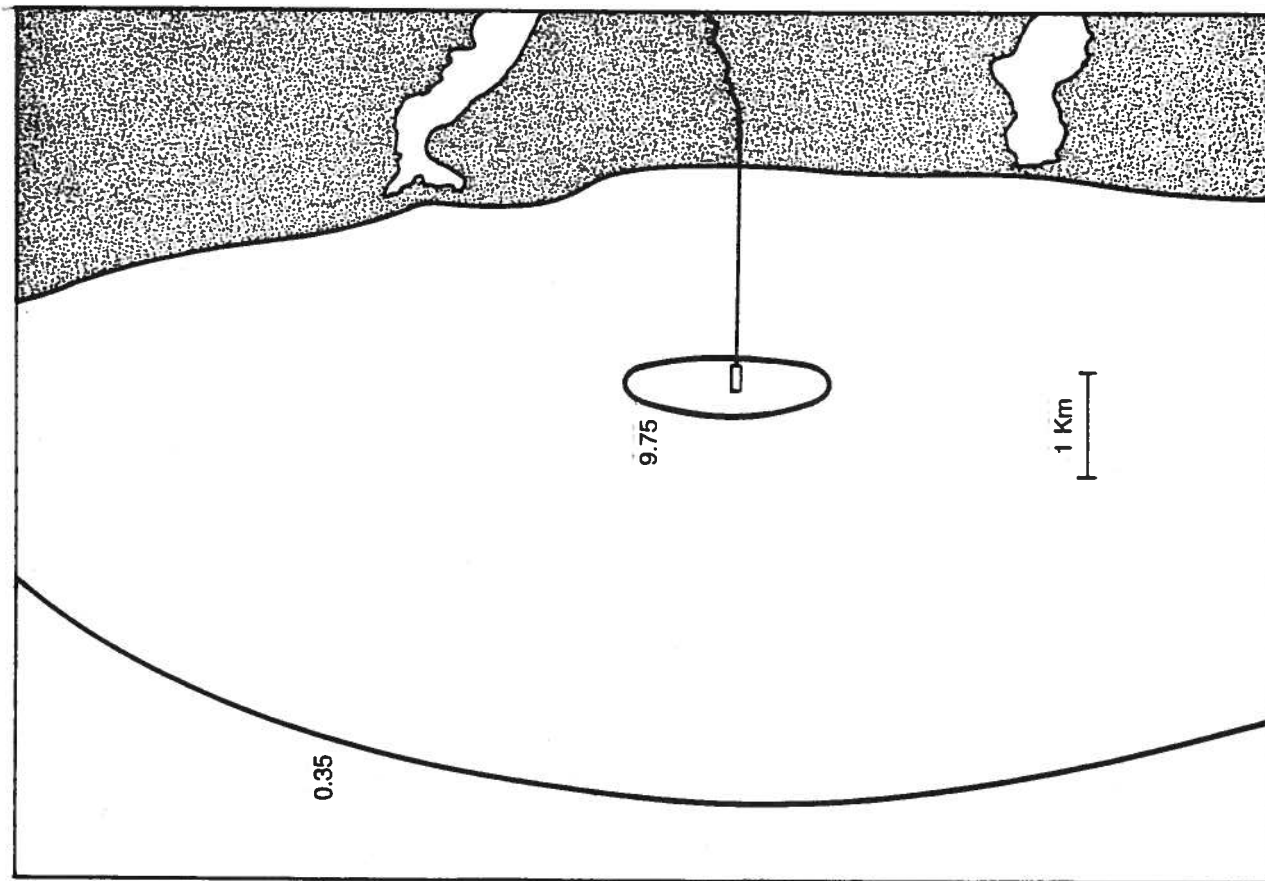


Fig 10. Sedimentation accumulation for 35m waste field using EPA model.

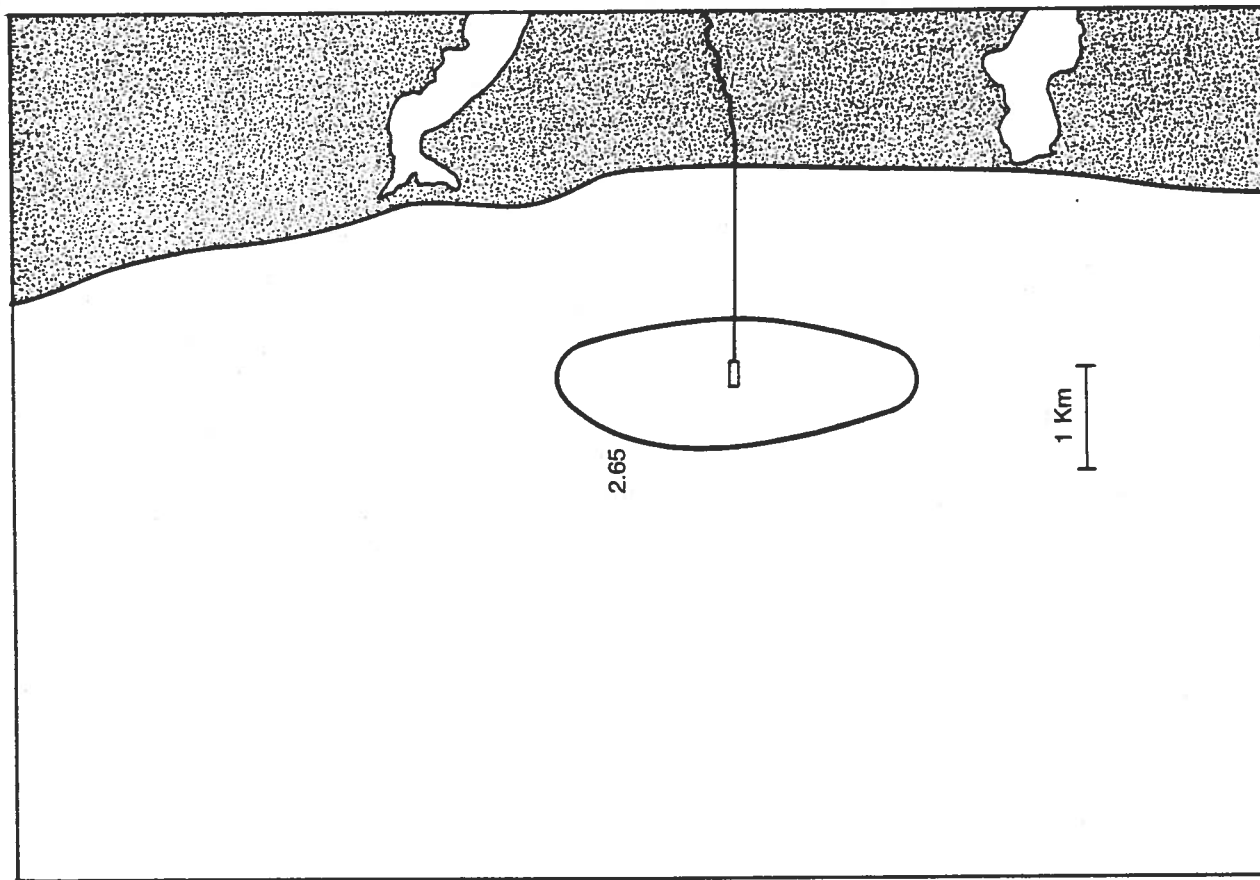


Fig 11. Sedimentation accumulation for 25m waste field using EPA model.

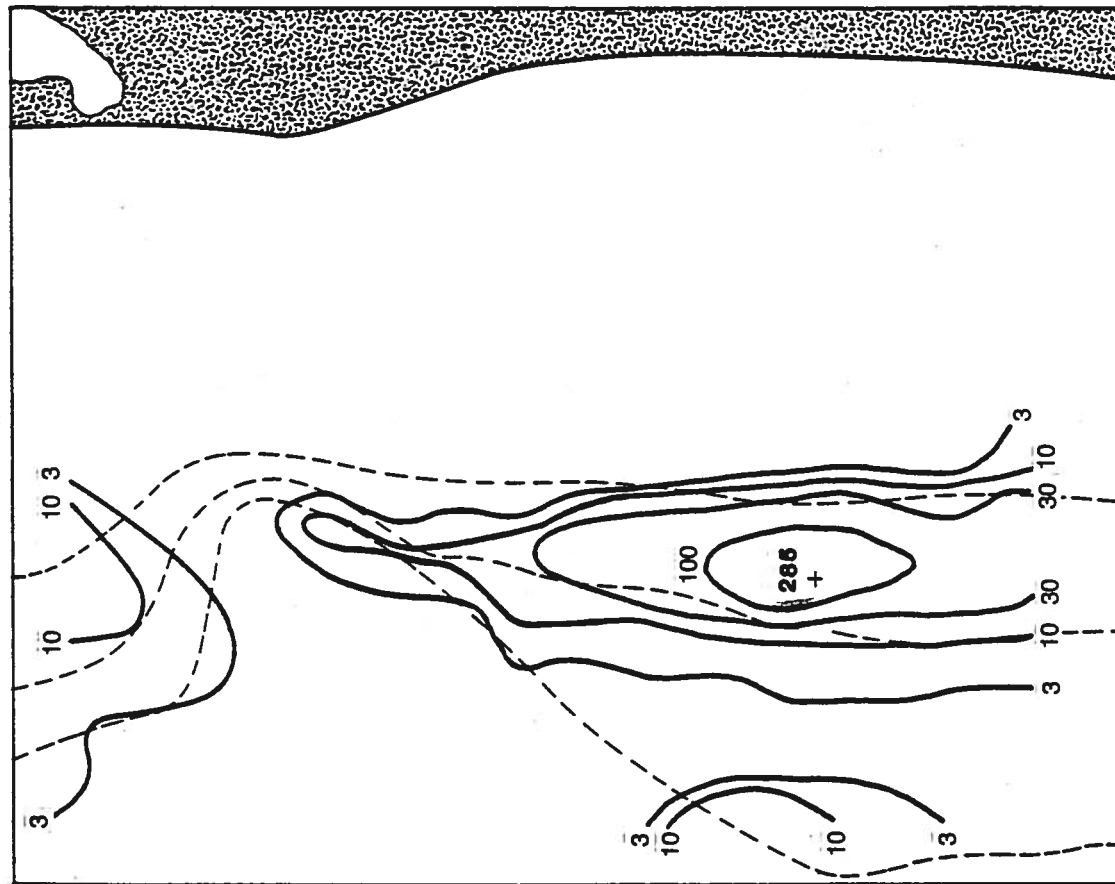


Fig 12. Sedimentation flux for 35m waste field using SEDF2D for July 13 to August 15, 1986.

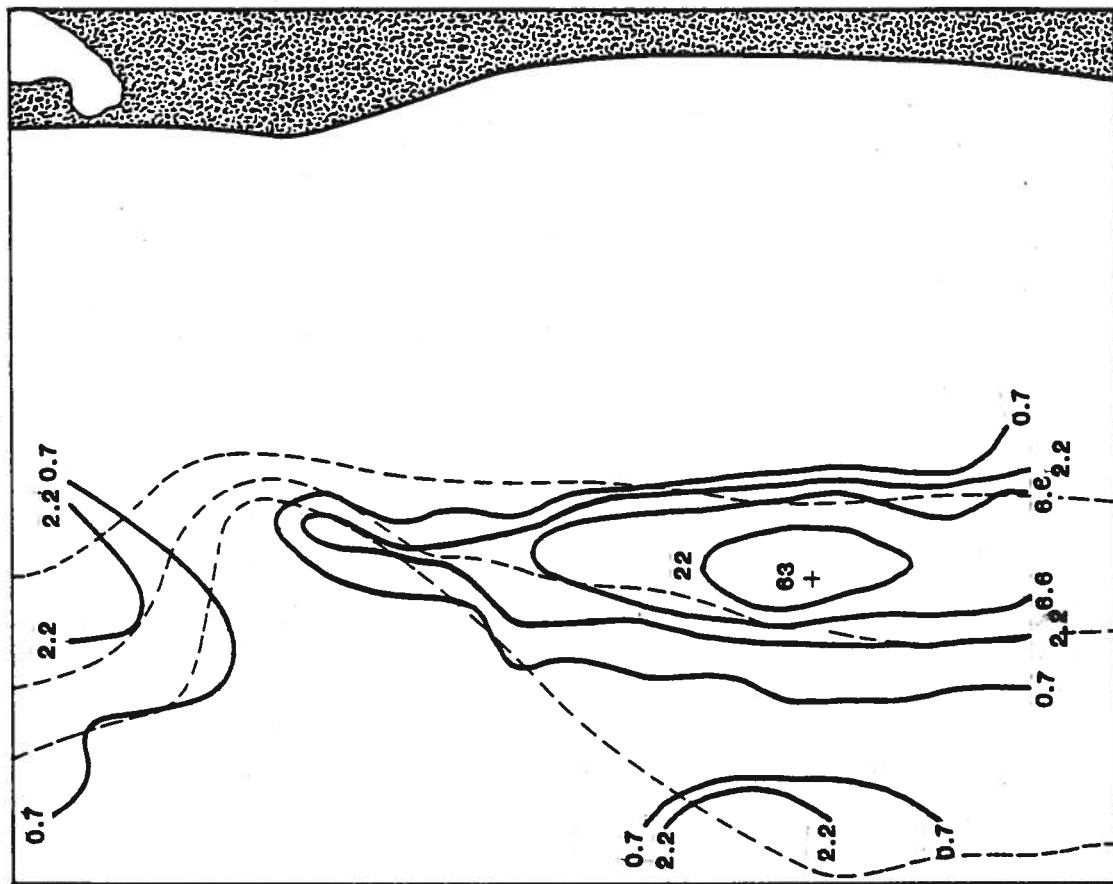


Fig 13. Sedimentation accumulation for 35m waste field using SEDF2D for July 13 to August 15, 1986.

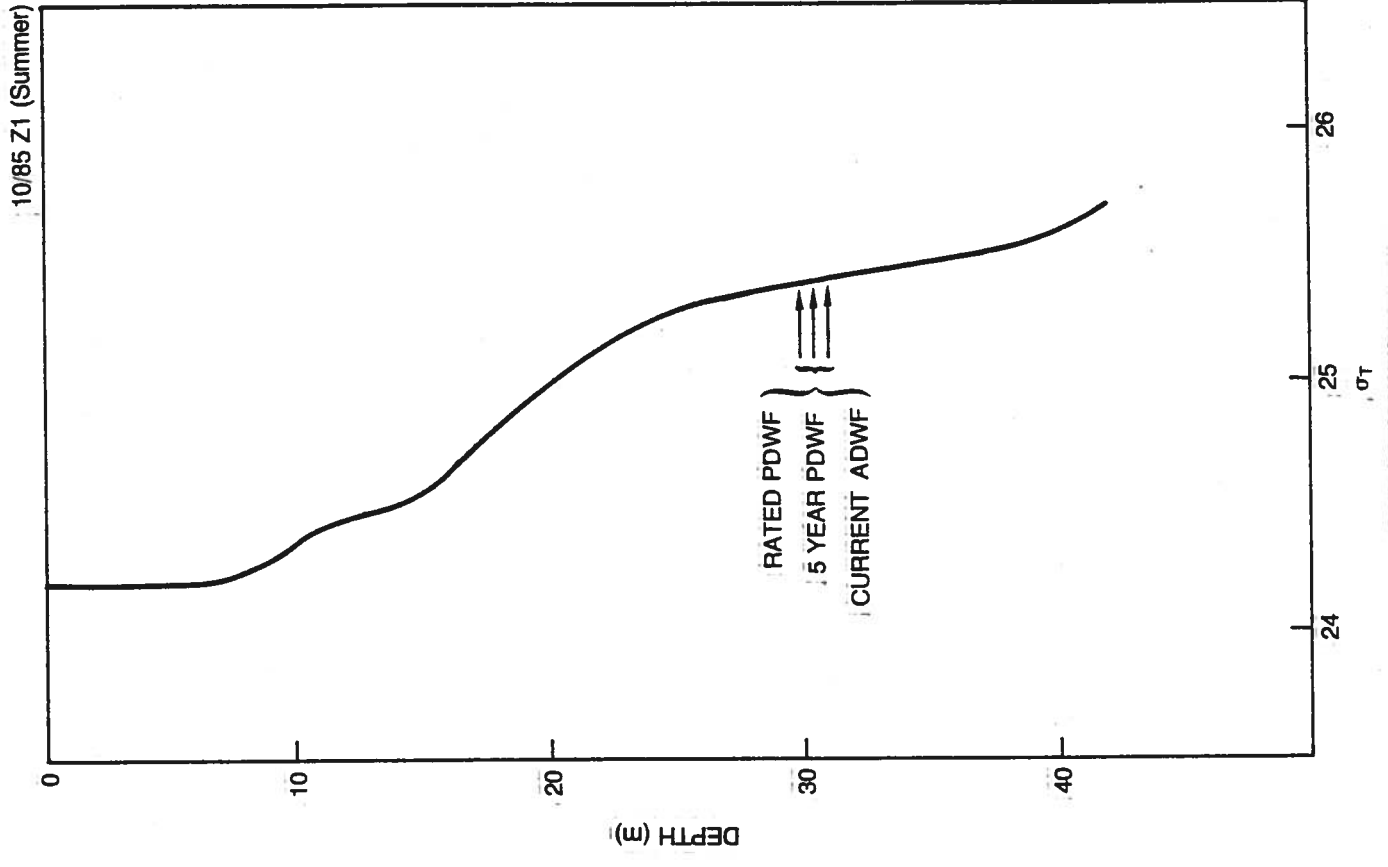


Fig 15. Density profile for Oct 1985.

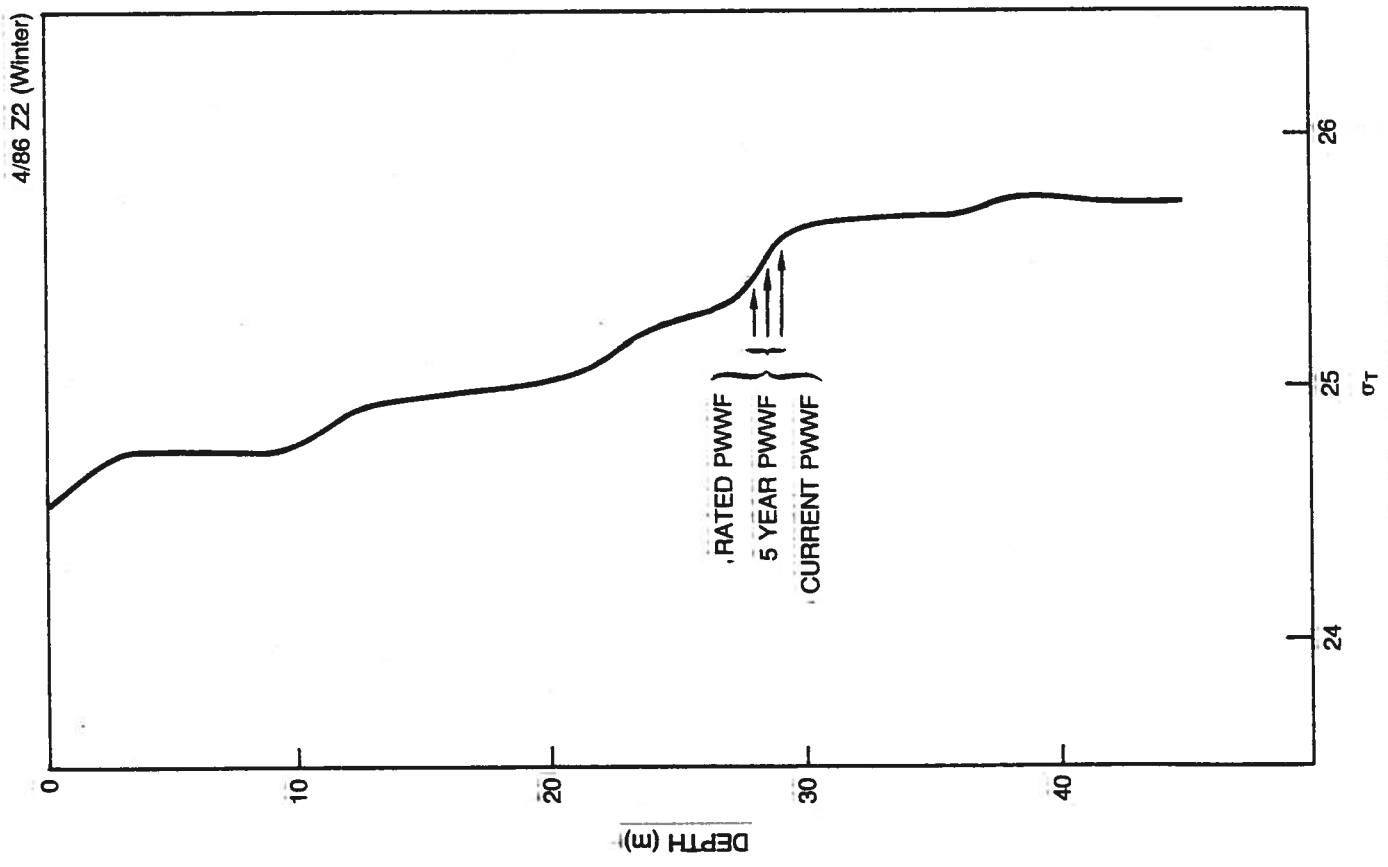


Fig 14. Density profile for April 1985.

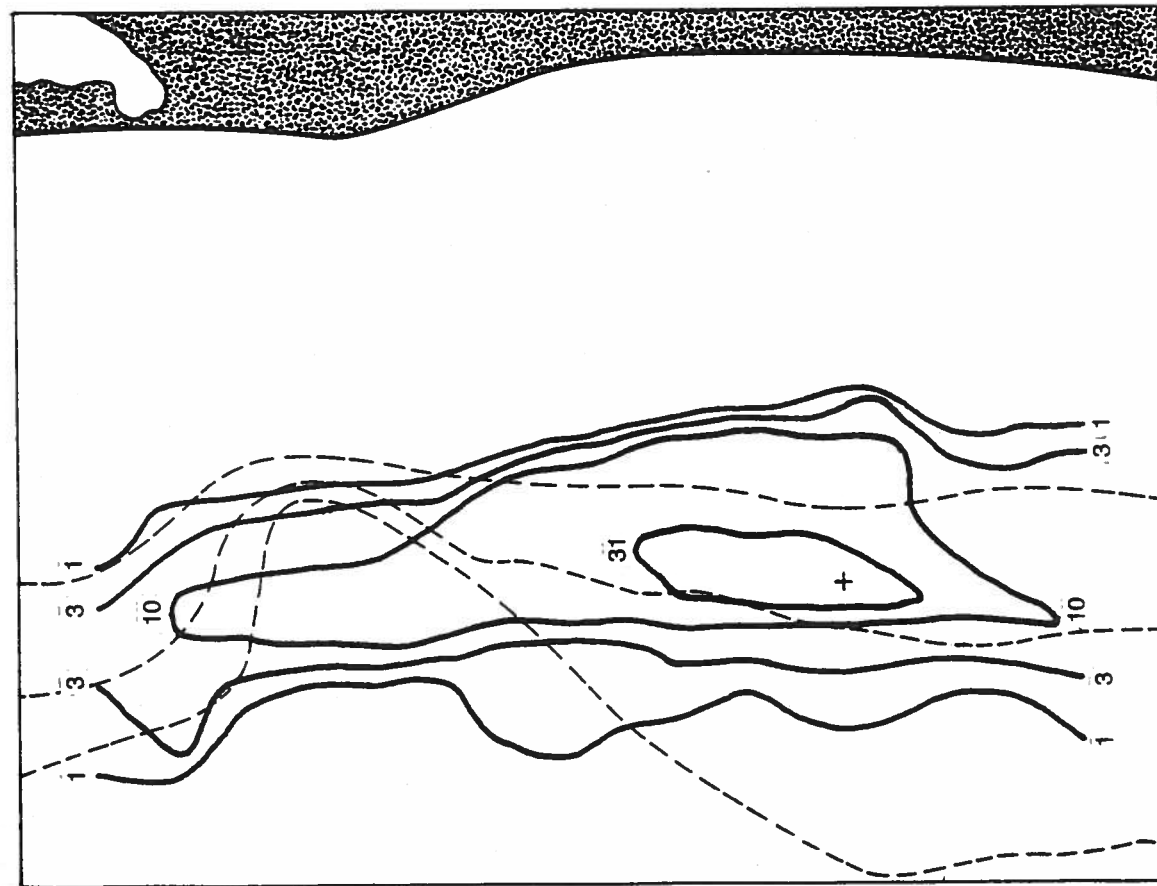


Fig 16(a). Probabilities from PXYT2D after 6 hours for 25m wastefield for August 15 to September 18, 1986

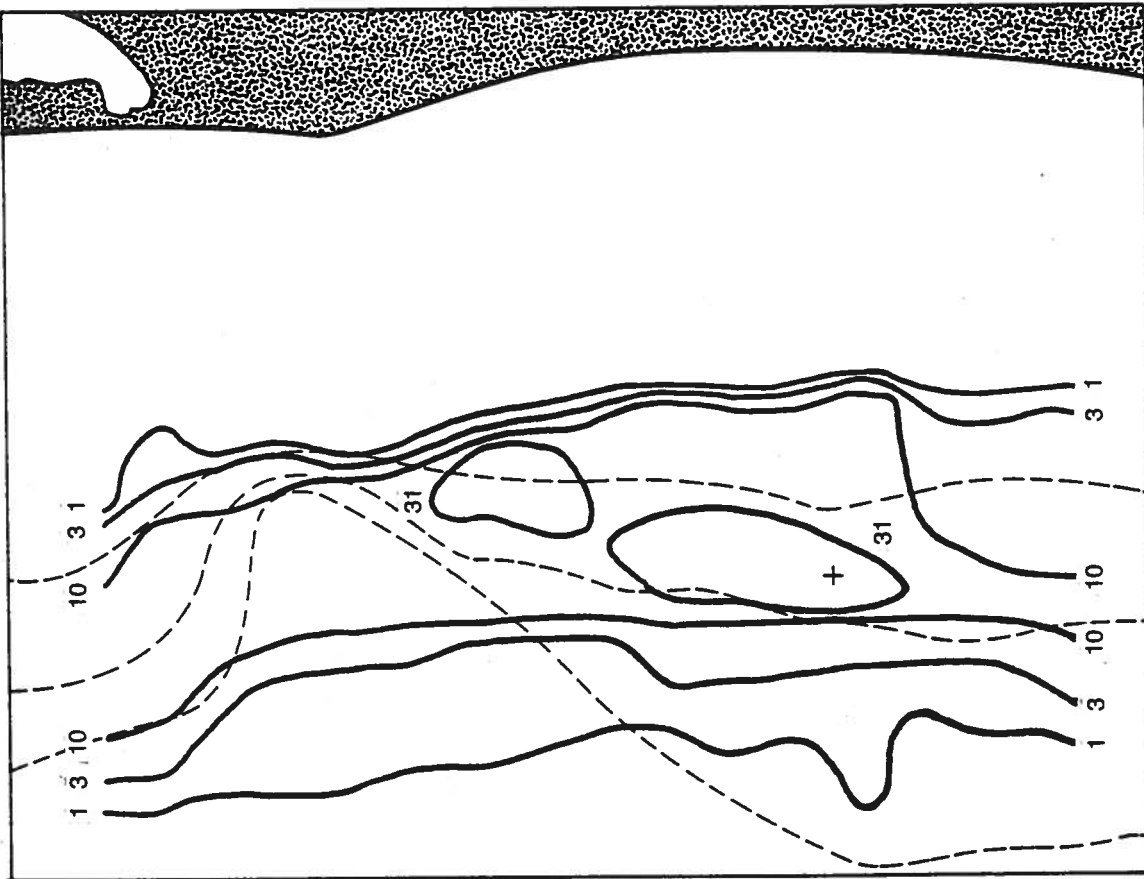


Fig 16(b). Probabilities from PXYT2D after 12 hours for a 25m wastefield for August 15 to September 18, 1986

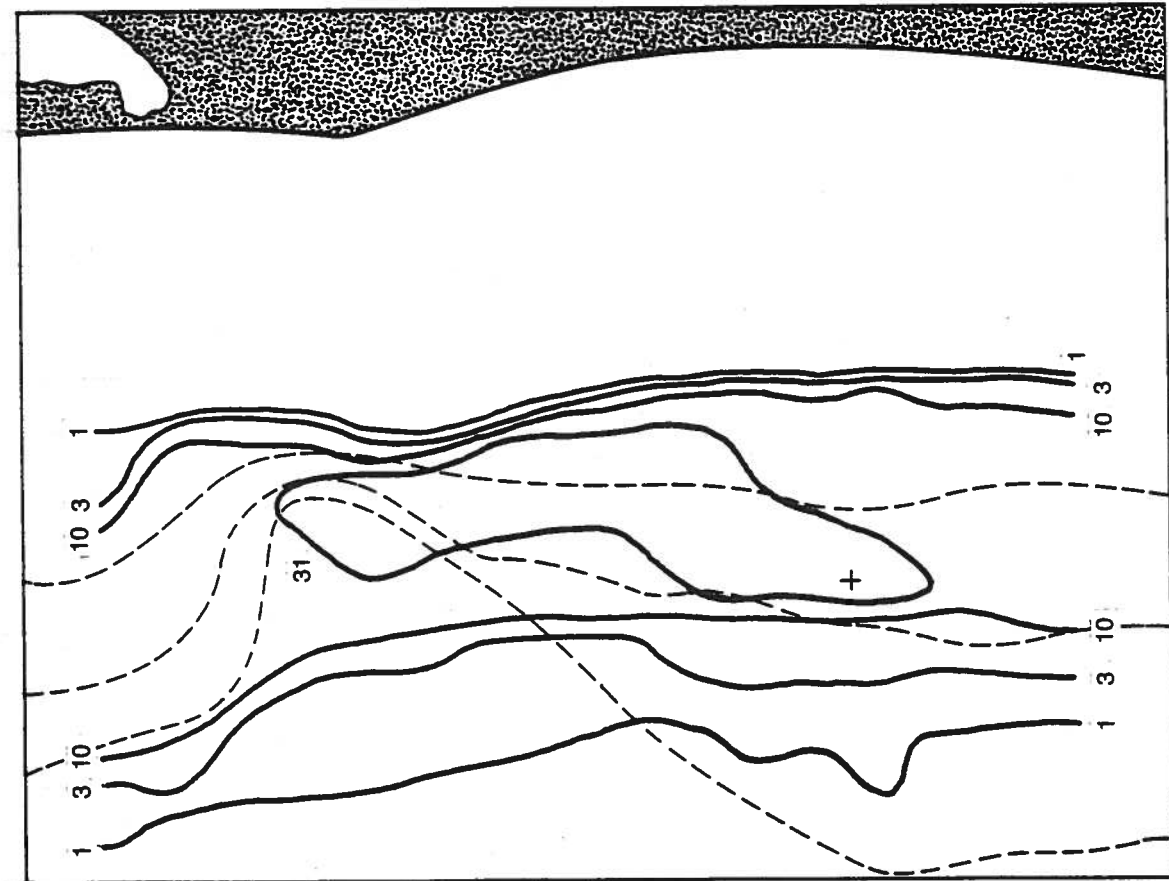


Fig 16(c). Probabilities from PXYT2D after 24 hours for a 25m wastefield for August 15 to September 18, 1986

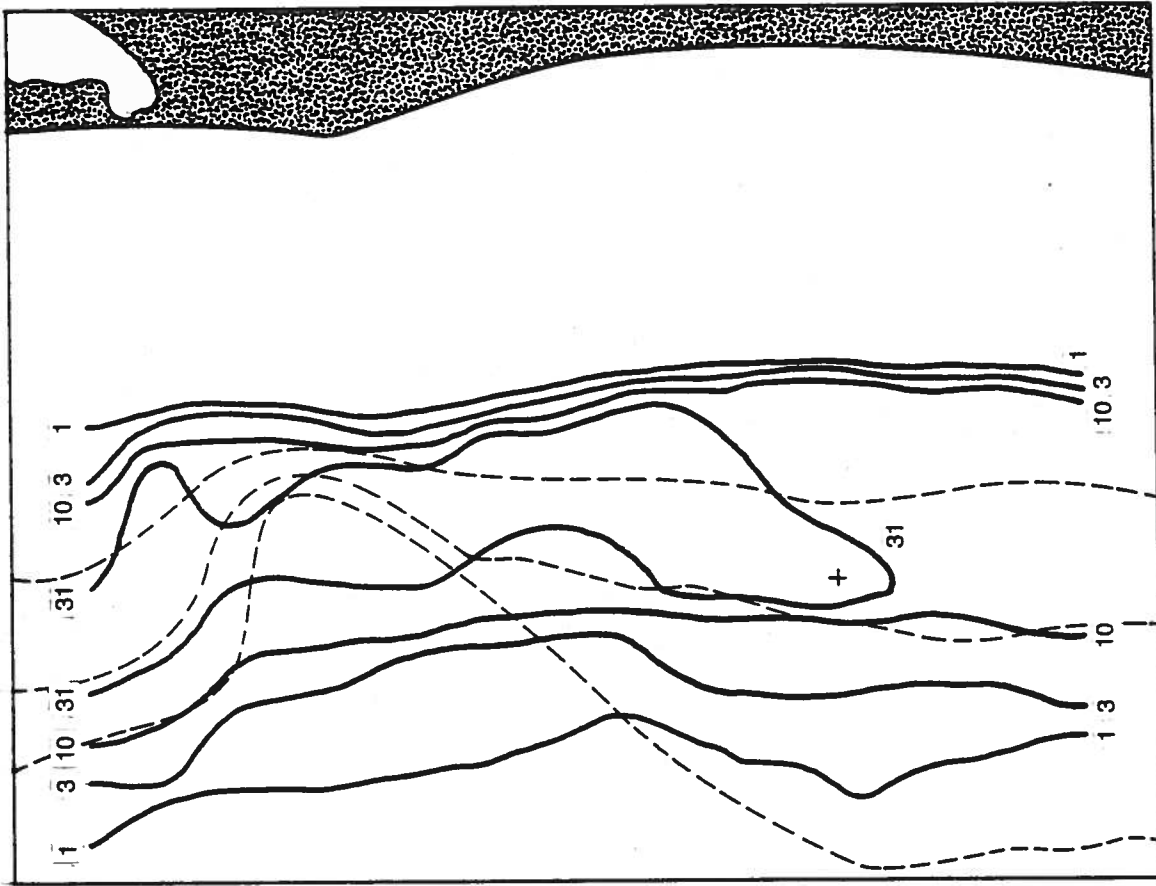


Fig 16(d). Probabilities from PXYT2D after 48 hours for a 25m wastefield for August 15 to September 18, 1986

APPENDIX A

PROBABILITY OF FLOW BY SPEED AND DIRECTION

Matrix numbers represent the number of observations.

[illegible]

STATION 1 (INSHORE)
12.5/25M - WINTER

SPEED/DIRECTION PROBABILITY MATRIX (NO. OCCURRENCES/ELEMENT)

DIR (M)	SPEED CM/SEC																				DIR PROB
	0	2	4	6	8	10	12	14	16	18	20	22	24	26	28	30	32	34	36	38	
0	2	3	5	3	5	1	.	1013
10	.	4	5	4	3	5013
20	1	2	6	4	3	.	.	1011
30	.	2	5	1	4	.	1008
40	2	6	2	6	1	.	1012
50	2	5	6	4	4	1014
60	.	1	4	5	4	1	1010
70	1	3	3	6	5	2	2014
80	.	3	5	11	3	2	2	1017
90	1	1	6	9	6	6	1	.	1020
100	2	1	5	9	3	3	2016
110	1	3	5	6	6	2015
120	.	4	.	11	5	4	1016
130	.	7	8	9	5	3	1	2	1023
140	.	6	4	8	2	2	2015
150	2	3	5	9	7	1	1	3020
160	1	2	6	9	7	4	6	1023
170	.	1	2	10	10	3	2	1	1019
180	.	6	8	10	6	13	3	.	1030
190	.	4	6	11	7	5	1	.	3024
200	.	2	5	11	7	5	1	1021
210	1	1	5	21	6	2	3025
220	.	6	6	16	7	3024
230	2	3	8	13	7	3	2024
240	1	4	4	14	10	4	3	.	.	.	1026
250	.	9	8	18	6	11	3035
260	2	6	8	17	15	6	1	5	3	.	1	.	.	.	1	1042
270	1	4	8	30	26	15	4	6	1	1	1062
280	2	6	10	27	26	28	11	9	11	5	3088
290	.	6	12	22	26	18	12	10	12	1	2	1	1	.	1080
300	3	4	23	27	37	25	13	4	4	.	2	2	.	1	.	.	.093
310	.	5	6	19	17	9	5	4	3	2	3	2	1	.	1	1050
320	.	4	11	16	13	6	1	.	1	1	.	1	.	.	.	1	.	.	.	1	.036
330	1	4	8	15	11	2	3	.	1	.	.	1	.	1	.	.	.	1	.	.	.031
340	.	2	7	9	6	2	1	.	1018
350	.	1	4	3	3	1	.	1008

SPD	.018	.147	.204	.058	.029	.008	.002	.003	0.000	.001	0.000	0.000	.002
PRB	.086	.271	.127	.032	.006	.003	0.000	.003	0.000	0.000	.001	0.000	

STATION 1 (INSHORE)
23/25M - WINTER

		SPEED CM/SEC																										
DIR		0	2	4	6	8	10	12	14	16	18	20	22	24	26	28	30	32	34	36	38	40	42	44	46	48	DIR	
(M)		1	3	5	7	9	11	13	15	17	19	21	23	25	27	29	31	33	35	37	39	41	43	45	47	49	PROB	
0	0	.	1	12	3	4	3	1	0.018	
10	.	.	4	4	8	6	0.018	
20	.	.	10	8	9	0.020	
30	.	2	4	2	5	1	1	0.011	
40	1	.	6	4	9	1	.	1	0.016	
50	.	2	6	7	4	1	0.015	
60	1	.	7	4	3	.	1	1	0.012	
70	.	3	8	10	4	1	2	0.020	
80	.	3	5	5	12	1	.	1	0.020	
90	.	2	4	12	9	1	0.020	
100	1	2	5	10	10	5	1	1	0.026	
110	.	1	6	6	12	4	1	1	.	1	0.023	
120	1	2	16	11	20	19	5	1	2	0.057	
130	2	1	6	11	20	28	20	19	5	5	2	3	1	0.091	
140	.	1	9	7	16	15	20	30	11	10	11	3	5	.	1	0.102	
150	.	1	6	6	11	5	7	11	11	10	3	1	3	.	1	0.056	
160	1	.	3	4	10	2	1	.	2	0.017	
170	.	.	4	3	5	1	1	1	0.011	
180	.	3	6	3	2	0.010	
190	.	2	4	2	2	.	1	0.008	
200	.	2	6	5	3	0.012	
210	1	.	2	4	1	1	0.007	
220	.	1	3	4	3	0.008	
230	.	.	5	2	1	1	0.007	
240	1</																											

SPD	.007	.156	.227	.083	.040	.015	.010	.002	0.000	0.000	0.000	0.000	0.000
PKB	.027	.159	.135	.092	.035	.008	.001	0.000	0.000	0.000	.002	0.000	

STATION 2 (OUTFALL)
20/46M - WINTER

DIR (M)	SPEED CM/SEC																				DIR PROB					
	0	2	4	6	8	10	12	14	16	18	20	22	24	26	28	30	32	34	36	38		40	42	44	46	48
***	1	3	5	7	9	11	13	15	17	19	21	23	25	27	29	31	33	35	37	39	41	43	45	47	49	****
0	1	8	19	19	10	5	1	2	1	.025
10	1	5	15	14	7	2	2	2018
20	.	9	9	18	6	3	1	.	2018
30	2	11	14	21	7	4	2022
40	1	10	12	14	12	3	.	1	1020
50	2	3	16	19	9	3017
60	3	7	13	17	18	4	2	.	1024
70	.	2	10	21	12	5	.	2019
80	.	7	13	22	7	5	2	1	2022
90	3	9	14	25	17	12	4	4	4	.	1034
100	.	7	7	18	18	12	3	6	2	1027
110	.	2	10	15	6	6	2	4017
120	3	3	15	9	8	6	2	3	1	.	1019
130	.	6	11	7	6	.	.	2	.	1	.	1012
140	1	5	4	13	3	.	1	1	.010
150	.	5	9	11	3	.	1	1	.011
160	1	2	10	6	2	.	1	1008
170	.	2	8	8	2	2	.	.	1008
180	1	5	12	8	2	2016
190	.	3	6	12	4	1013
200	1	5	9	12	4	2	2013
210	2	8	15	9	7	2	2	.	1017
220	.	3	6	12	1	1	1	2010
230	.	1	5	14	7	4	1	3	.	1013
240	1	3	12	16	9	9	5	3	6	2	2	2	2	.	.	1027
250	1	6	6	15	12	9	8	17	14	6	6	2	1													

SPD	.011	.181	.175	.060	.033	.013	.003	.002	0.000	.001	0.000	0.000	.001
PRB	.081	.263	.102	.054	.013	.004	.001	.001	0.000	.000	0.000	0.000	

STATION 2 (OUTFALL)
44/46M - WINTER

[illegible][illegible]

STATION 4 (CANYON)
20/46M - WINTER


```

.....SPEED CM/SEC.....
DIR    0  2  4  6  8 10 12 14 16 18 20 22 24 26 28 30 32 34 36 38 40 42 44 46 48    DIR
(M)    1  3  5  7  9 11 13 15 17 19 21 23 25 27 29 31 33 35 37 39 41 43 45 47 49    PROB
***    .....*****

```

	.017	.352	.091	.025	.017	.006	.001	.001	0.000	.000	0.000	0.000	.001
SPD													
PKB	.156	.260	.050	.013	.006	.002	0.000	.001	0.000	0.000	0.000	0.000	

STATION 4 (CANYON)
44/46M - WINTER

SPEED/DIRECTION PROBABILITY MATRIX (NO. OCCURRENCES/ELEMENT)

DIR (M)	SPEED (KNOTS)																				DIR PROB
	0	2	4	6	8	10	12	14	16	18	20	22	24	26	28	30	32	34	36	38	
0	2	4	8	10	8	4	4	3037
10	2	5	6	7	6	5	3030
20	1	7	9	7	5	1	1	2029
30	1	3	4	3	3	2	.	1015
40	1	6	2	1	2	4014
50	1	4	6	5	3	1	.	1018
60	4	2	9	1	.	3	.	1017
70	2	.	4	3	3	.	1011
80	1	1	2	1004
90	.	.	4	.	5	1009
100	1	4	4	2	4	2015
110	1	2	6	6	4	4	1021
120	2	4	4	3	8	6	1024
130	2	1	11	13	22	15	5066
140	3	8	12	4	10	17	5	8	3	3064
150	.	3	7	3	8	9	5	1	3	2	1	.	2038
160	.	4	6	2	5	5	3	2	3	1	.	2029
170	1	4	4	1	3	.	4	2	1	1	2	2	.	.	1023
180	6	3	3	5	4	1	1	.	1021
190	.	2	3	2	4016
200	1	1	4	1	1007
210	1	2	7	5	2015
220	1	2	5	3	1	1011
230	2	1	3	2	1008
240	2	2	2	3008
250	.	1	6	4	1	1011
260	.	2	6	4	1	1012
270	2	3	4	.	.	3010
280	1	3	11	8	4	2025
290	.	4	13	8	6	2029
300	1	8	10	9	12	8	4045
310	1	5	10	8	20	15	6	5051
320	.	7	13	10	17	20	15	6	3	.	1080
330	1	9	13	9	24	13	9	7	2	1077
340	3	4	13	12	15	17	8	9	2072
350	1	1	10	7	9	8	5	2	2039

*** **

SPD	.042	.213	.193	.071	.017	.003	.002	.001	0.000	0.000	0.000	0.000	0.000
PRB	.106	.150	.149	.044	.007	.003	0.000	0.000	0.000	0.000	0.000	0.000	0.000

STATION 1 (INSHORE)
12.5/25M - SUMMER

SPEED/DIRECTION PROBABILITY MATRIX (NO. OCCURRENCES/ELEMENT)

		SPEED CM/SEC																					
DIR	0 2 4 6 8 10 12 14 16 18 20 22 24 26 28 30 32 34 36 38 40 42 44 46 48	DIR																					
(N)	1 3 5 7 9 11 13 15 17 19 21 23 25 27 29 31 33 35 37 39 41 43 45 47 49	PROB																					
***		*****																					
0	. . 0 13 3 2 .																						

*** **

SPD .002 .173 .200 .027 .013 .005 0.000 .001 0.000 0.000 0.000 0.000 .001
 PRR .033 .435 .088 .020 .002 0.000 0.000 0.000 0.000 0.000 0.000 0.000

STATION 1 (INSHORE)
 23/25M - SUMMER

		SPEED CM/SEC																								
DIR	0	2	4	6	8	10	12	14	16	18	20	22	24	26	28	30	32	34	36	38	40	42	44	46	48	VIR
(M)	1	3	5	7	9	11	13	15	17	19	21	23	25	27	29	31	33	35	37	39	41	43	45	47	49	PROB
***																										****
0	.	1	15	18	11	6	.	3	.	.	L026
10	.	.	26	11	12	3	1022
20	.	.	13	9	9	2	1016
30	1	.	17	6	3	2014
40	.	.	18	3	3011
50	.	1	8	6	1	1	.	1008
60	.	.	14	4	4	1011
70	.	.	16	6	1	3009
80	.	.	3	7	3	.	1007
90	.	.	7	9	6	3012
100	.	1	3	7	5	2	1009
110	.	.	10	11	13	7	.	1026
120	.	.	5	8	11	23	13	1029
130	.	.	1	9	17	27	29	24	10	8	1059
140	.	.	4	5	13	23	14	31	8	7	.	1050
150	.	.	2	7	15	20	15	11	1	1	1034
160	2	.	3	8	15	13	3	6	.	1	.	1024
170	.	.	2	6	8	2008
180	.	.	2	2	8	3	1007
190	.	2	2	4	4006
200	.	.	1	1	4	1003
210	.	1	3	4	3	1006
220	.	.	4	2	4	1005
230	.	3	7	3	1	1067
240	.	1	5	6066
250	.	.	4	6	1067
260	.	2	8																							

	SFD	PRB	0.002	.126	.195	.121	.037	.016	.007	.007	.000	.006	0.000	0.000	0.000	0.000
			.009	.140	.187	.097	.034	.007	.000	.003	0.000	.000	.006	0.000		

STATION 2 (OUTFALL)
16/46M - SUMMER

SPEED/DIRECTION PROBABILITY MATRIX (NO. OCCURRENCES/ELEMENT)

		SPEED CHASE																																									
DIR	0	2	4	6	8	10	12	14	16	18	20	22	24	26	28	30	32	34	36	38	40	42	44	46	48	DIR																	
(M)	1	3	5	7	9	11	13	15	17	19	21	23	25	27	29	31	33	35	37	39	41	43	45	47	49	PROB																	
###	*****																																								*****		
0	1	4	11	4	4	1	1013																
10	1	6	3	4	4009																
20	.	5	7	3	3009																
30	1	4	6	2	1007																
40	1	3	8	4	1009																
50	1	5	3	1	1006																
60	.	5	8	5009																
70	1	5	3	4	1	1008																
80	.	3	6	6	2009																
90	.	8	8	7	5014																
100	2	7	10	10	4	1	2018																
110	.	6	12	6	4	1	2	.	.	1016																
120	1	1	5	6	6	4	.	3	1	1	.	.	1015																
130	1	4	6	7	3	8	5	5	1	2	4	1024																
140	.	5	5	14	14	9	10	7	4	2	2	2	2	.	.	1039																
150	1	5	6	15	12	9	3	2	6	3	4	2	1	1035																
160	3	7	5	9	8	7	5	4	9	1	4	1	1	.032																
170	2	6	7	7	5	5	2	4	1	1	2	.	.	.	1022																
180	.	7	3	7	3	3	3013																
190	1	4	7	4	3	1	1011																
200	1	2	5	2	.	.	1	.	1006																
210	1	2	4	1	1005																
220	.	2	10	1007																
230	.	5	1	1004																
240	.	6	6006																
250	2	7	1	.	1006																
260	.	3	4	3	1	1006																
270	.	7	6	7	2	4	3	3	3	1	3	4	.	.	1022																
280	3	4	12	10	13	14	13	8	10	3	5	3	1	1	.	2	.	.	1	1	.052																
290	3	11	15	21	14	24	31	20	14	8	14	5	5	2	2	2	.	.	1	1	.097																
300	1	13	28	38	53	37	35	34	22	8	18	4	7	3	4	3	.	.	9	5	1	.163																
310	.	14	27	61	41	28	24	17	25	5	8	3	4	.	1	4	.	.	4	.	.	3	.	.	4	.138																	
320	.	13	22	42	27	9	7	3	8	4	5	1	3	.	2	.	.	.	1	1	.075																	
330	.	13	29	34	12	3	3	5	2	.	2	1052																
340	2	7	9	15	5	2	5	3024																
350	4	9	16	8	6	2023																

	.017	.163	.131	.078	.054	.036	.012	.006	0.000	.009	0.000	0.000	.005
PRB	.110	.186	.088	.059	.020	.013	.003	.006	0.000	.004	.002	0.000	

STATION 4 (OUTFALL)
16/46M - SUMMER

		SPEED CM/SEC																					
DIR	0 2 4 6 8 10 12 14 16 18 20 22 24 26 28 30 32 34 36 38 40 42 44 46 48	DIR																					
(M)	1 3 5 7 9 11 13 15 17 19 21 23 25 27 29 31 33 35 37 39 41 43 45 47 49	PROB																					
***		***																					

STATION 4 (CANYON)
44/46M - SUMMER

SPEED/DIRECTION PROBABILITY MATRIX (NO. OCCURRENCES/ELEMENT)

DIR (M)	SPEED CM/SEC																				DIR PRB
	0	2	4	6	8	10	12	14	16	18	20	22	24	26	28	30	32	34	36	38	
0	1	3	5	7	9	11	13	15	17	19	21	23	25	27	29	31	33	35	37	39	.015
10	1	3	7	5015
20	.	.	5	2	2008
30	.	2	5	1	2	2011
40	1	2	6	9	3	1020
50	.	2	3	10	2	2018
60	.	1	4	4	1	1016
70	.	5	6	4	1	1	2018
80	1	1	6	6013
90	1	2	5	5012
100	.	2	1	6	1	.	1016
110	.	4	3	6	2014
120	.	1	4	5	1016
130	.	2	3	3	2	1010
140	.	1	4	5	1016
150	.	3	3	6	1	1013
160	.	5	10	7	3	2025
170	.	1	6	4010
180	.	2	7	7	4	.	1019
190	1	.	4	5	6015
200	.	1	10	4	2	3	1019
210	.	2	2	8	5	1018
220	.	1	6	3	5014
230	.	1	3	4	4	4	1	.	1017
240	.	3	6	2	5	1	.	1018
250	.	5	4	4	2	6	2	3	2026
260	.	3	9	13	16	4	5	5	5050
270	.	1	10	9	13	10	14	7	1	1	1062
280	.	1	4	22	19	20	8	2	4074
290	.	2	10	16	21	19	13	.	1076
300	.	6	16	36	34	22	1106
310	1	5	17	26	28	4075
320	.	5	15	22	16	2	1056
330	.	5	21	31	7	1	1061
340	.	3	11	15	9	1036
350	.	4	5	8	2	1	1019

*** **

SPD	.006	.229	.197	.048	.013	.001	0.000	0.000	.001	0.000	0.000	0.000	0.000
PRB	.081	.306	.101	.017	.001	0.000	0.000	0.000	0.000	0.000	0.000	0.000	0.000

STATION 5 (UPCOAST)
44/46M - SUMMER

SPEED/DIRECTION PROBABILITY MATRIX (NO. OCCURRENCES/ELEMENT)

DIR (M)	SPEED CM/SEC																				DIR PROB
	0	2	4	6	8	10	12	14	16	18	20	22	24	26	28	30	32	34	36	38	
0	1	3	4	1008
10	.	3	2	4008
20	.	4	3	1007
30	.	.	2	2004
40	.	1	2	3	.	1006
50	.	.	3	3	1	1007
60	.	1	4	3	1008
70	.	1	5	5	5015
80	.	1	4	4	2	2012
90	.	3	3	3	5	1014
100	.	.	6	8	1	.	2	.	1017
110	.	2	.	4	3	3	2	1014
120	1	1	6	3	3	4	1	1	1	.	.	1020
130	.	1	5	6	3	4	4	.	5026
140	.	.	2	7	8	3	.	2	3023
150	1	2	7	7	9	3	2029
160	1	.	3	7	5	2	3	2021
170	.	.	3	2	2	4	.	1	1012
180	.	1	3	.	1	1	2	2	1010
190	.	2	1	1	3	.	.	1007
200	.	2	6	2	1010
210	.	1	1	2004
220	.	1	3	2006
230	.	.	5005
240	.	2	4	1006
250	.	2	4	3	.	.	2010
260	.	3	4	1	.	1	2	1	.	1	1013
270	.	2	7	5	1	12	10	7	10	4	8	1	1	.	.	1064
280	.	.	10	9	13	28	29	25	18	4	15	6	4	1	7	4	.	2	.	.	.160
290	.	7	11	18	24	39	15	20	16	7	11	5	6	.	5	4	.	2	1	.	.182
300	1	2	13	33	30	19	9	12	6	4	3	1	4	.	1	5	.	2	.	1	.137
310	.	3	15	17	11	10	2	2	2	1058
320	.	3	14	18	9	.	.	1	2	.	1044
330	.	1	6	6	5	.	.	2018
340	.	2	4	4	1010
350	.	1	1	2004

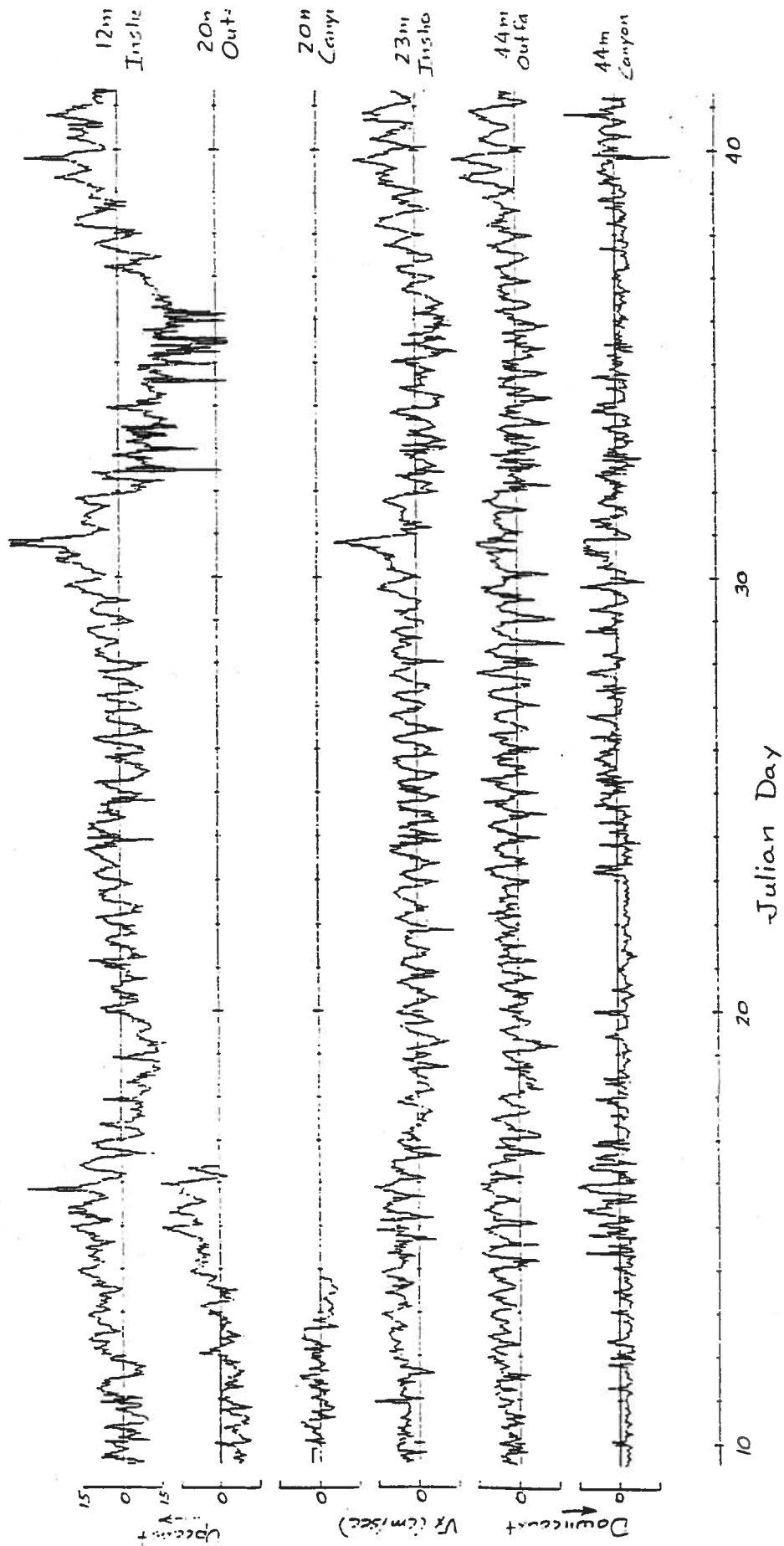
*** **

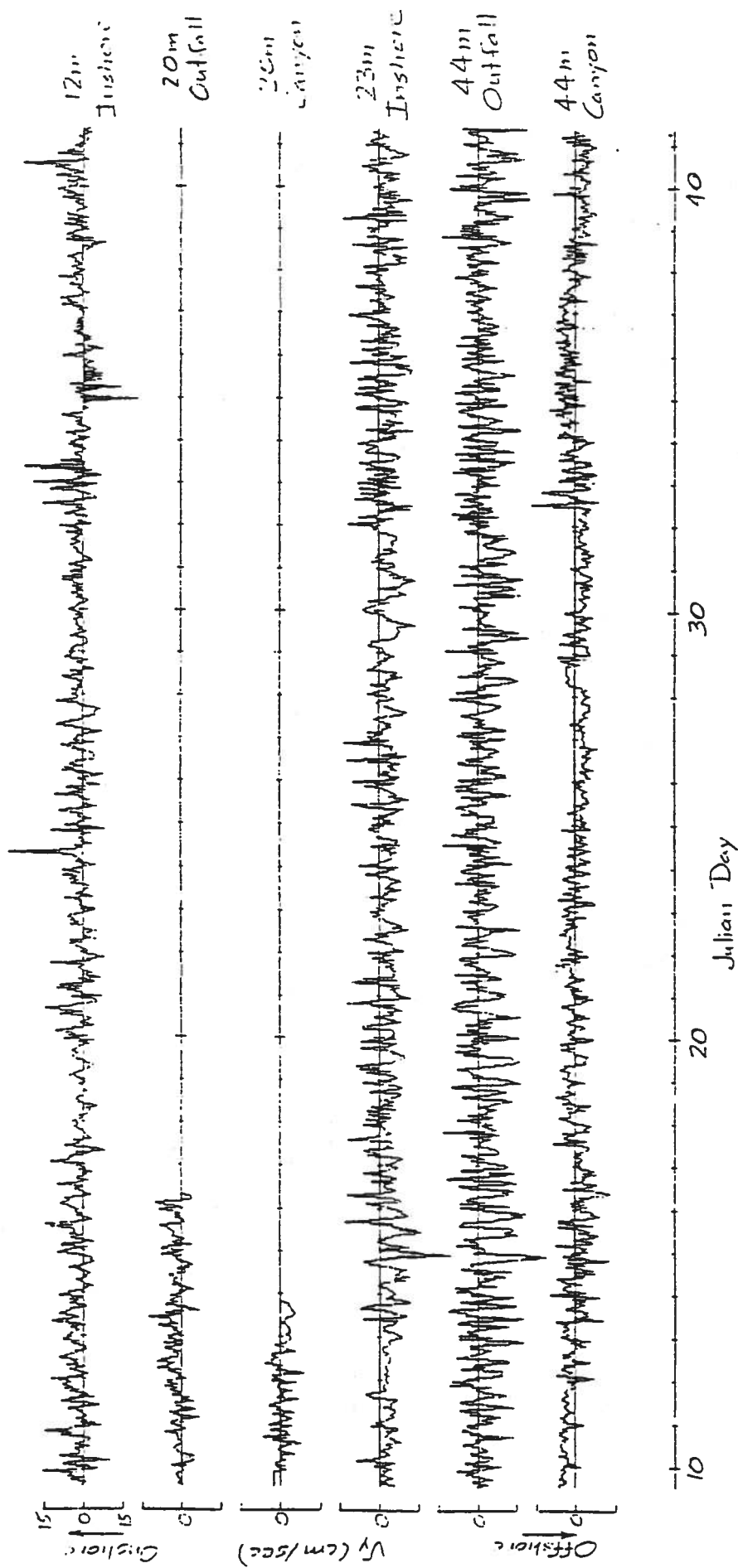
SPD	.005	.162	.135	.074	.061	.036	.015	.012	0.000	.006	0.000	0.000	.006
FRB	.053	.181	.126	.078	.019	.013	.001	.013	0.000	.001	.004	0.000	

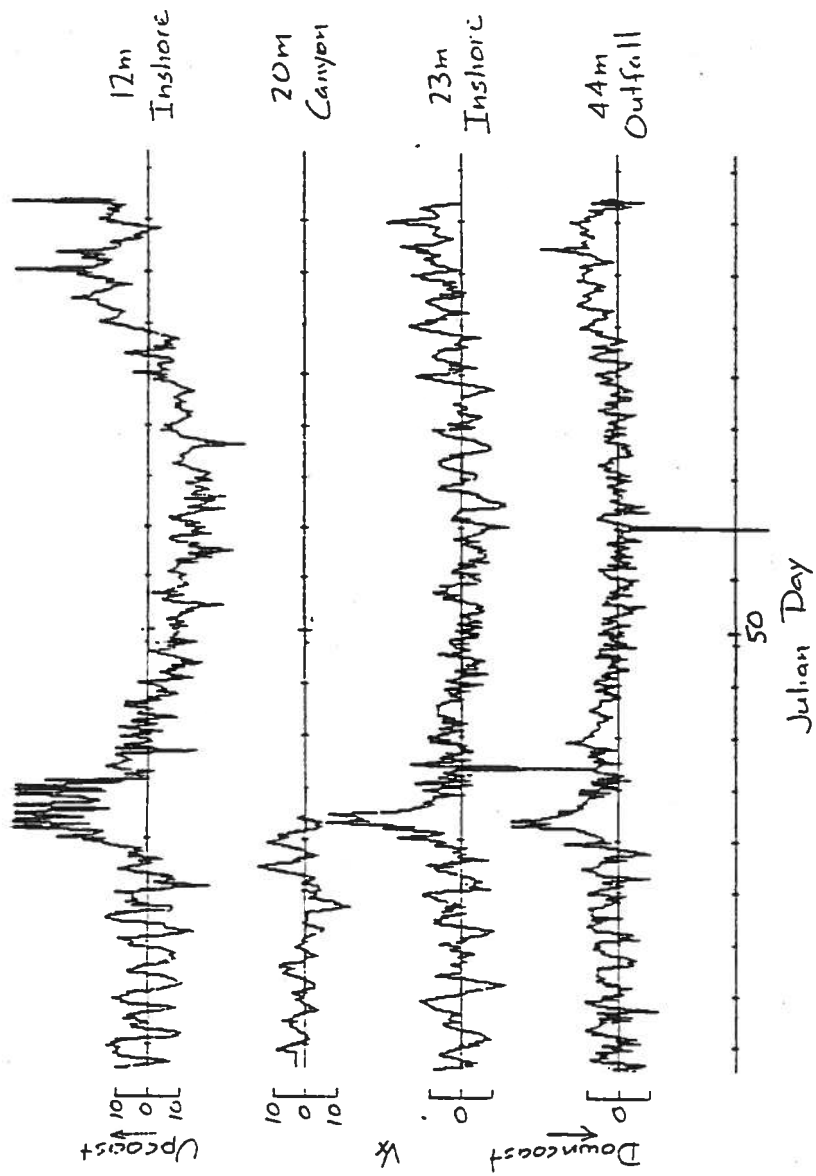
STATION 5 (UPCOAST)
16/46M - SUMMER

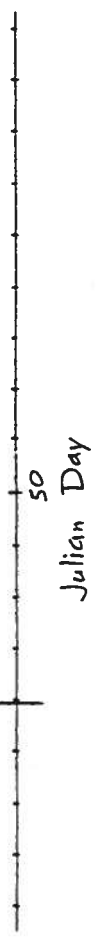
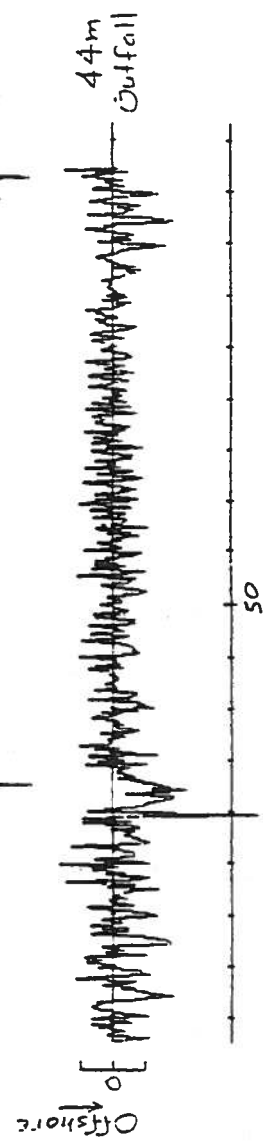
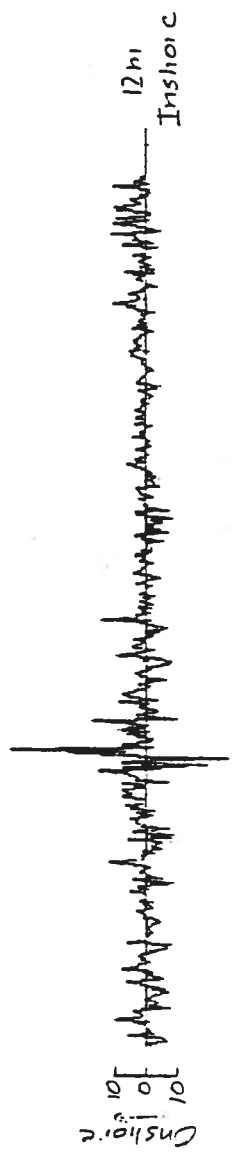
APPENDIX B

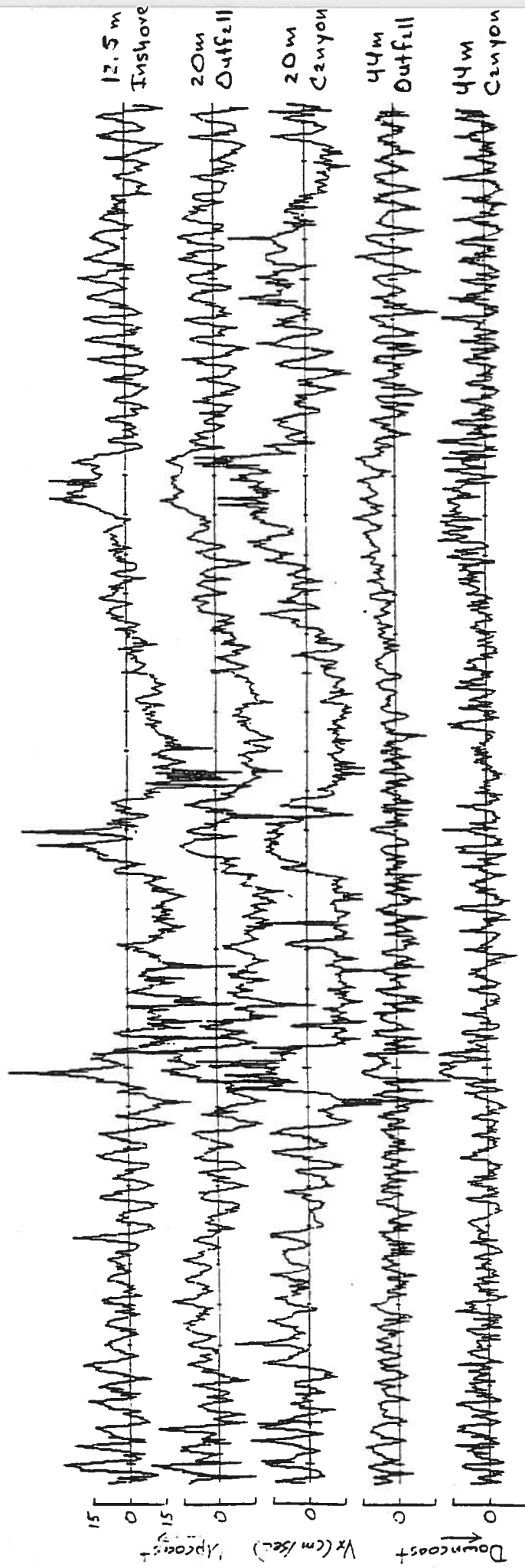
**LONGSHORE AND CROSS-SHORE COMPONENTS OF THE FLOW
FOR JULIAN DAYS 009-094 AND 227-261**

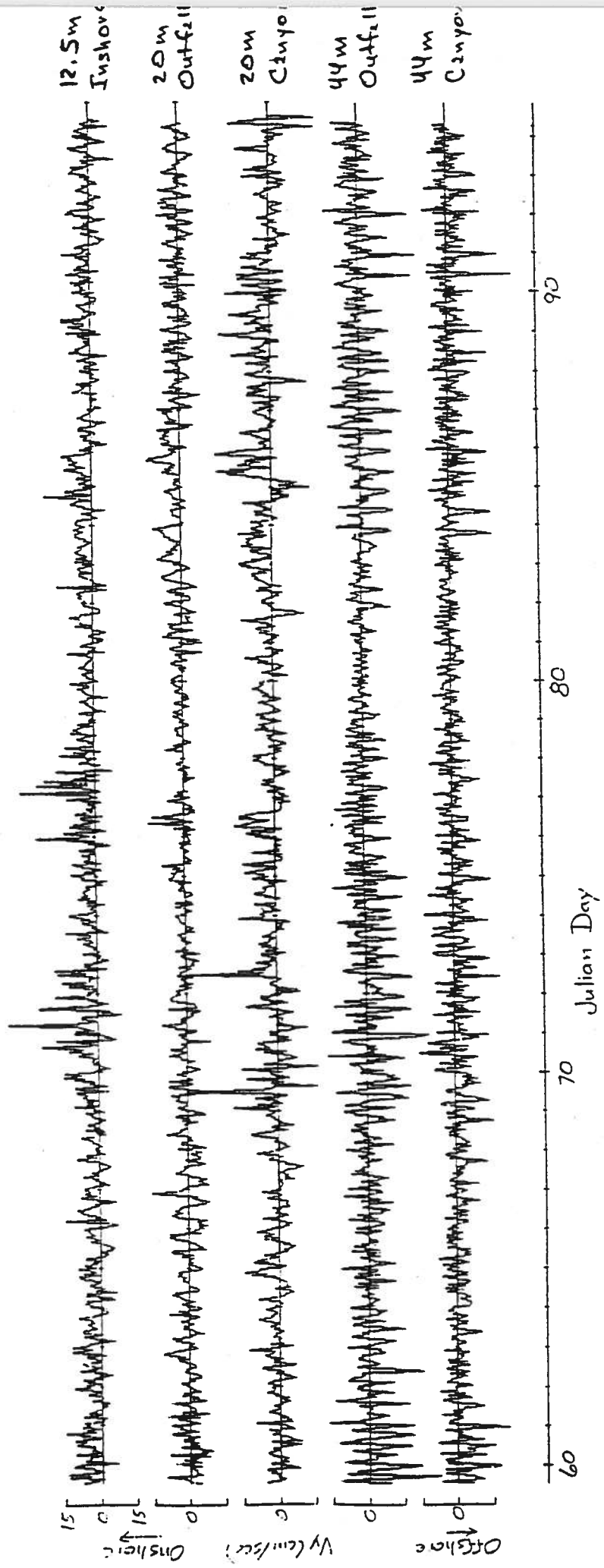


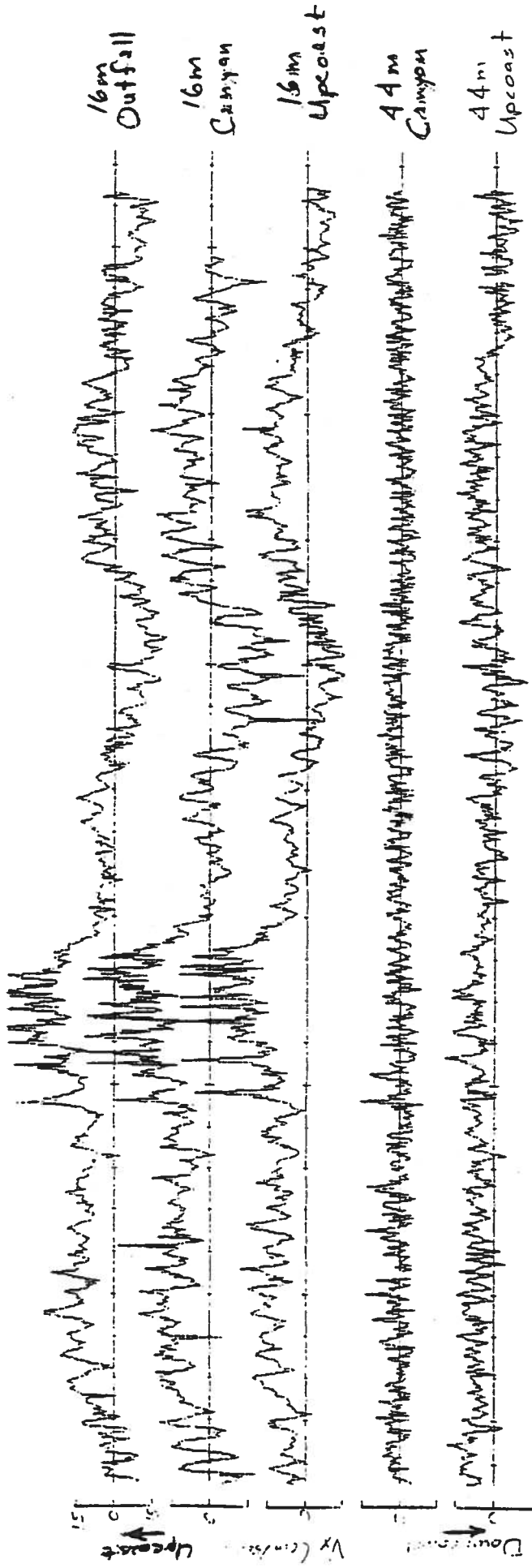


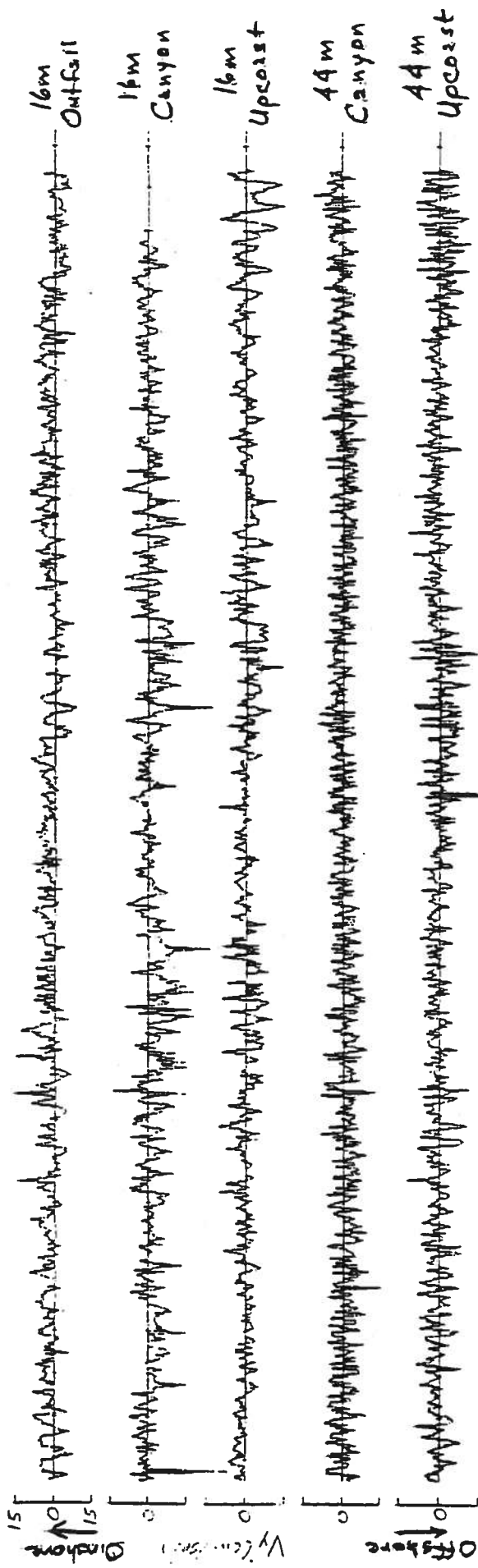










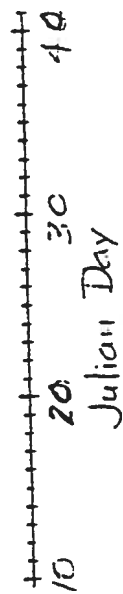
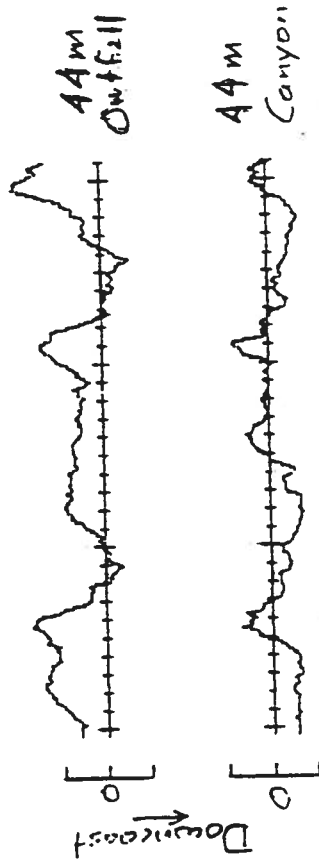
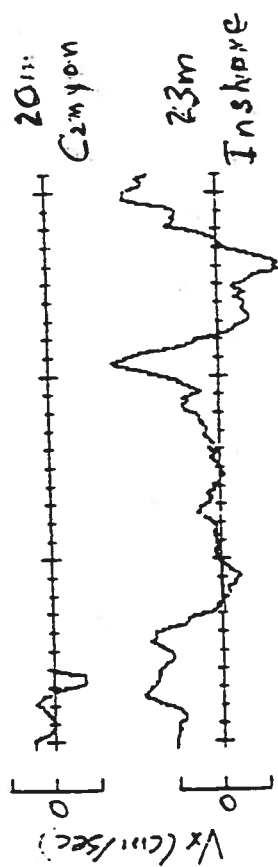
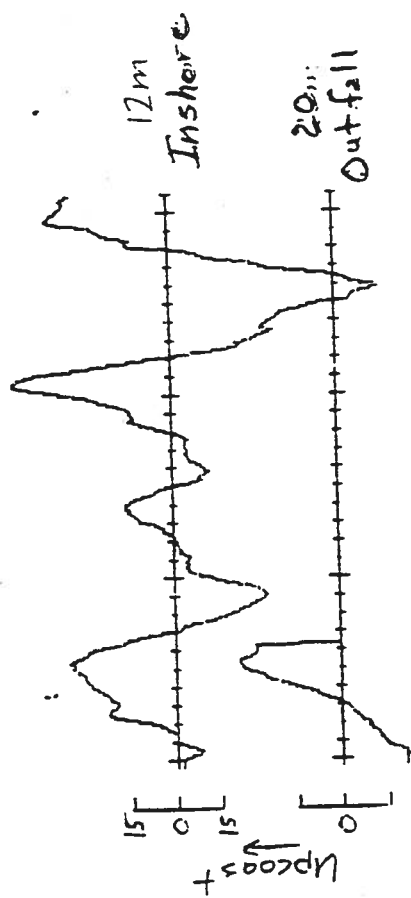


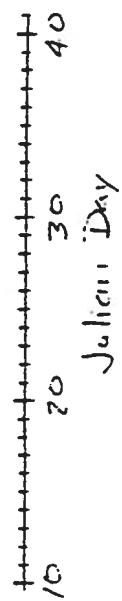
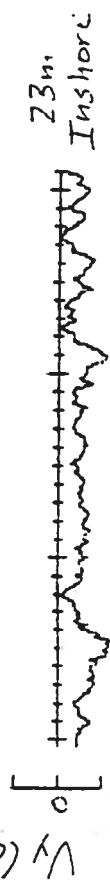
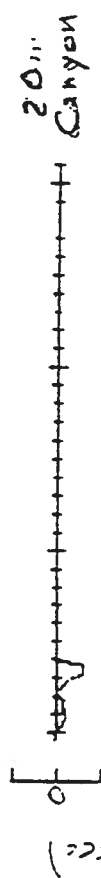
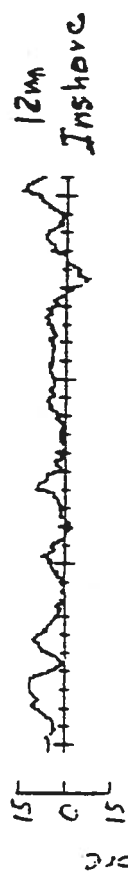
260

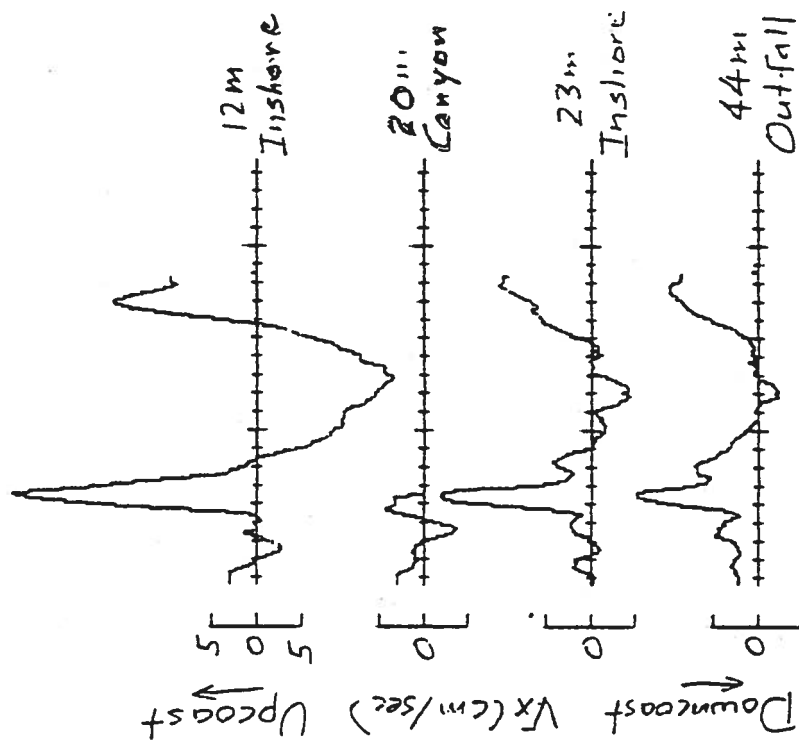
250

240

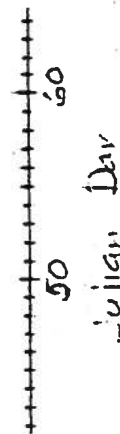
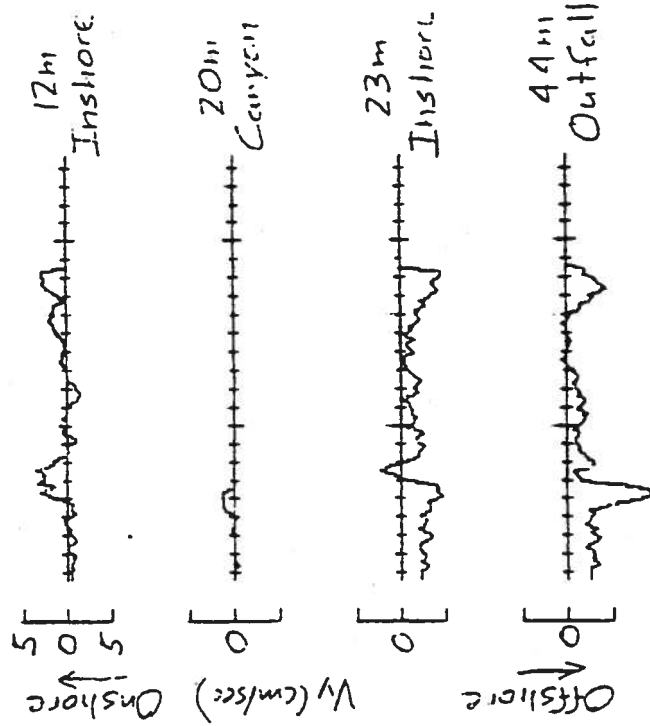
Julian Day

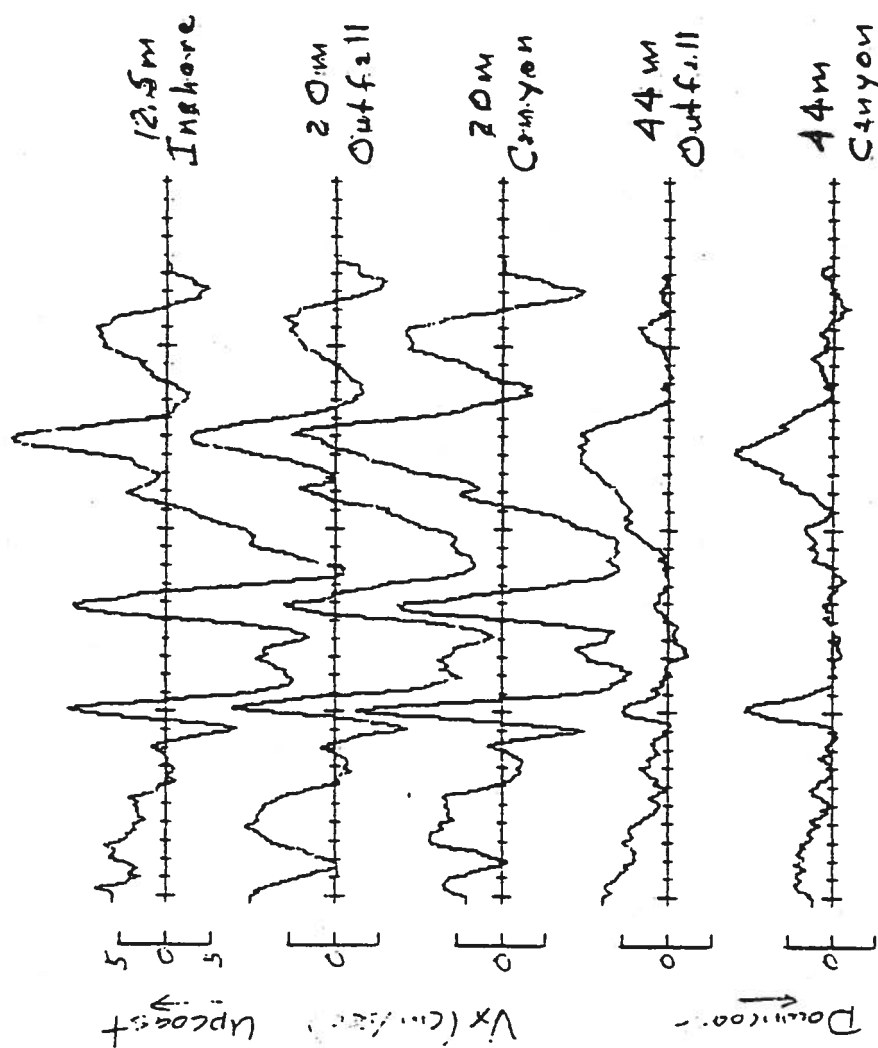






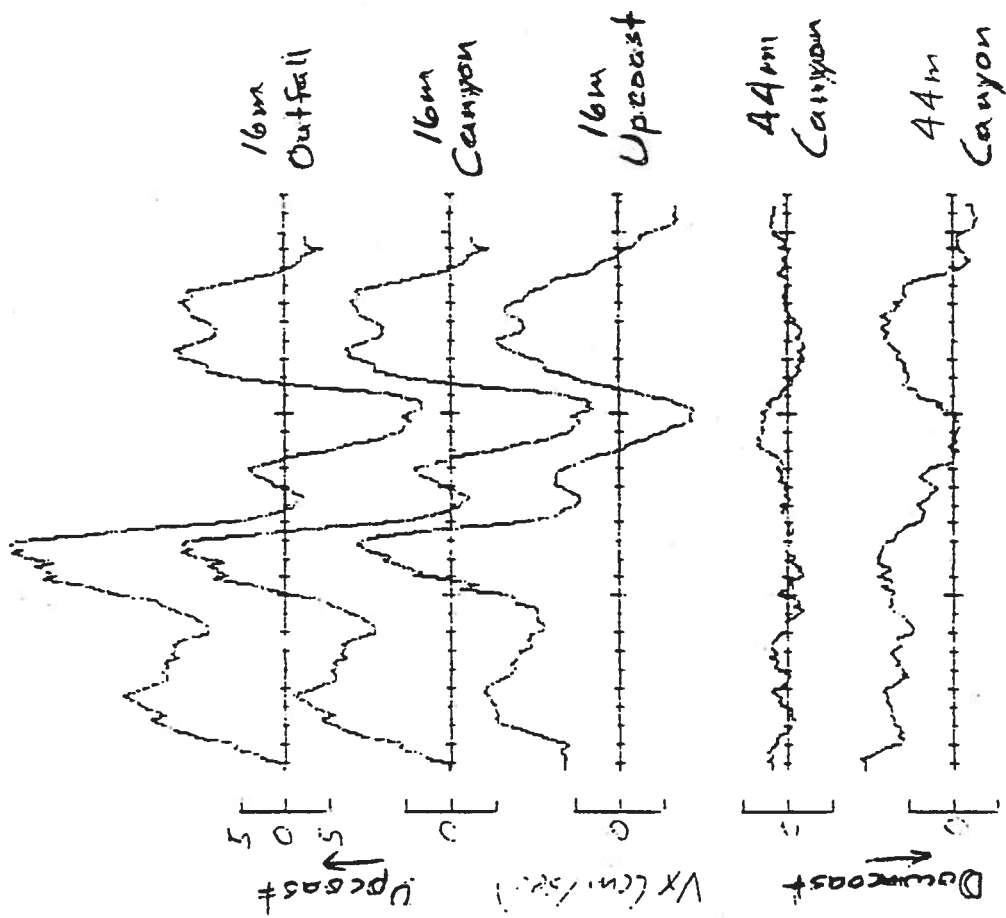
50 60
Julian Day



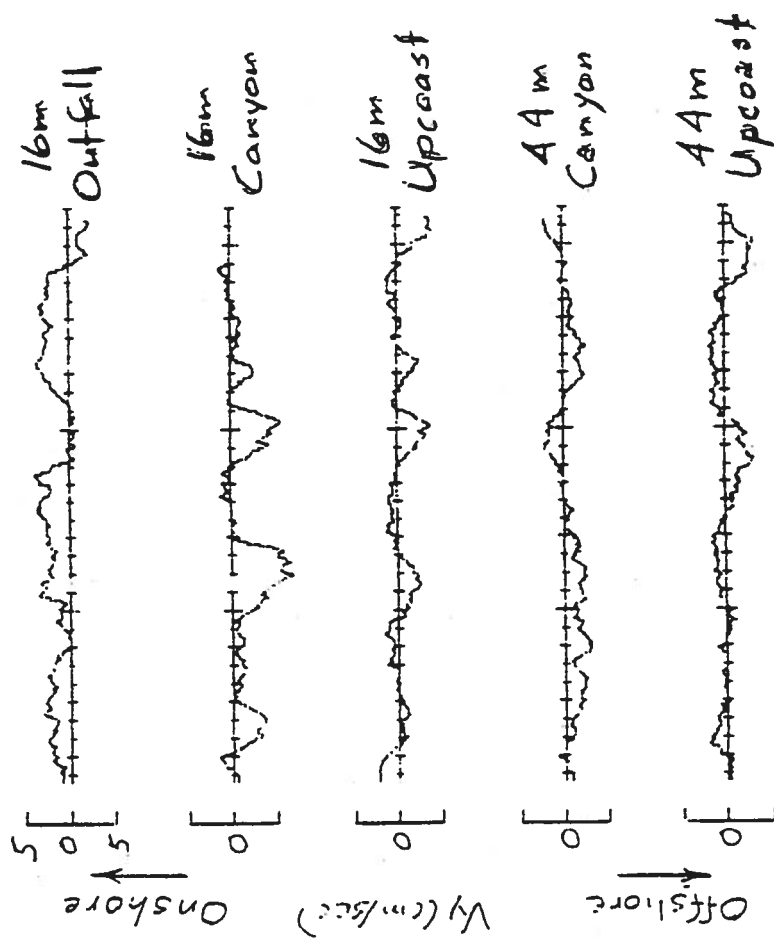


60 70 80 90

Julian Day



240 250 260
Julian Day

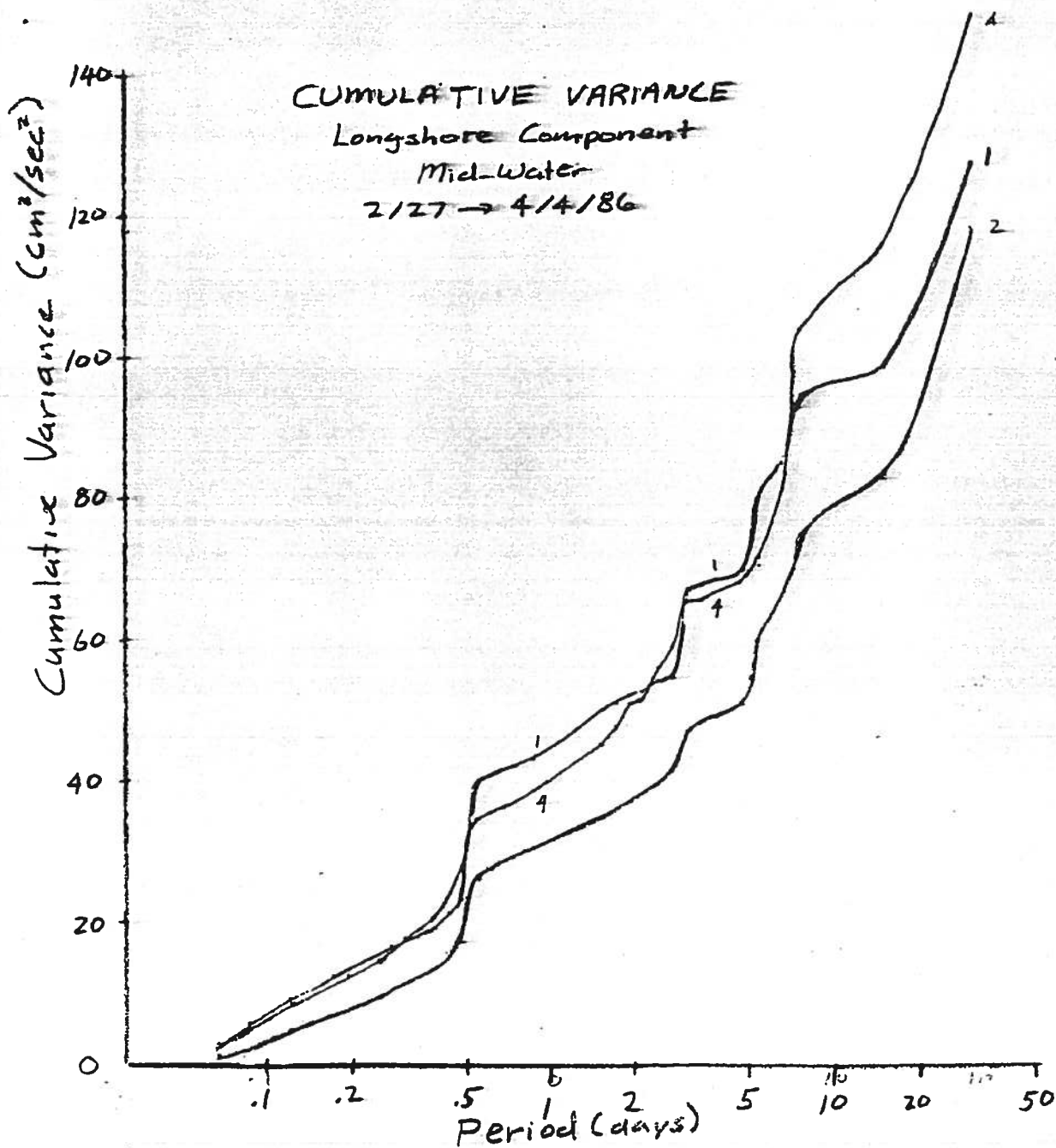


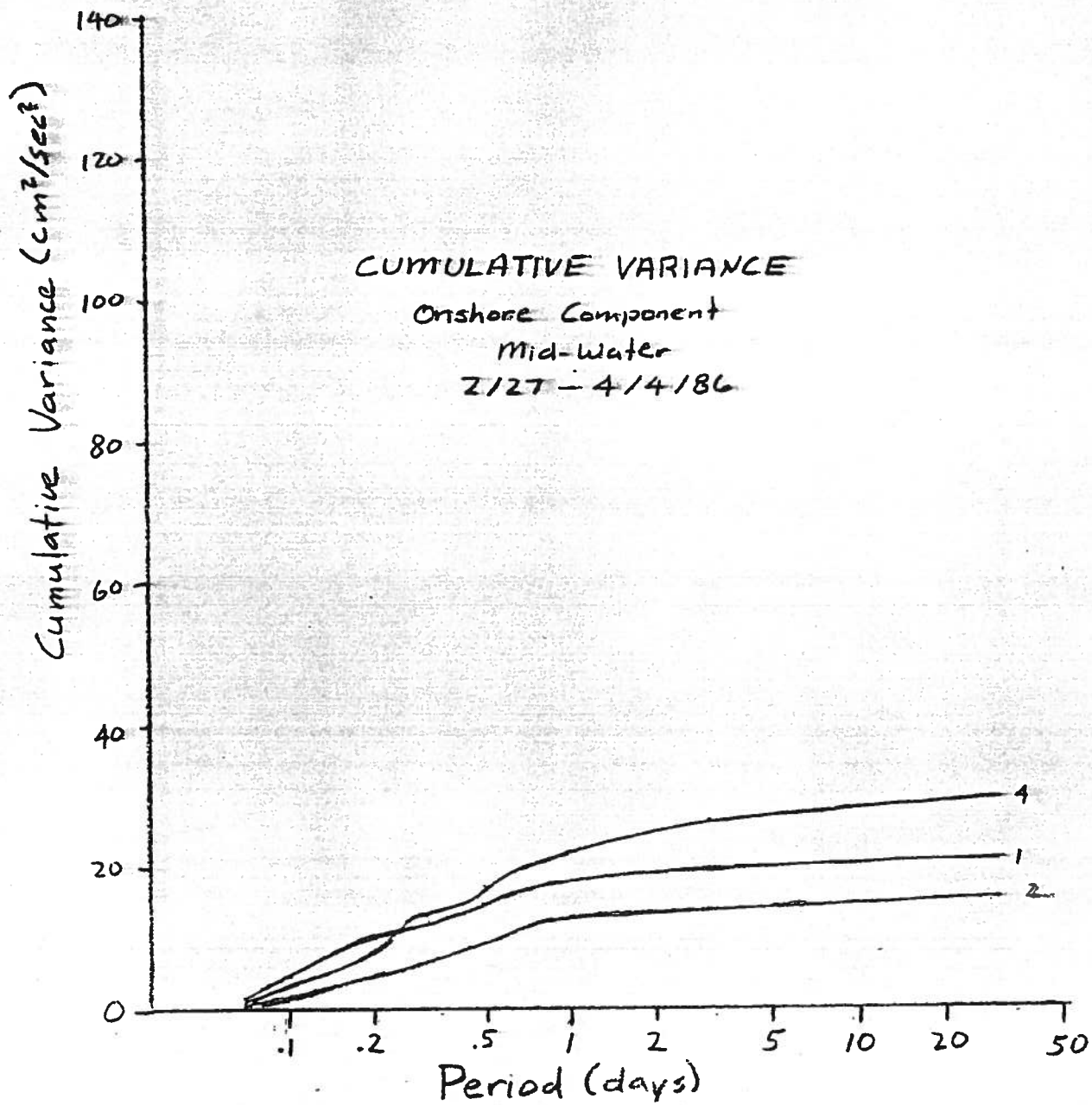
240 250 260

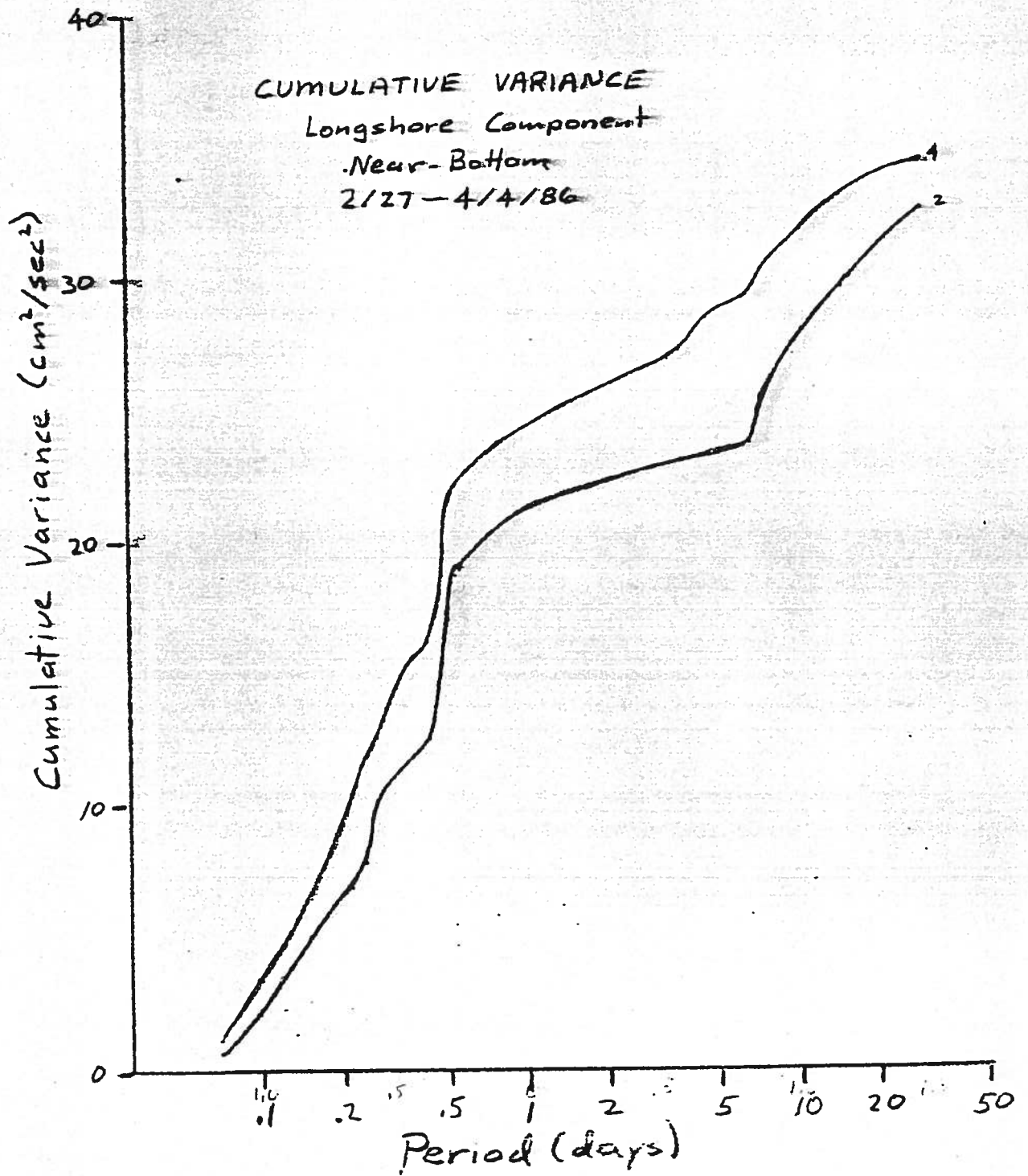
Julian Day

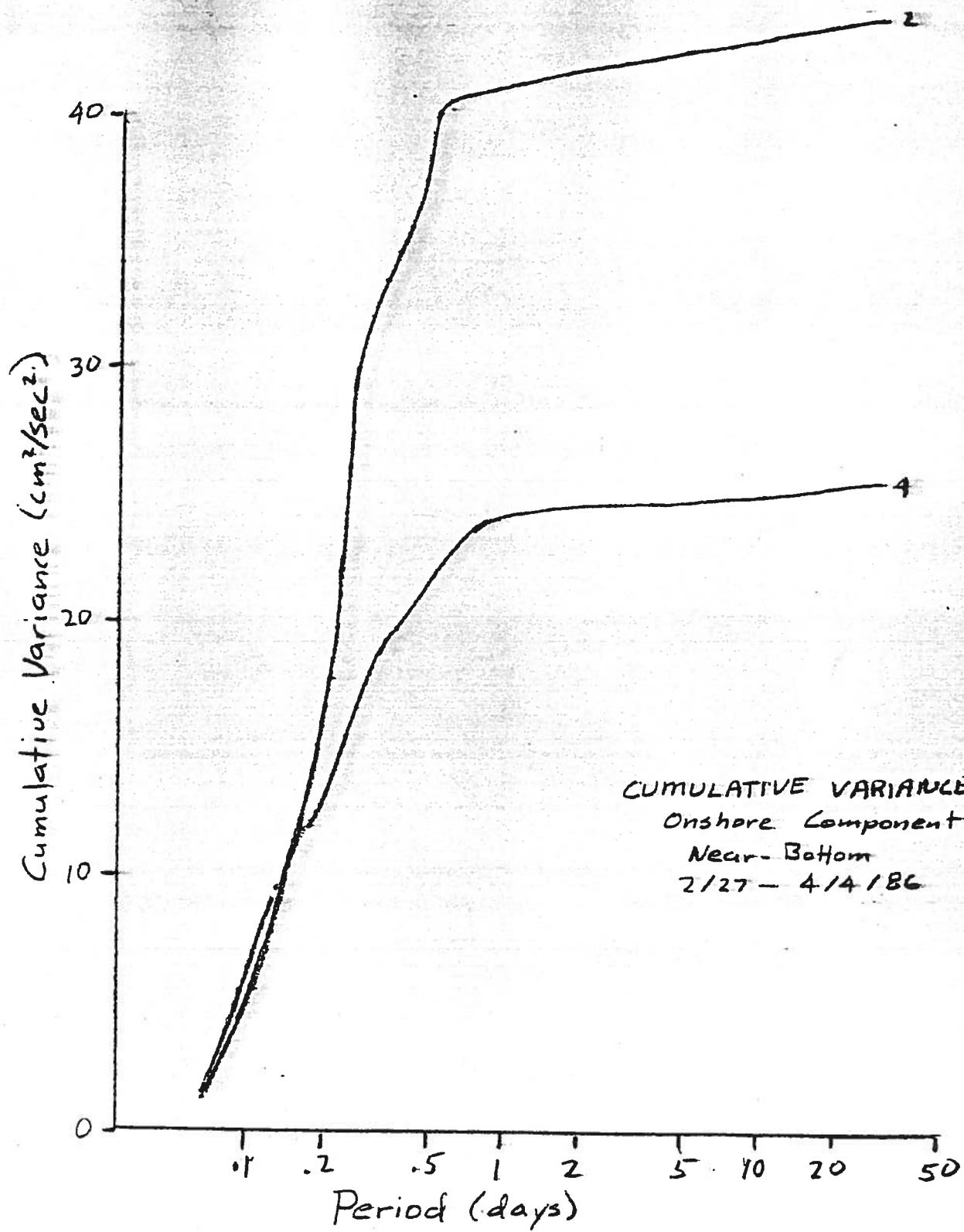
APPENDIX C

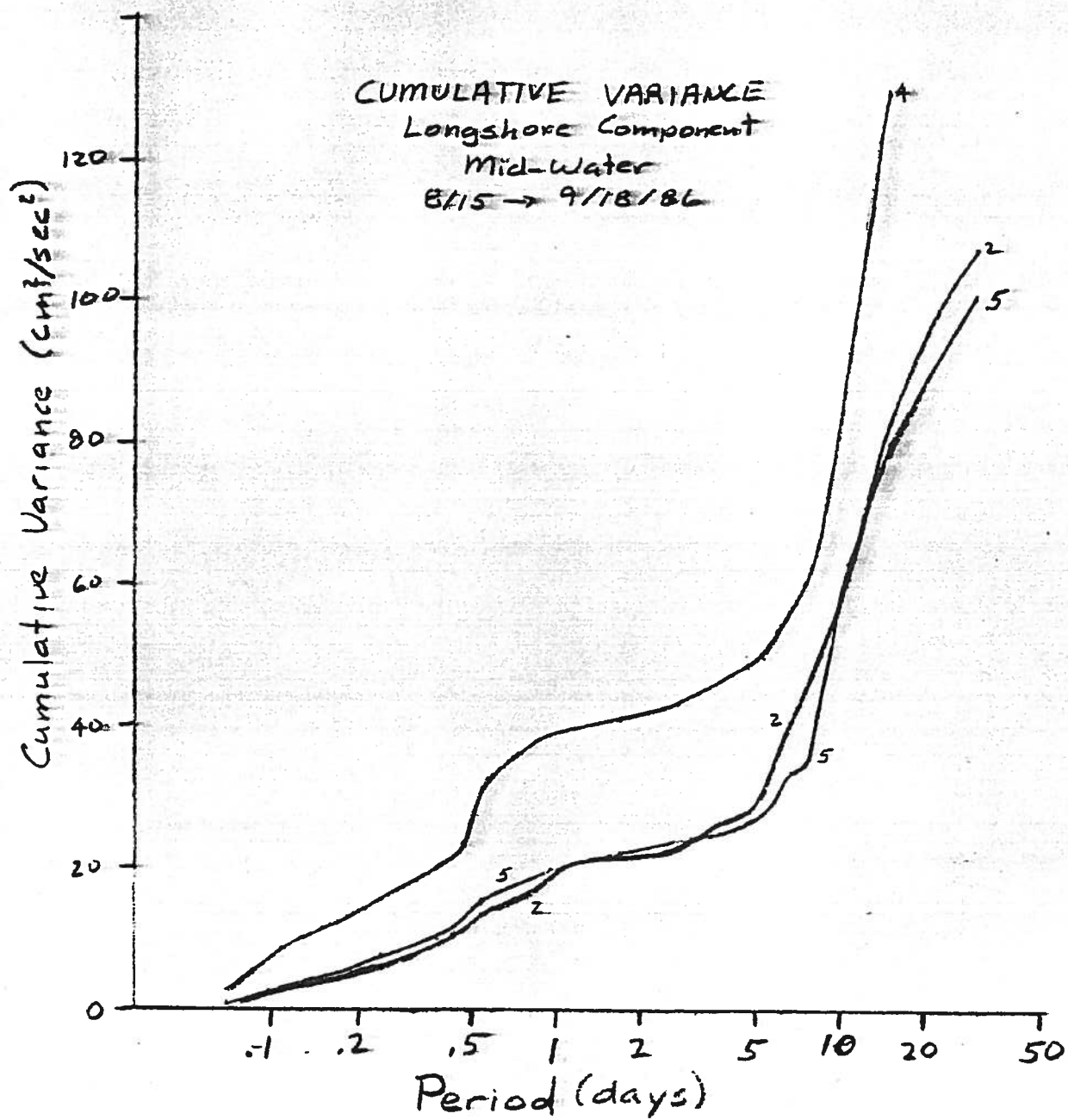
CUMMULATIVE VARIANCE AS A FUNCTION OF PERIODICITY

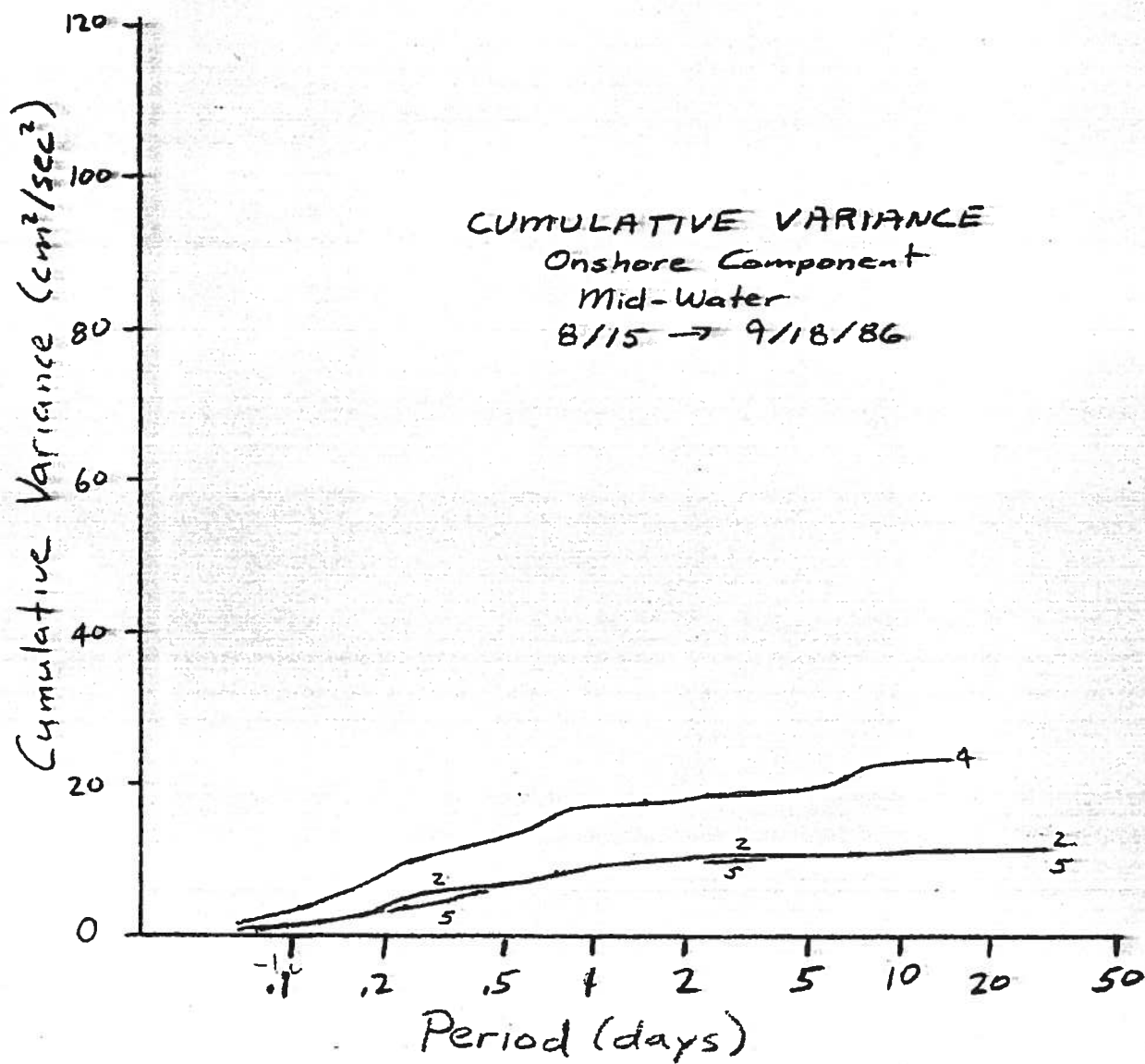


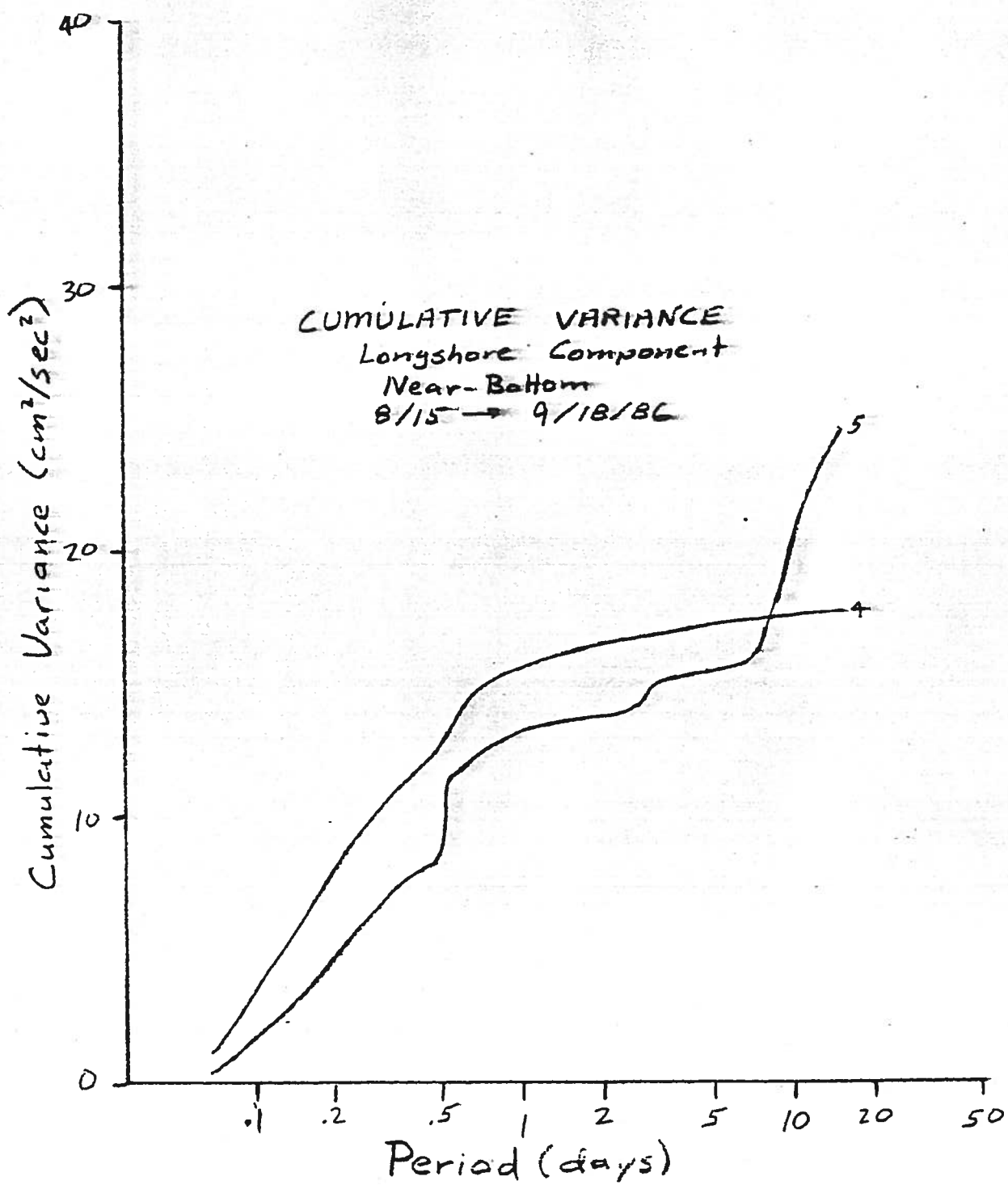


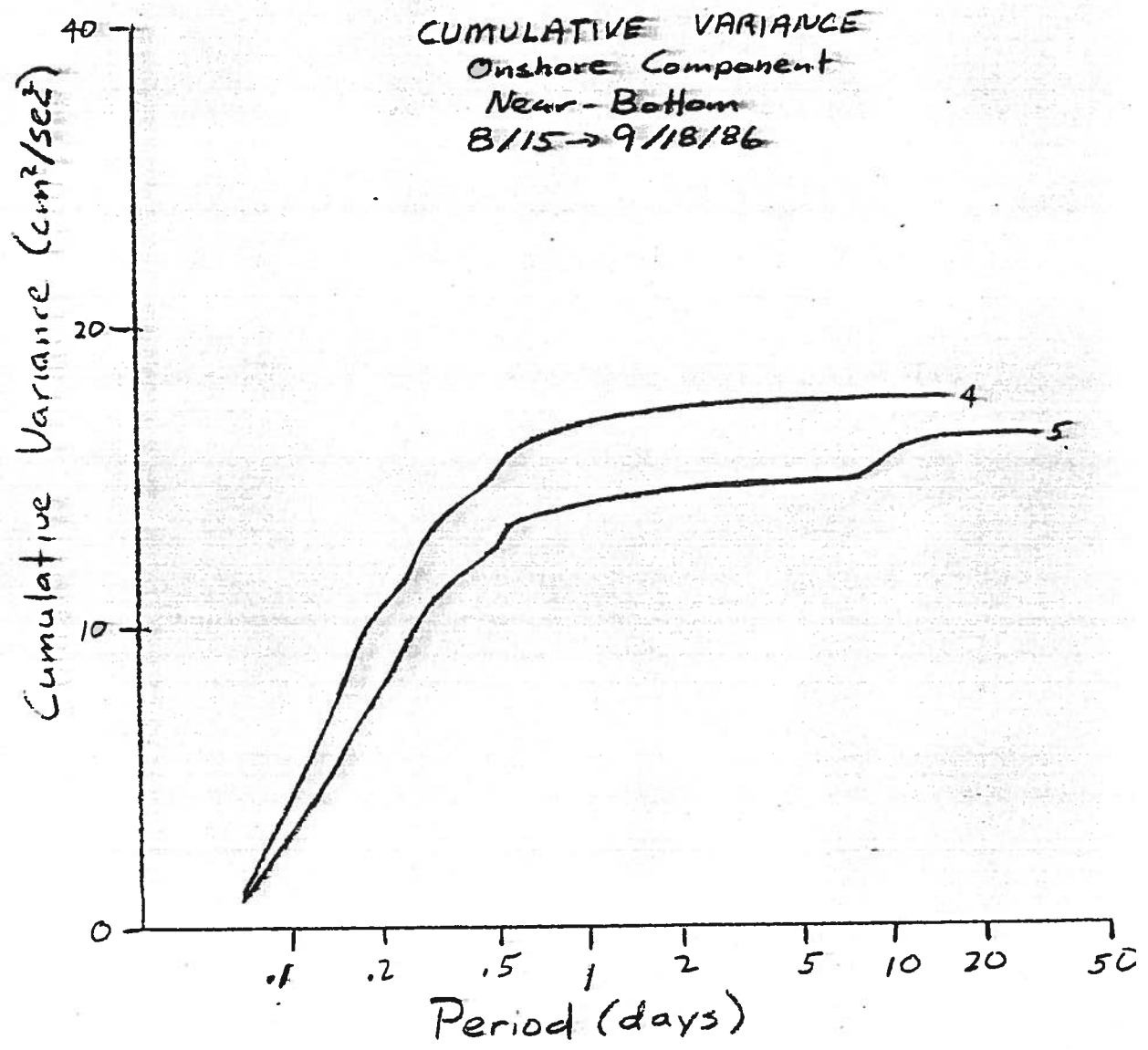












APPENDIX D
DENSITY PROFILES

APPENDIX D

DENSITY PROFILES

(Expressed in sigma-t units: density(gm/cm**3)=1.+.001*sigma-t)

Depth (m)	07/85 (Z1)	07/85 (Z2)	08/85 (Z1)	08/85 (Z2)	09/85 (Z1)	09/85 (Z2)	10/85 (Z1)	10/85 (Z2)
*****	*****	*****	*****	*****	*****	*****	*****	*****
0	24.08	24.02	23.89	23.94	24.02	24.02	24.20	24.1
3	24.28	24.65	24.00	23.94	24.08	24.08	24.20	24.2
6	24.82	25.05	24.02	23.94	24.08	24.15	24.20	24.2
9	24.82	25.22	24.05	24.02	24.15	24.41	24.28	24.2
12	25.11	25.33	24.33	24.08	24.20	24.58	24.46	24.2
15	25.27	25.37	24.58	24.58	24.65	24.82	24.53	24.7
18	25.37	25.37	24.79	24.82	25.93	25.07	24.82	25.1
21	25.48	25.48	25.00	25.22	25.22	25.27	25.05	25.2
24	25.54	25.58	25.46	25.35	25.33	25.44	25.22	25.3
27	25.58	25.64	25.44	25.44	25.48	25.68	25.33	25.5
30	25.64	25.64	25.82	25.64	25.58	25.78	25.37	25.5
33	25.64	25.64	25.84	25.84	25.64	25.78	25.44	25.6
36	25.68	25.64	25.84	25.84	25.78	25.84	25.48	25.6
39	25.68	25.64	25.84	25.84	25.84	25.84	25.54	25.6
42	25.84	25.68	25.85	25.78	25.84	25.84	25.68	25.6
45	25.87	25.78	-	-	25.84	25.84	-	-
	11/85 (Z1)	11/85 (Z2)	12/85 (Z1)	12/85 (Z2)				
	*****	*****	*****	*****				
0	24.93	25.00	25.37	25.37				
3	25.00	25.00	25.37	25.37				
6	25.00	25.00	25.37	25.37				
9	25.00	25.00	25.37	25.37				
12	25.00	25.00	25.37	25.37				
15	25.00	25.00	25.37	25.37				
18	25.33	25.22	25.37	25.37				
21	25.64	25.64	25.37	25.37				
24	25.74	25.74	25.44	25.44				
27	25.74	25.74	25.64	25.64				
30	25.74	25.74	25.84	25.84				
33	25.74	25.74	25.84	25.84				
36	25.78	25.74	25.84	25.84				
39	25.78	25.78	25.87	25.84				
42	25.78	25.78	25.93	25.84				
45	-	-	-	-				

Depth (m)	01/86 (Z1)	01/86 (Z2)	02/86 (Z1)	02/86 (Z2)	02/86 (S-1)	02/86 (S-2)	03/86 (Z1)	03/86 (Z2)
*****	*****	*****	*****	*****	*****	*****	*****	*****
0	25.22	25.16	25.22	25.33	24.85	24.72	24.77	24.77
3	25.22	25.22	25.27	25.33	24.85	24.77	25.00	25.00
6	25.22	25.22	25.27	25.33	24.85	24.77	25.22	25.11
9	25.22	25.22	25.27	25.33	24.85	24.84	25.44	25.48
12	25.22	25.22	25.27	25.33	24.85	24.86	25.64	25.64
15	25.27	25.22	25.27	25.37	24.85	24.98	25.84	25.78
18	25.33	25.22	25.27	25.37	24.85	25.08	25.87	25.87
21	25.44	25.37	25.27	25.37	24.85	25.10	25.93	25.97
24	25.54	25.44	25.27	25.37	24.85	25.31	25.97	25.97
27	25.54	25.48	25.27	25.37	24.95	25.38	26.02	26.02
30	25.54	25.54	25.27	25.37	25.06	25.45	26.02	26.02
33	25.58	25.54	25.33	25.33	25.20	25.46	26.02	26.02
36	25.58	25.64	25.33	25.37	25.22	25.46	26.06	26.02
39	25.58	25.64	25.37	25.44	25.41	25.48	26.06	26.02
42	25.58	25.64	25.44	25.48	25.54	25.55	26.11	26.02
45	-	25.68	25.58	25.64	25.65	25.59	-	26.06
	04/86 (Z1)	04/86 (Z2)	04/86 (S)	05/86 (Z1)	05/86 (Z2)	06/86 (Z1)	06/86 (Z2)	06/86 (S)
*****	*****	*****	*****	*****	*****	*****	*****	*****
0	24.65	24.53	24.85	24.63	24.65	23.68	23.70	23.67
3	24.82	24.75	25.16	25.05	24.86	23.76	23.76	23.78
6	24.89	24.75	25.32	25.37	25.07	23.86	24.02	23.87
9	24.91	24.75	25.46	25.68	25.44	24.72	24.96	24.16
12	25.00	24.89	25.56	25.76	25.64	25.22	25.22	25.05
15	25.11	24.96	25.57	25.87	25.74	25.82	25.87	25.42
18	25.18	25.00	25.68	25.91	25.84	25.91	25.87	25.47
21	25.44	25.05	25.74	25.95	25.84	25.97	25.95	25.55
24	25.82	25.22	25.77	25.93	25.84	26.00	26.02	25.75
27	25.84	25.33	25.79	25.93	25.84	26.02	26.02	25.88
30	25.80	25.64	25.79	25.93	25.84	26.02	26.02	25.91
33	25.84	25.68	25.79	25.93	25.80	26.02	26.02	25.92
36	25.84	25.68	25.79	25.93	25.80	26.02	26.02	25.92
39	25.84	25.74	25.80	25.93	25.84	26.02	26.02	26.00
42	25.95	25.72	25.80	25.93	25.84	26.02	26.02	26.01
45	25.97	25.74	25.80	25.93	25.84	26.02	26.02	26.01

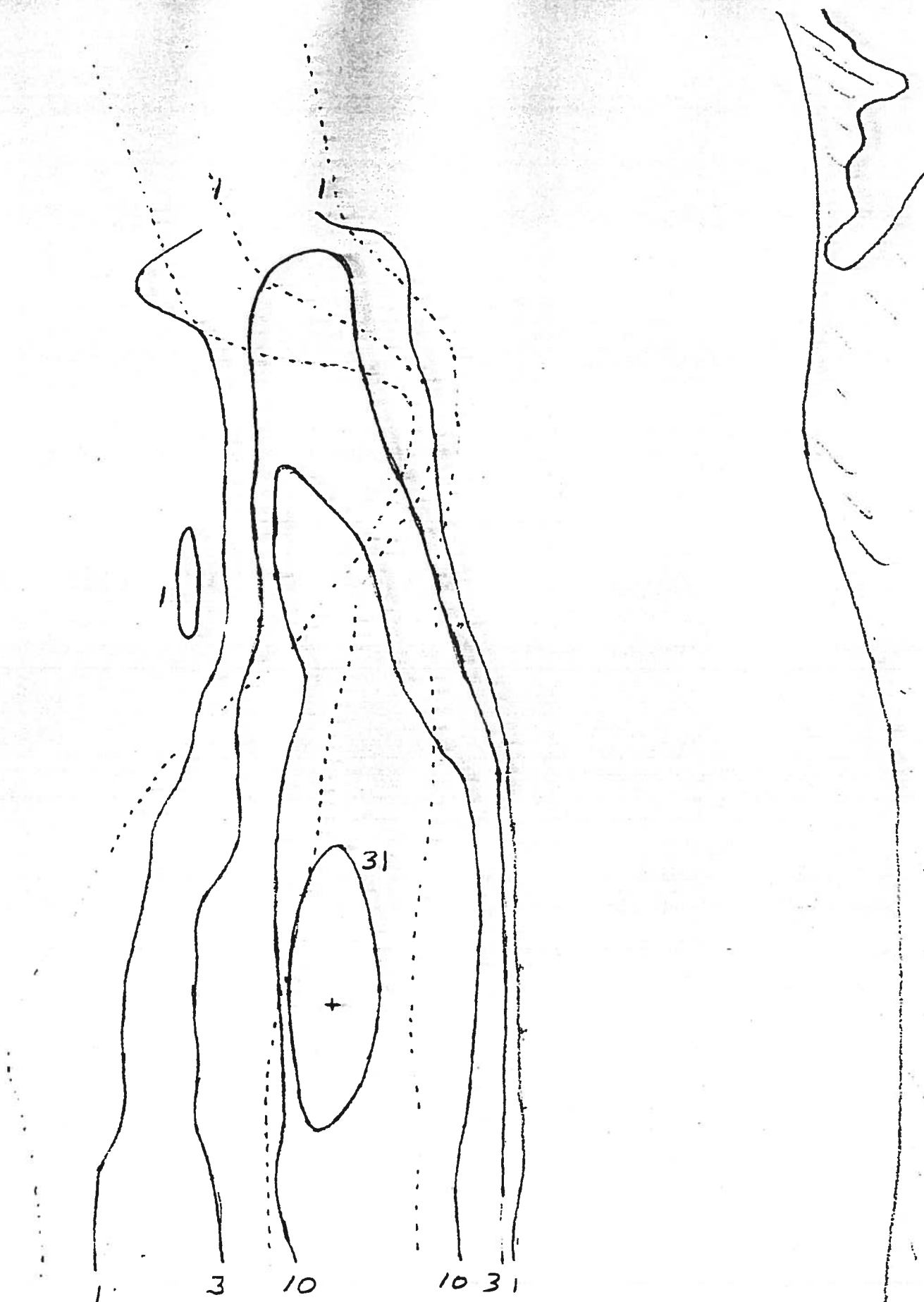
Depth (m)	07/86 (Z1)	07/86 (Z2)	08/86 (Z1)	08/86 (Z2)	08/86 (S)	09/86 (Z1)	09/86 (Z2)	09/86 (S)
*****	*****	*****	*****	*****	*****	*****	*****	*****
0	24.02	24.02	23.73	23.70	24.18	24.36	24.38	23.94
3	24.08	24.08	24.00	23.97	24.66	24.46	24.43	24.15
6	24.13	24.13	24.48	24.77	24.91	24.53	24.53	24.08
9	24.82	25.00	25.11	25.09	25.31	24.67	24.72	24.12
12	25.40	25.35	25.37	25.37	25.31	24.89	24.91	24.19
15	25.54	25.56	25.60	25.44	25.47	25.22	25.33	24.34
18	25.62	25.68	25.68	25.60	25.57	25.44	25.46	24.55
21	25.72	25.76	25.80	25.66	25.49	25.54	25.54	24.70
24	25.84	25.78	25.84	25.82	25.59	25.64	25.60	24.96
27	25.89	25.80	25.84	25.84	25.58	25.68	25.60	25.01
30	25.91	25.85	25.87	25.84	25.61	25.70	25.64	25.11
33	25.93	25.89	25.87	25.84	25.61	25.76	25.64	25.18
36	25.97	25.93	25.87	25.84	25.62	25.78	25.66	25.23
39	25.98	25.97	25.87	25.84	25.62	25.76	25.68	25.29
42	25.98	25.98	25.87	25.84	25.62	25.78	25.70	25.32
45	25.98	25.98	25.87	25.84	25.62	25.82	25.80	25.31

	10/86 (Z1)	10/86 (Z2)
*****	*****	*****
0	24.43	24.33
3	24.46	24.41
6	24.48	24.48
9	24.51	24.48
12	24.53	24.48
15	25.05	24.53
18	25.22	24.70
21	25.33	24.89
24	25.42	24.93
27	25.48	25.14
30	25.48	25.27
33	25.52	25.27
36	25.58	25.31
39	25.60	25.33
42	25.60	25.42
45	25.58	25.70

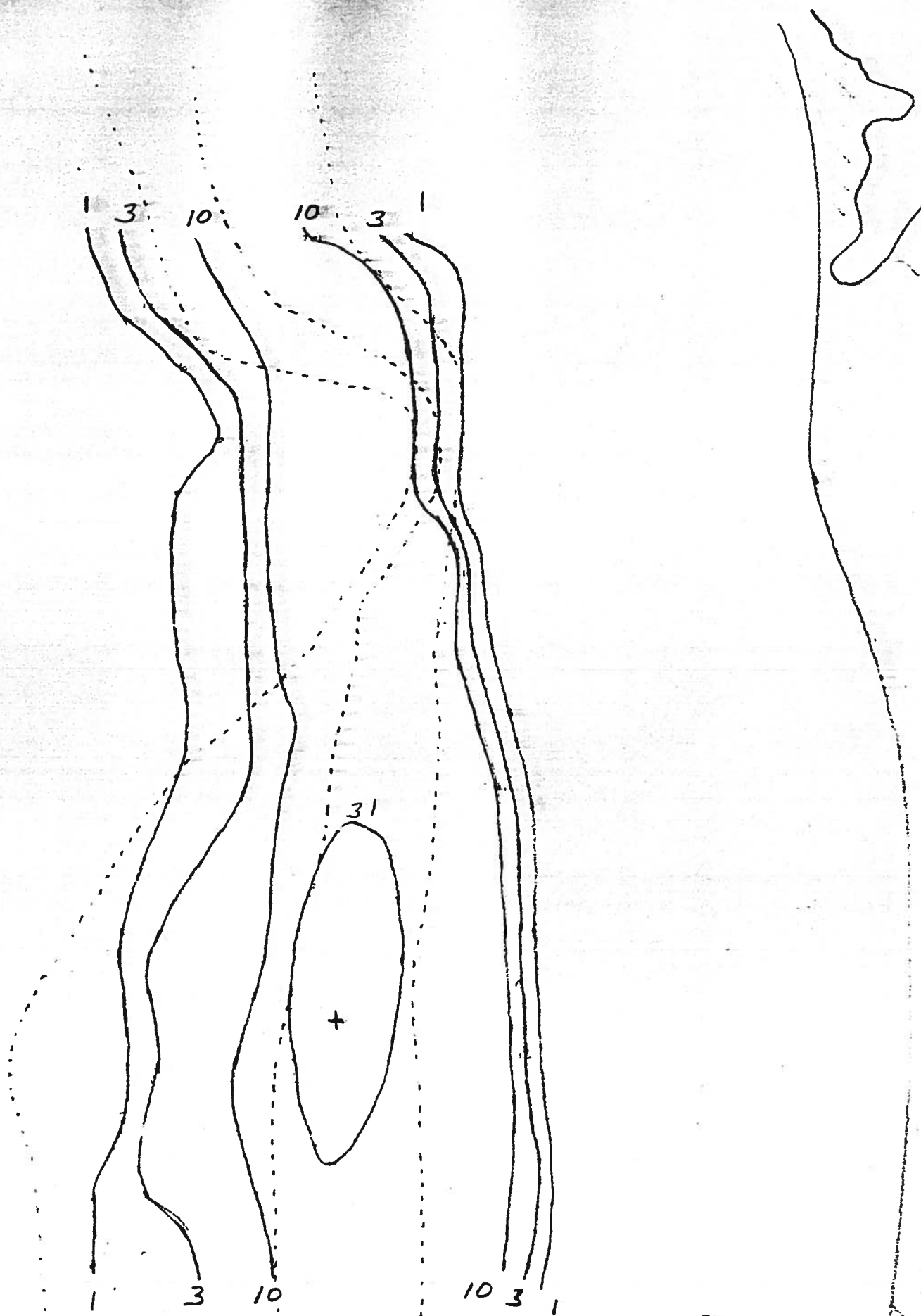
APPENDIX E

PXYT2D SIMULATIONS FOR THE PERIODS 009-041 AND 194-227

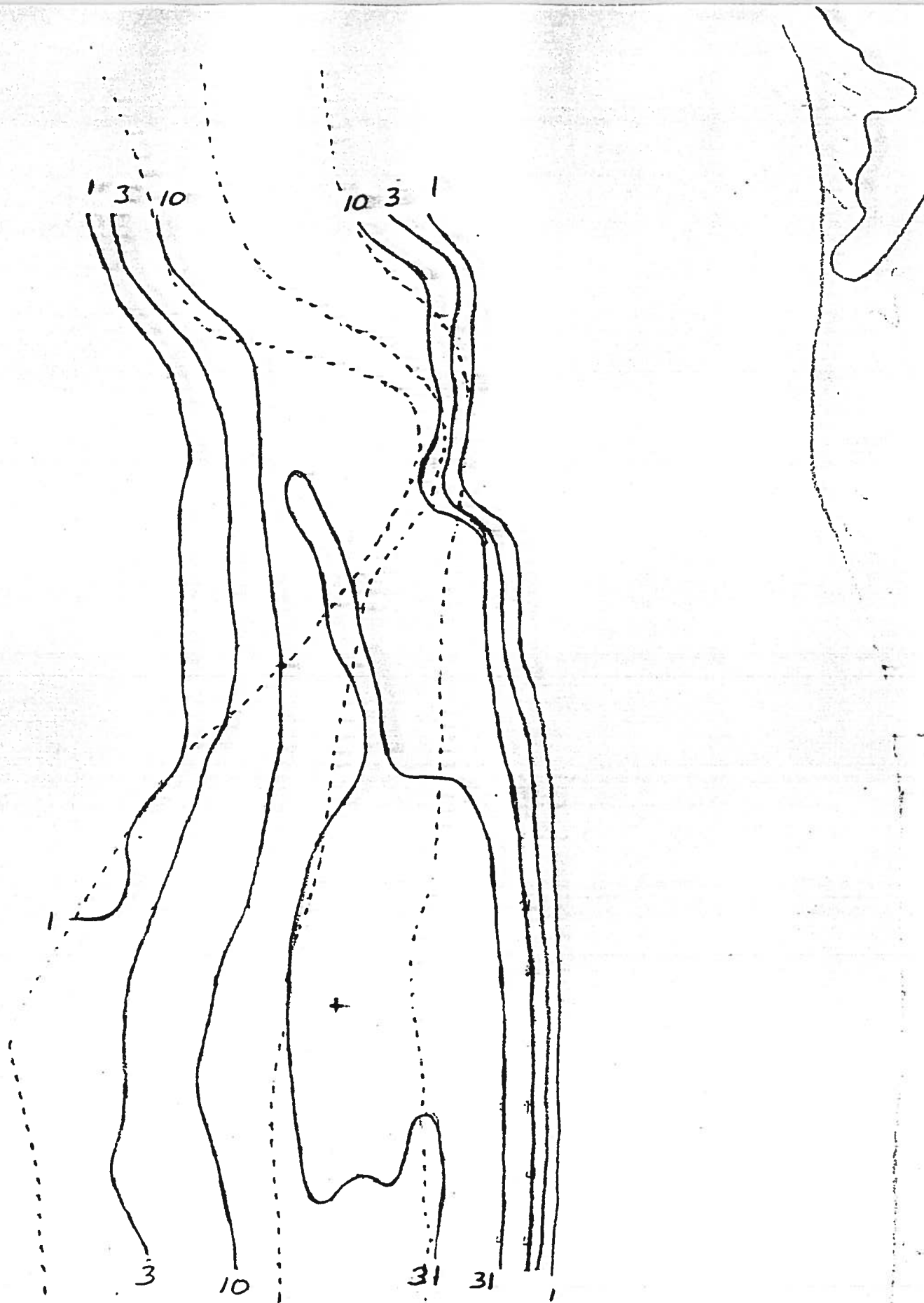
Contours indicate the probability that wastewater with an "age" less than or equal to the indicated lapse time since discharge will be found in the area.



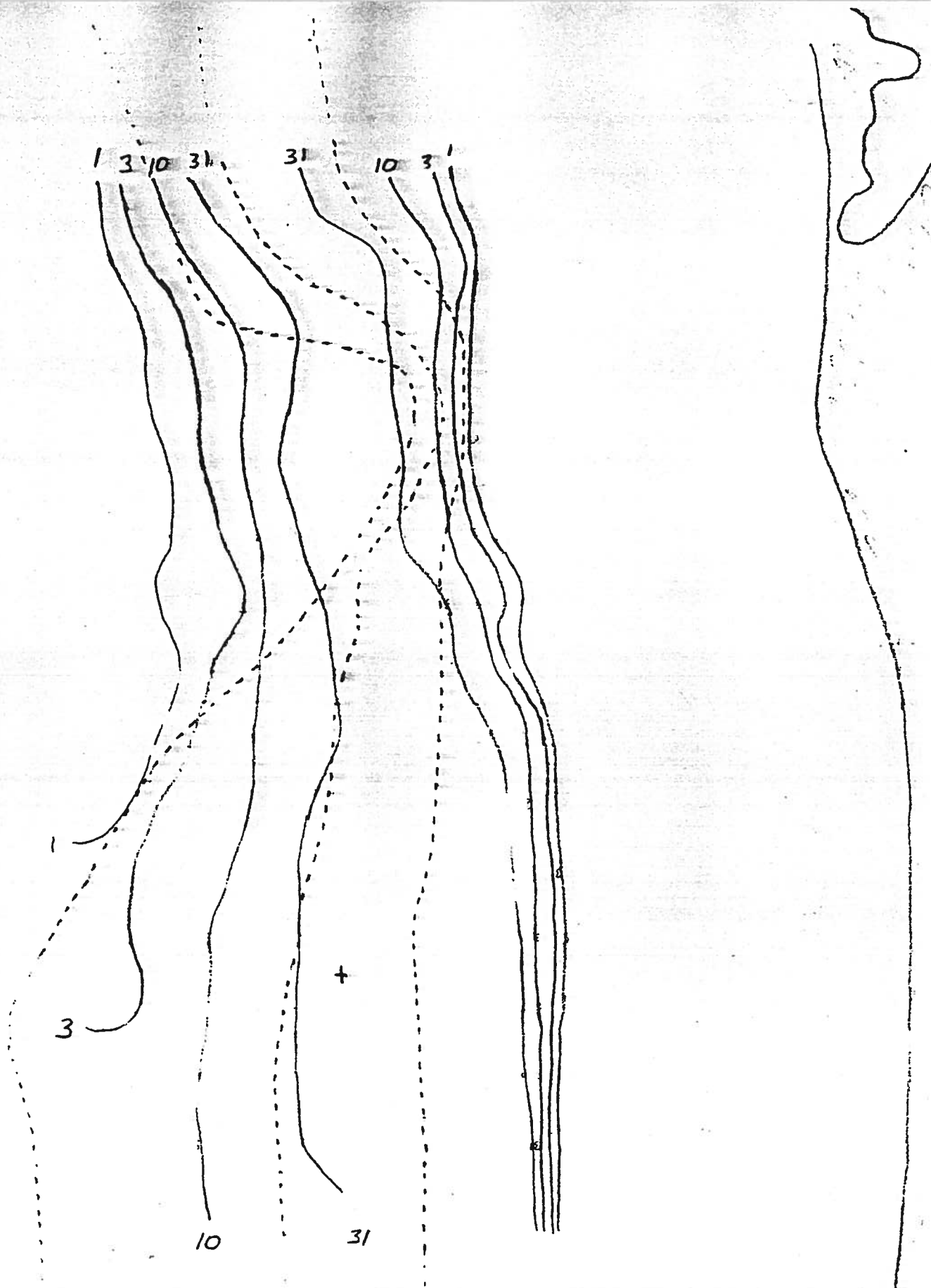
Probabilities for PXYT2D after 6 hours for a
25m deep wastefield - Jan. 9 to Feb. 10, 1986.



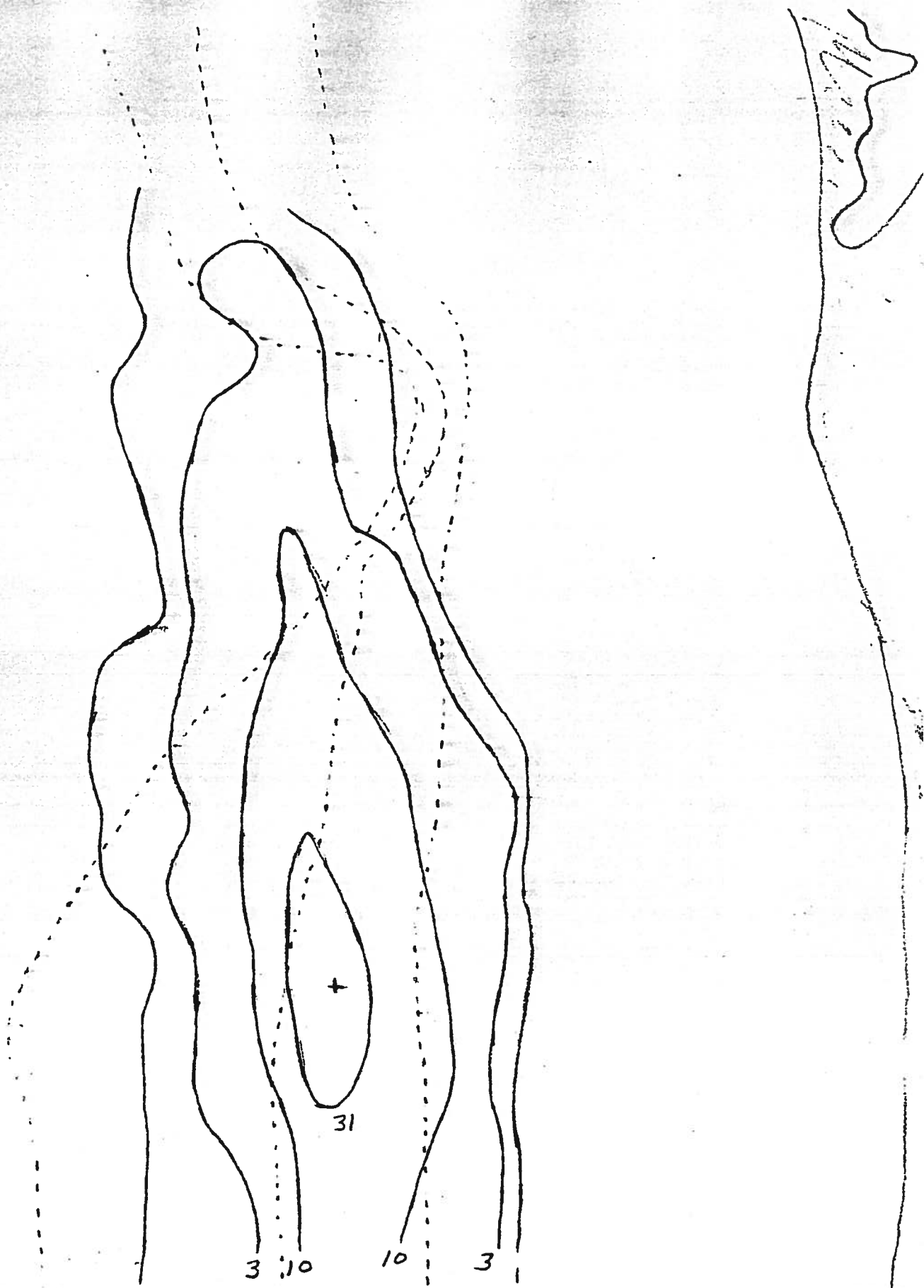
Probabilities for PXYT2D after 12 hours for a
25m deep wastefield - Jan. 9 to Feb. 10, 1986.



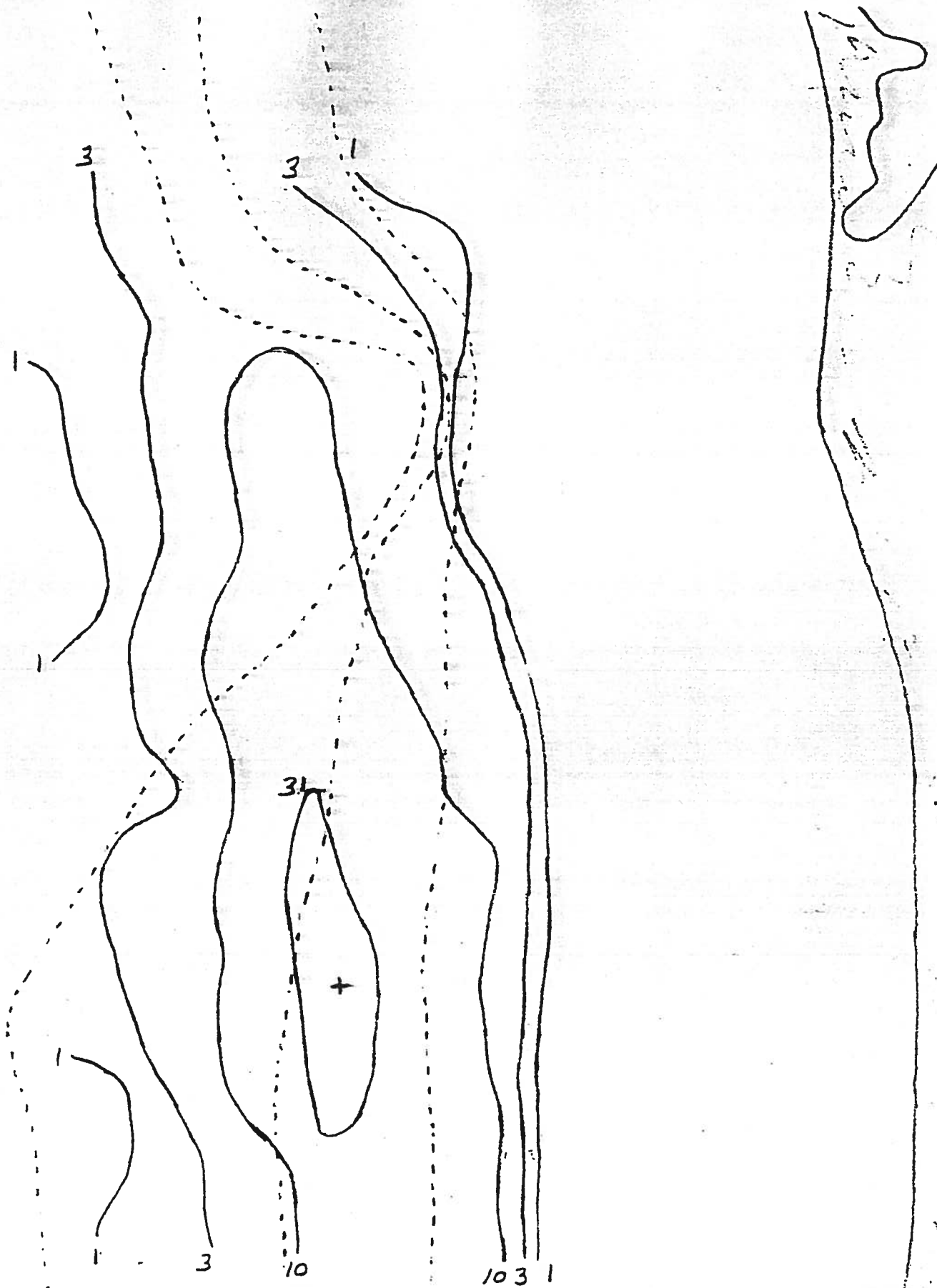
Probabilities for PXYT2D after 24 hours for a
25m deep wastefield - Jan. 9 to Feb. 10, 1986.



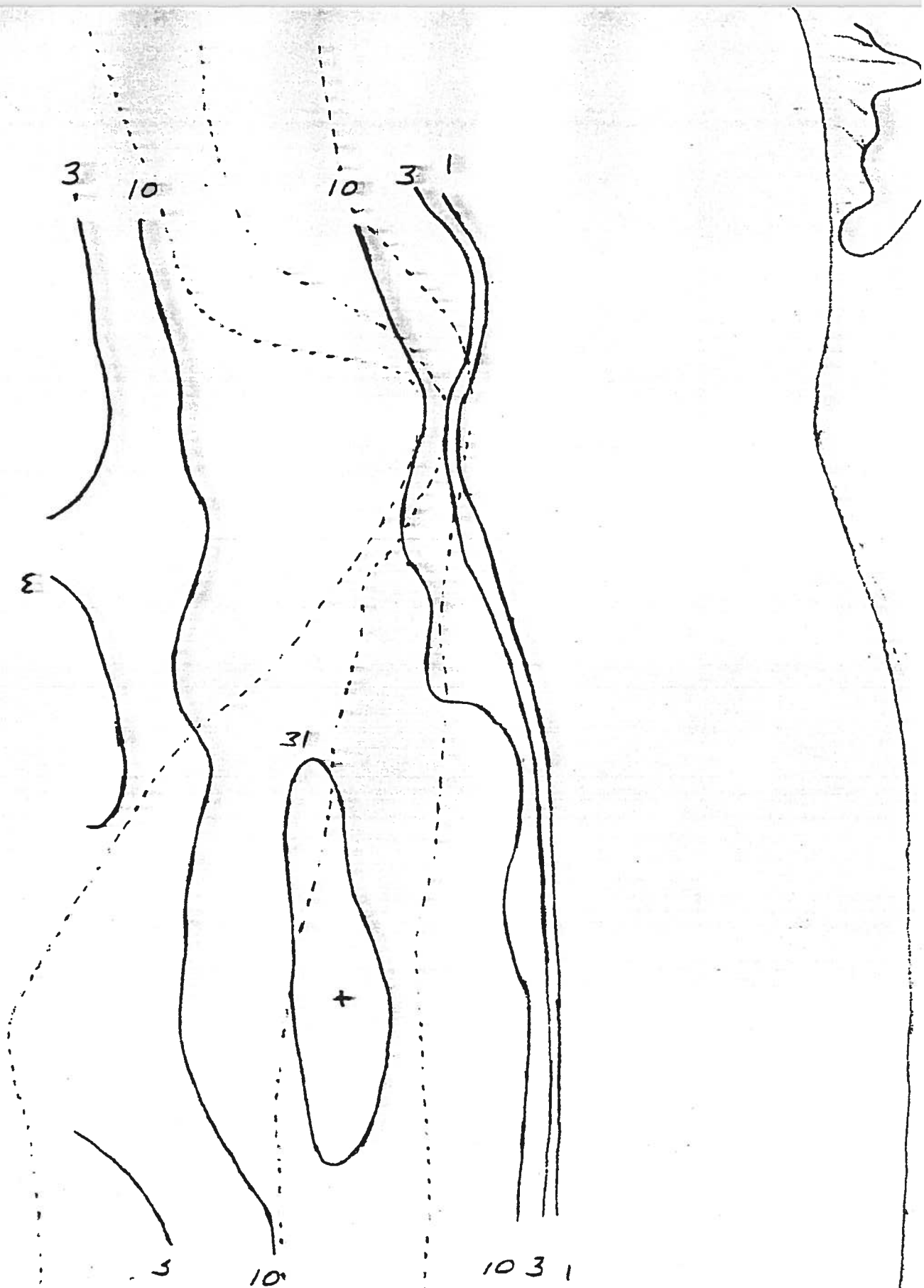
Probabilities for PXYT2D after 48 hours for a
25m deep wastefield - Jan. 9 to Feb. 10, 1986.



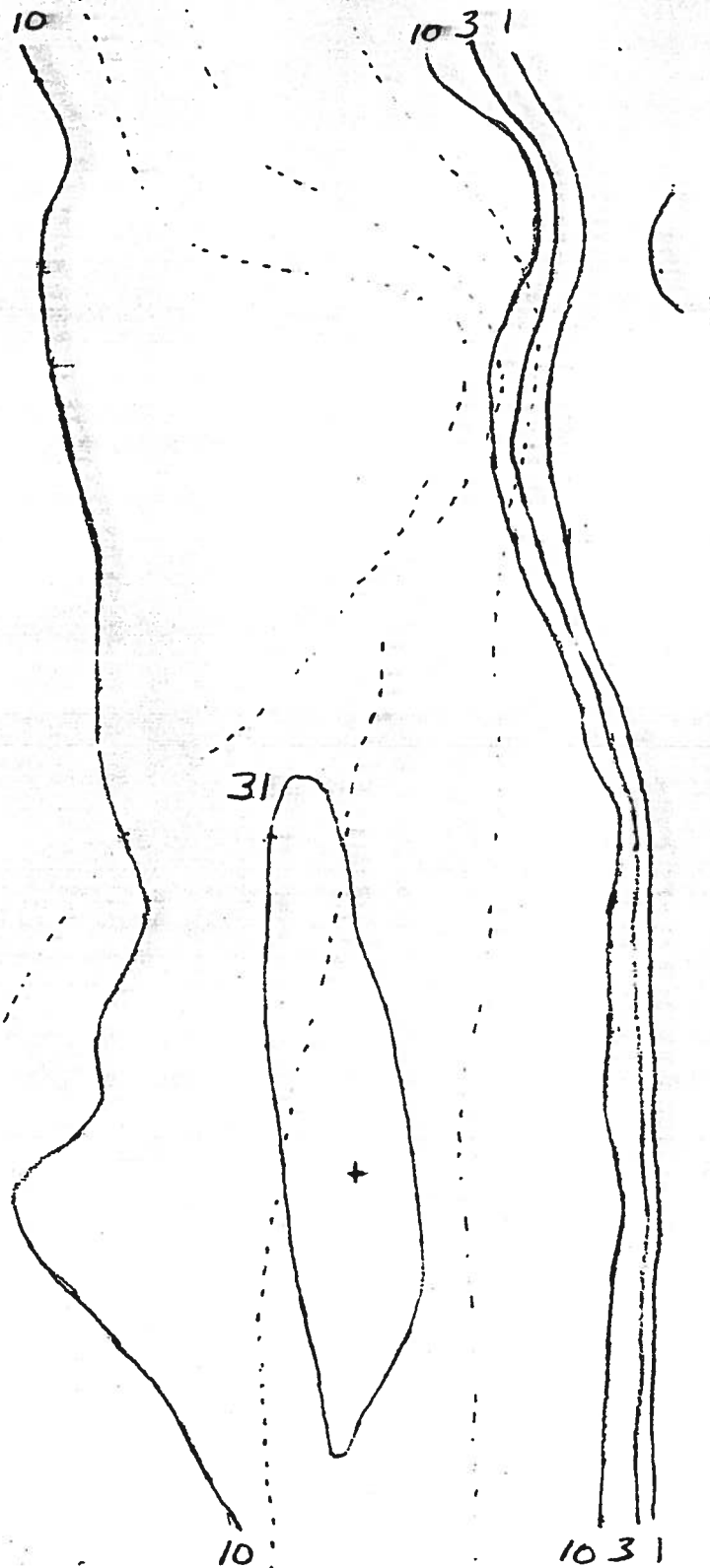
Probabilities for PXYT2D after 6 hours for a
25m deep wastefield - Feb. 27 to April 4, 1986.



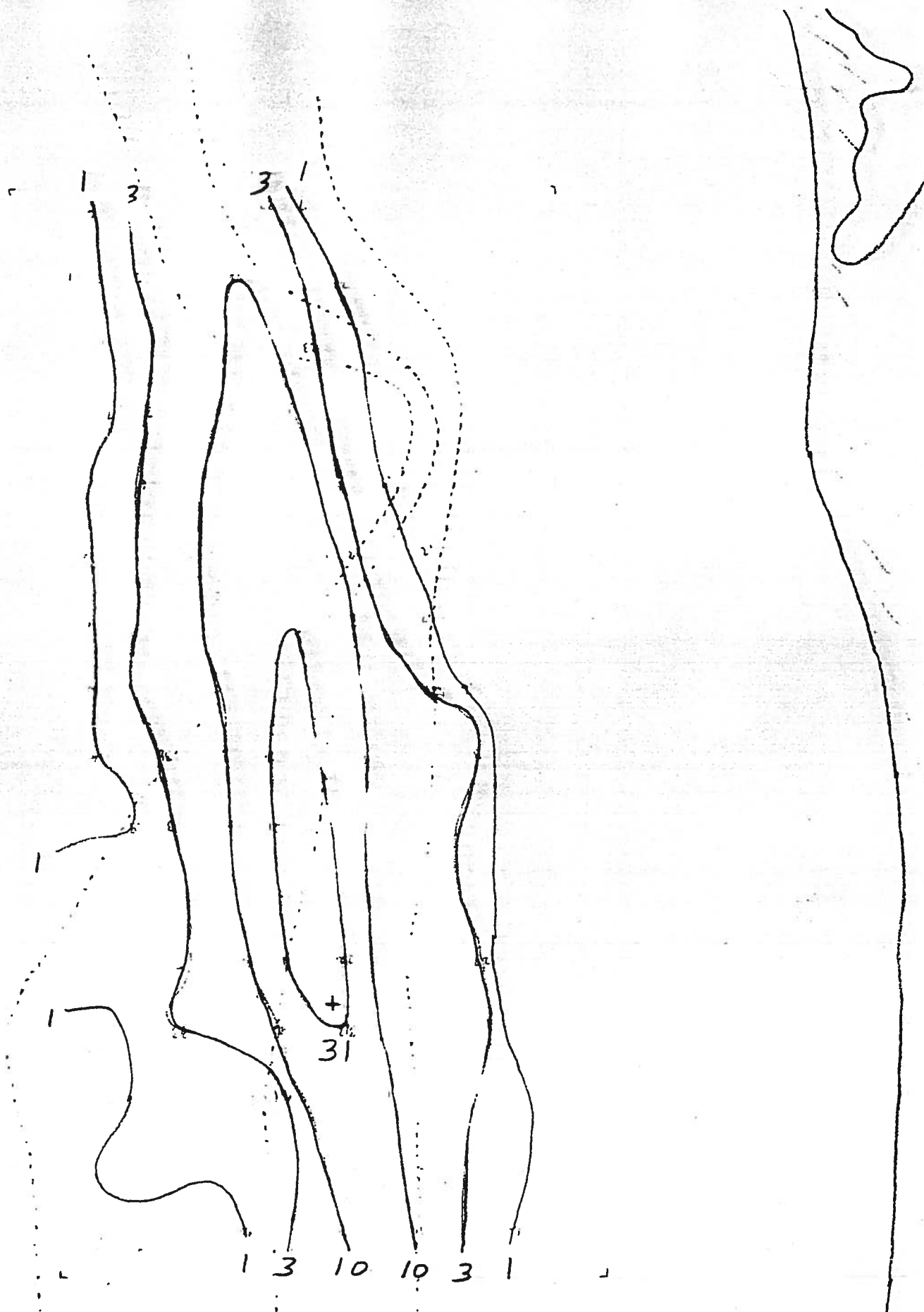
Probabilities for PXYT2D after 12 hours for a
25m deep wastefield - Feb. 27 to April 4, 1986.



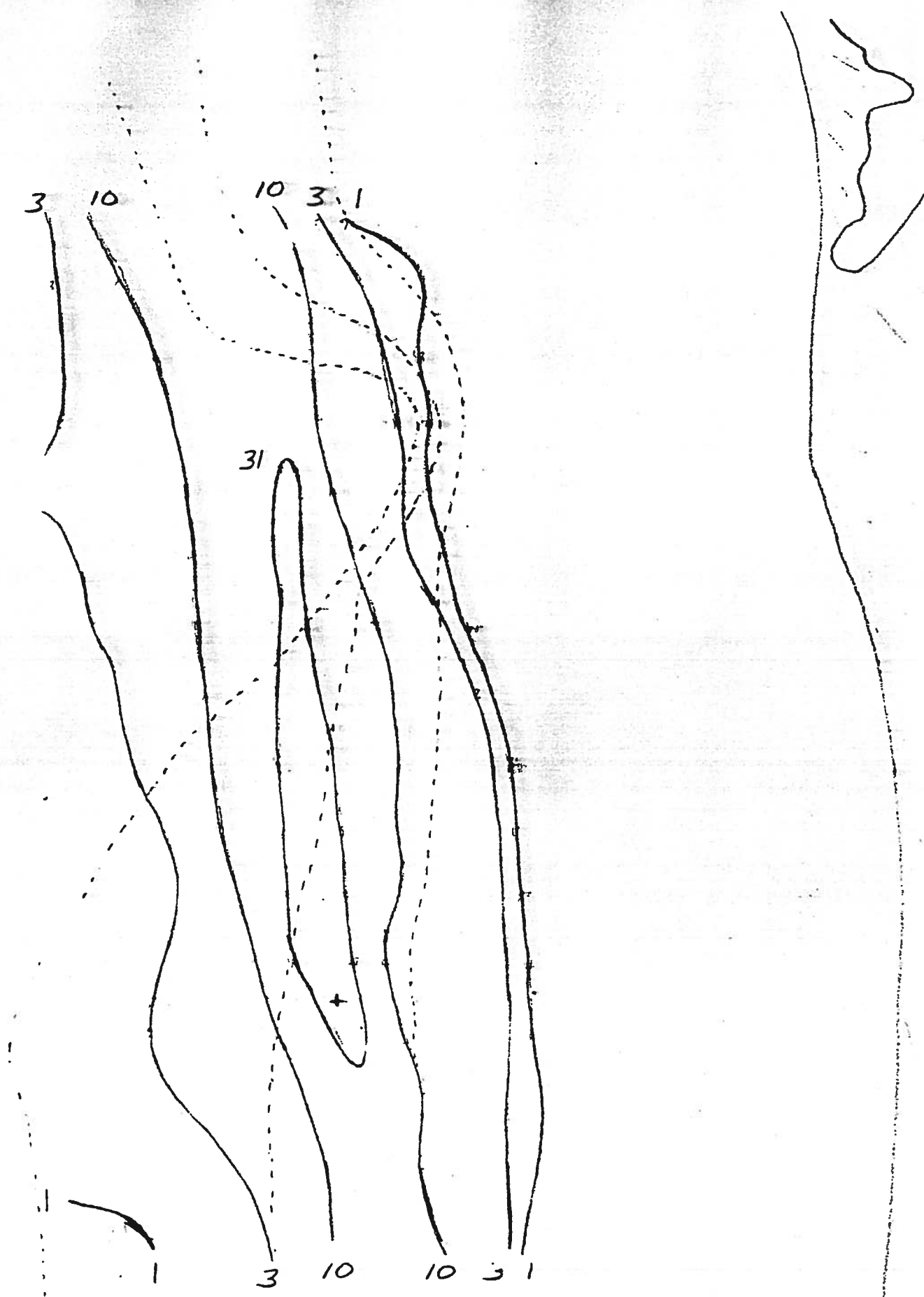
Probabilities for PXYT2D after 24 hours for a
25m deep wastefield - Feb. 27 to April 4, 1986.



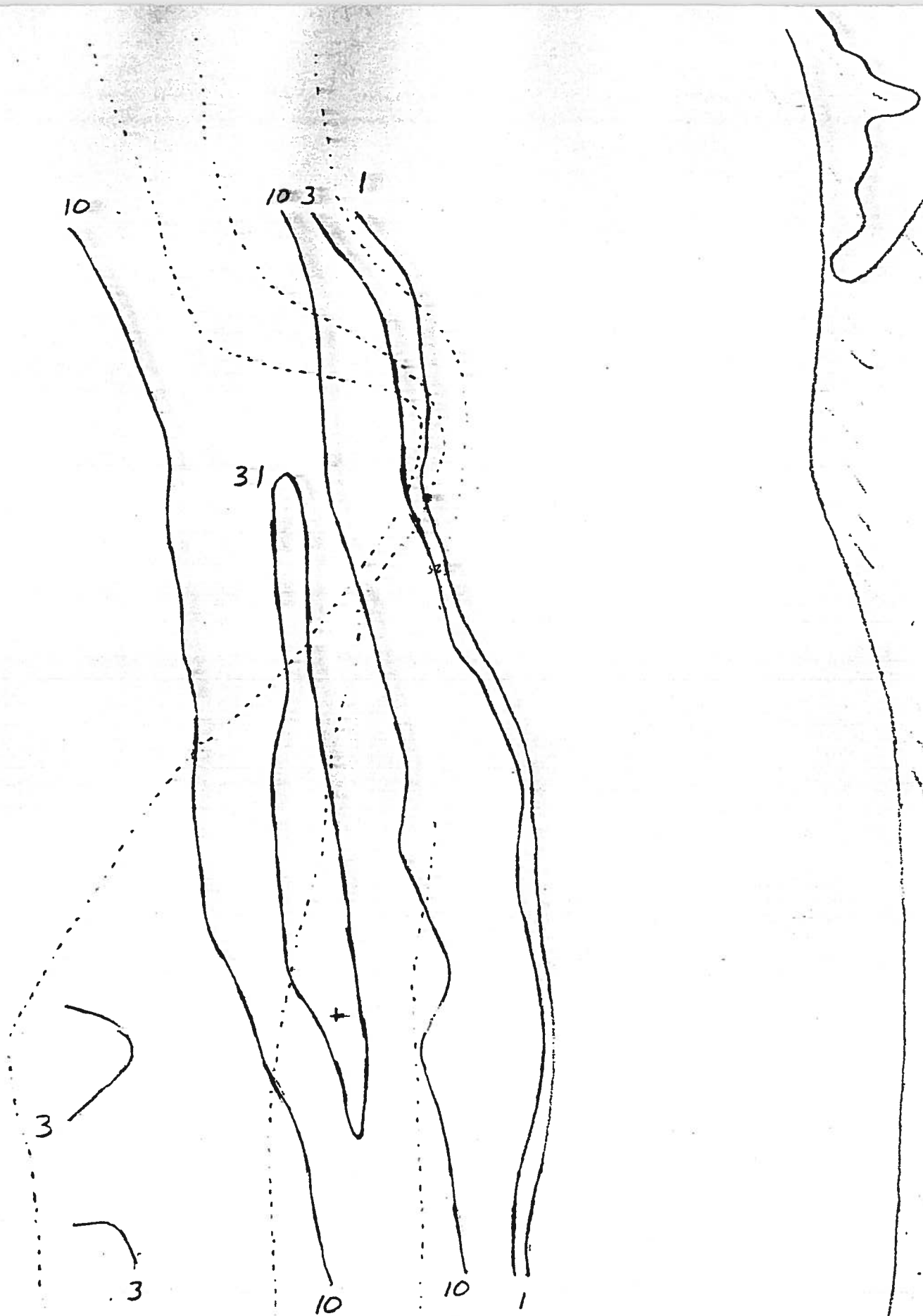
Probabilities for PXYT2D after 48 hours for a
25m deep wastefield - Feb. 27 to April 4, 1986.



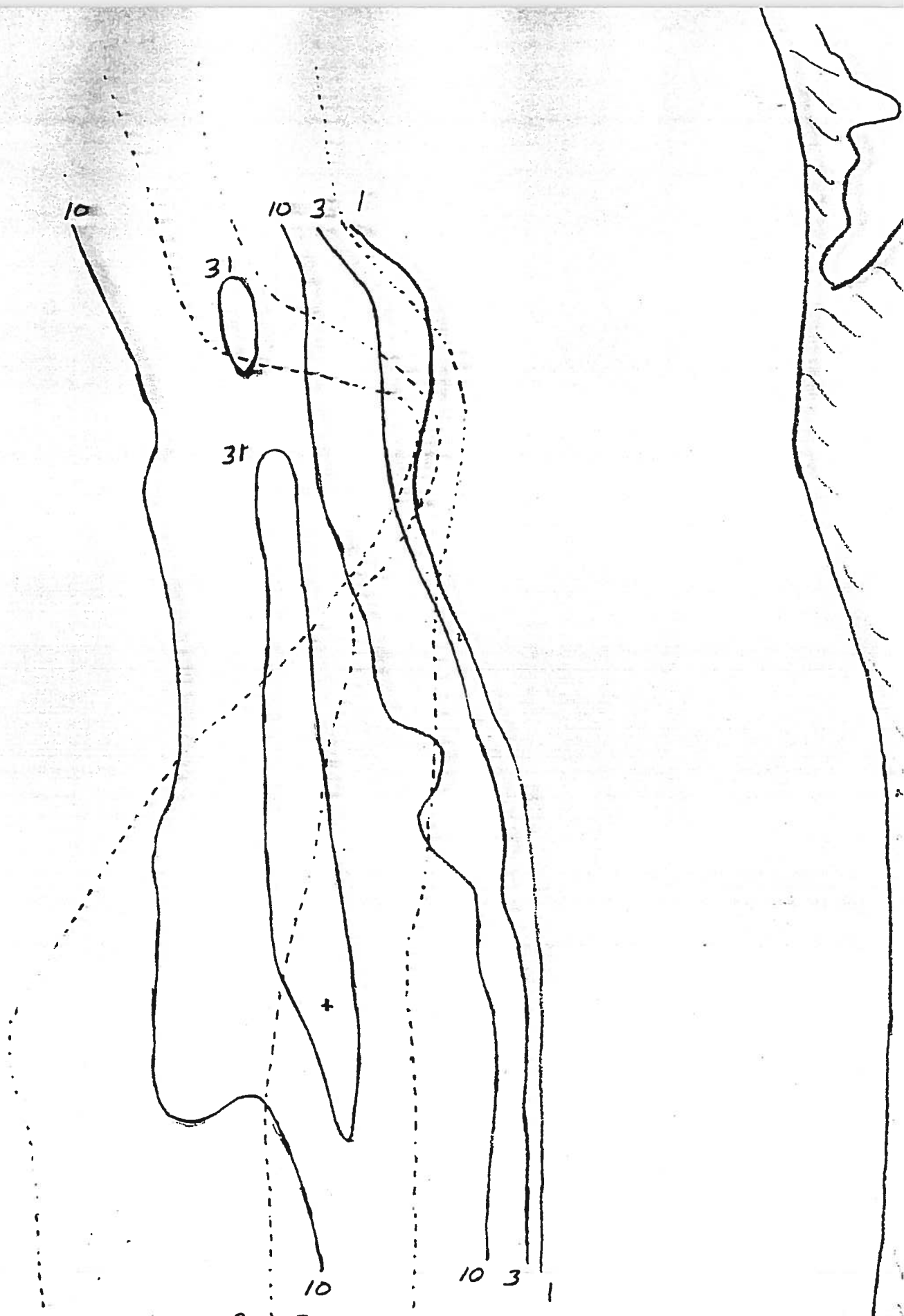
Probabilities for PXYT2D after 6 hours for a
25m deep wastefield - July 13 to Aug. 16, 1986.



Probabilities for PXYT2D after 12 hours for a
25m deep wastefield - July 13 to Aug. 16, 1986.



Probabilities for PXYT2D after 24 hours for a
25m deep wastefield - July 13 to Aug. 16, 1986.

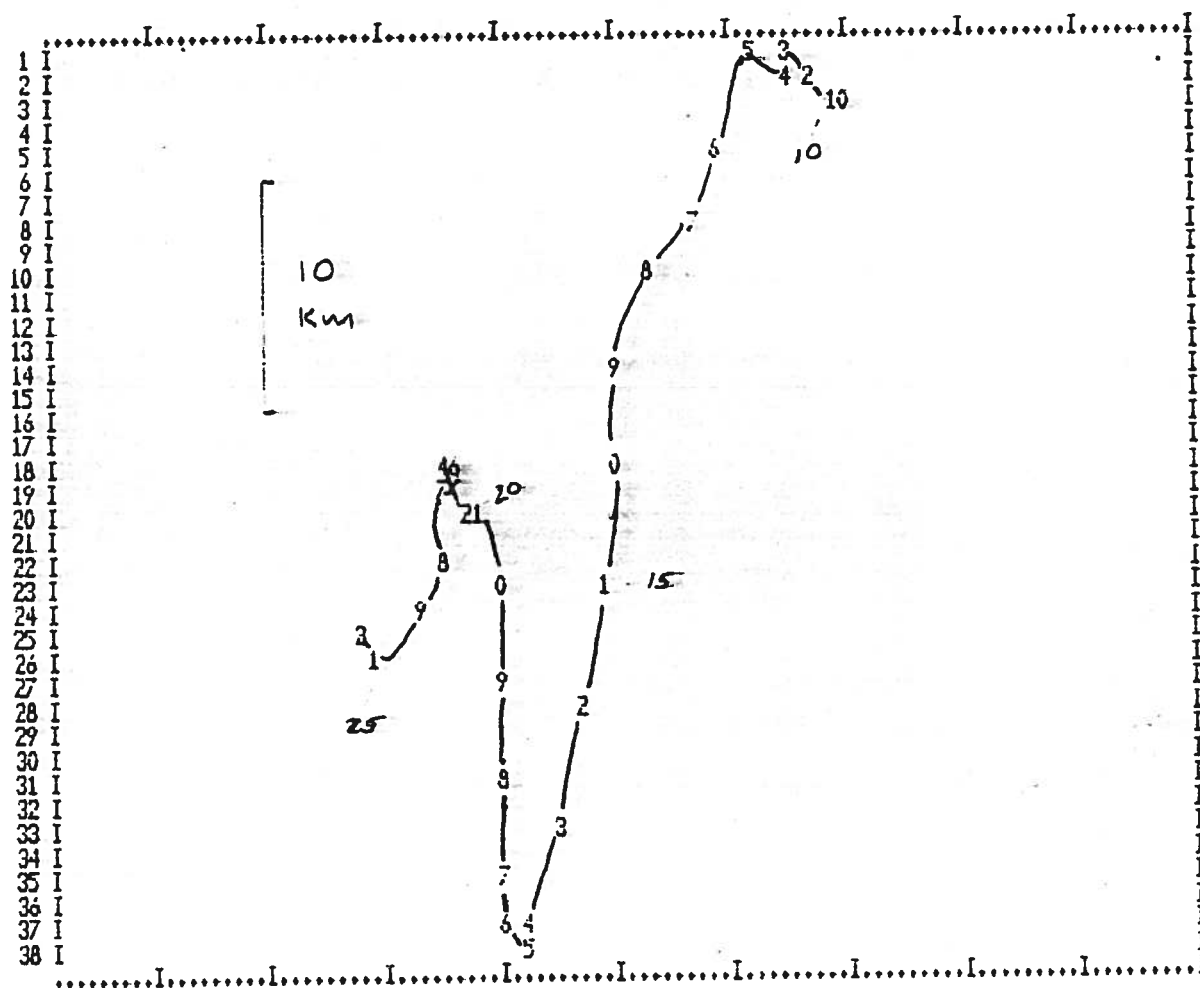


Probabilities for PXYT2D after 48 hours for a
25m deep wastefield - July 13 to Aug. 16, 1986.

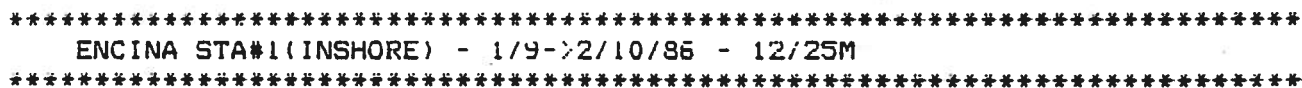
APPENDIX F

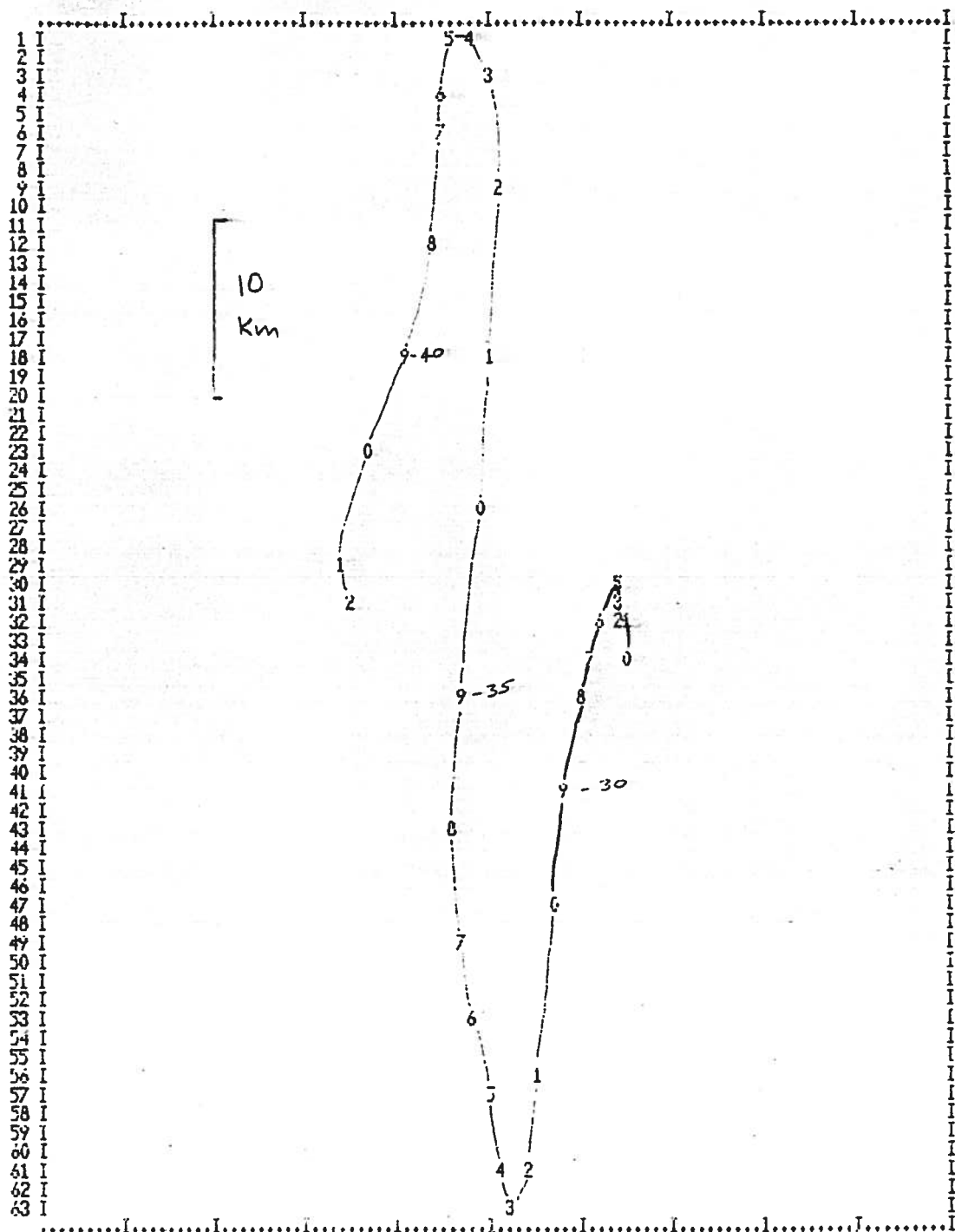
PROGRESSIVE VECTOR DIAGRAM

Numbers connected by lines indicate 12-hour intervals, offset numbers indicate Julian day. Downcoast movements are to the top of the page, offshore movements are to the right.

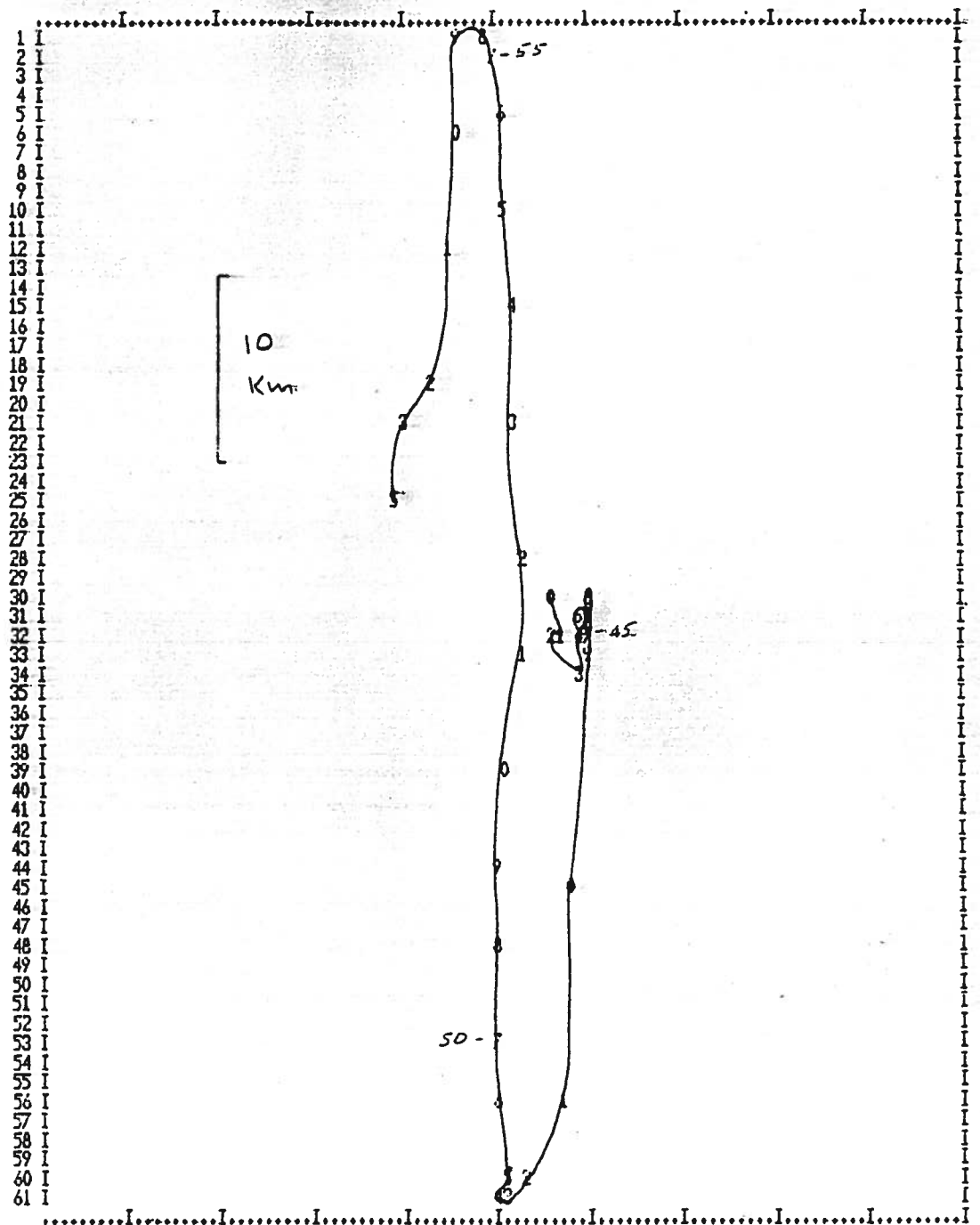


 ENCINA STA#1 (INSHORE) - 1/9->2/10/86 - 12/25M

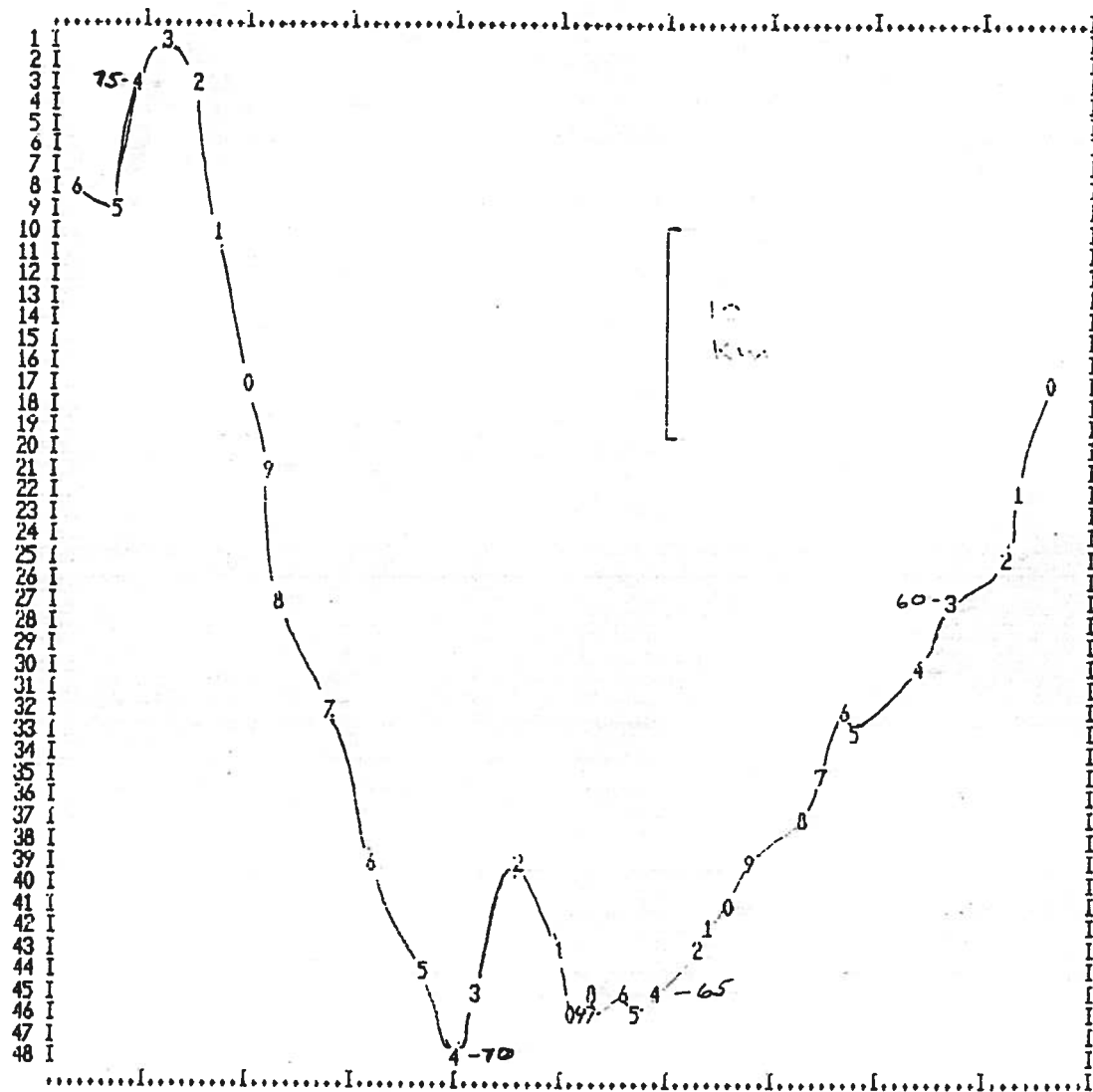




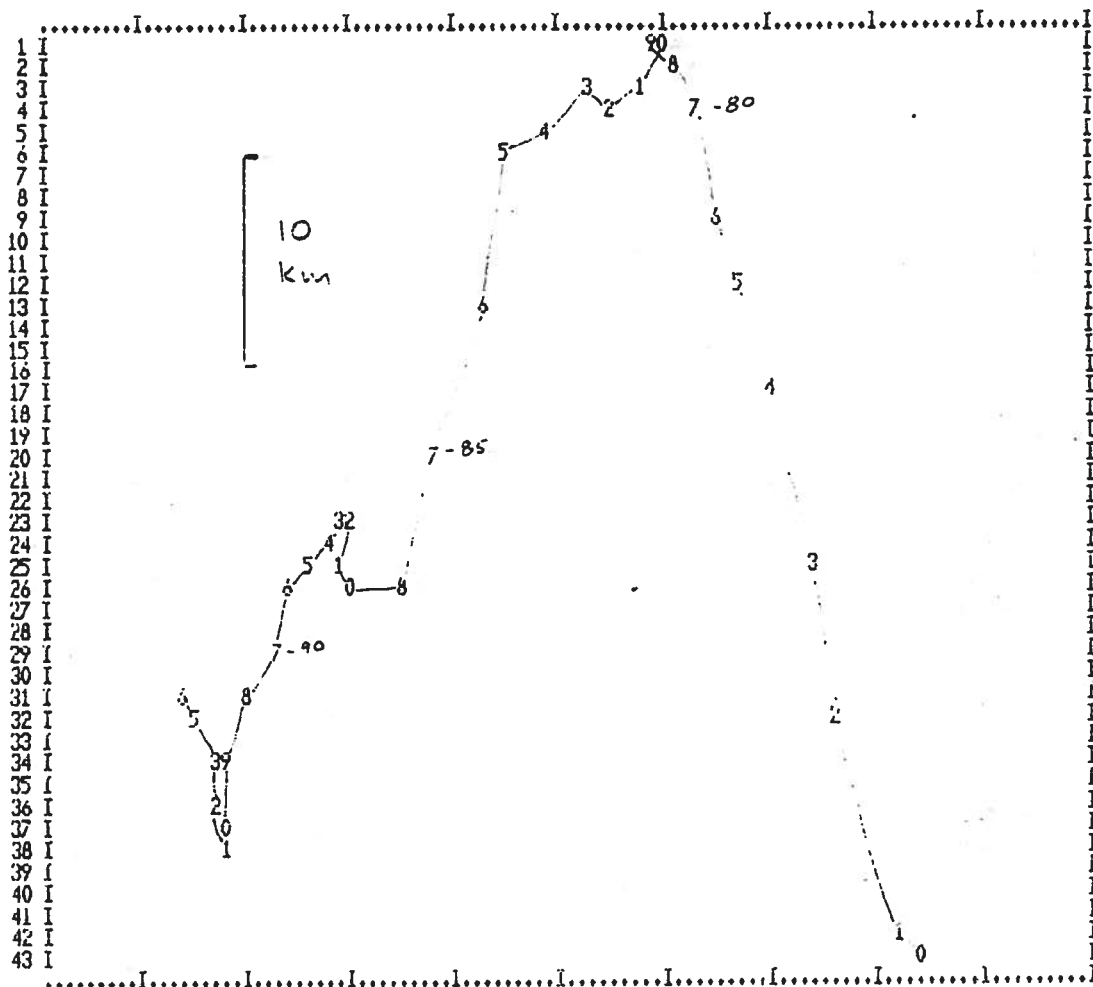
 ENCINA STA#1 (INSHORE) - 1/9->2/10/86 - 12/25M



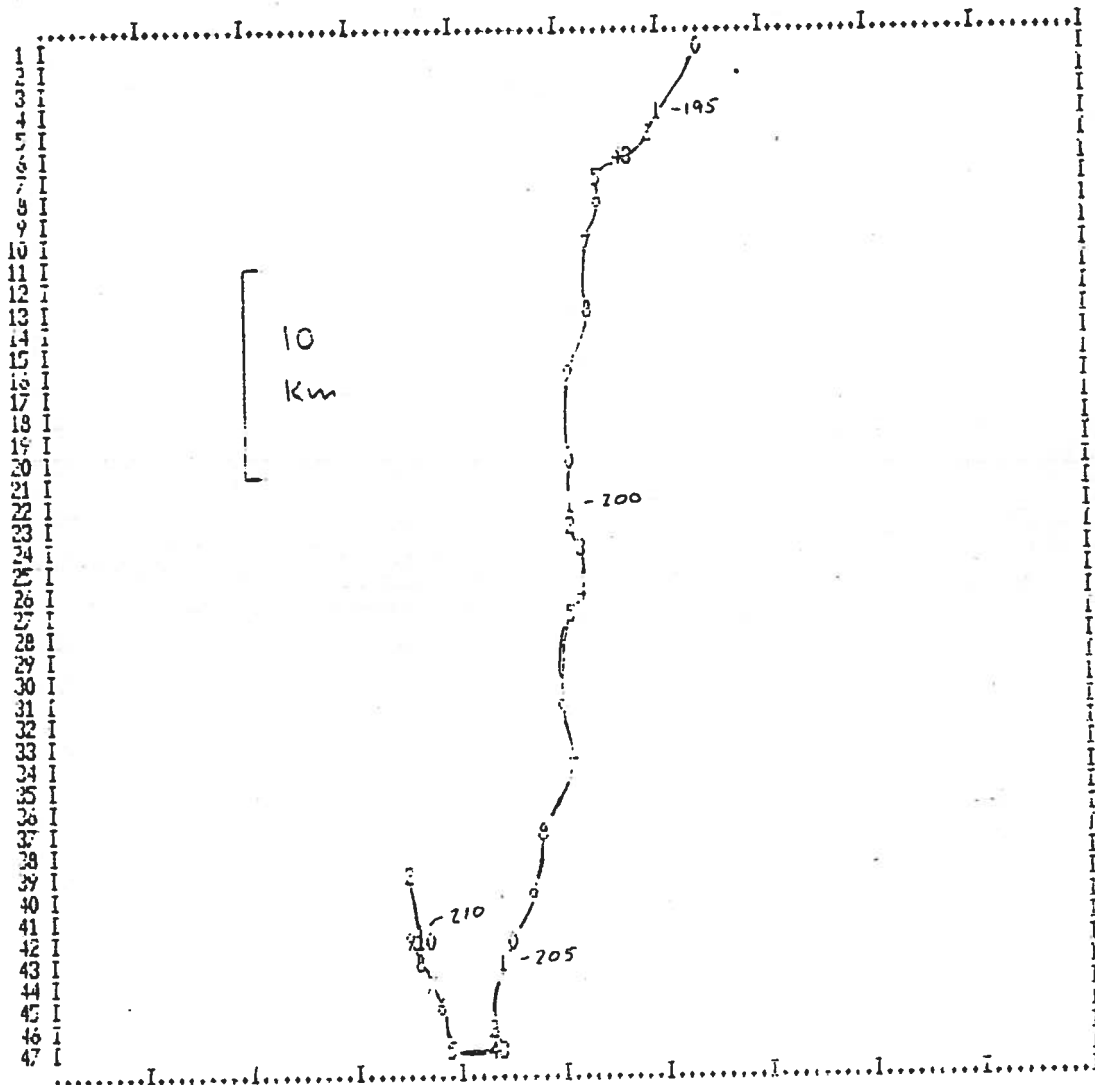
 ENCINA (STAI-INSIDE) - 2/10->2/27/86 - 12/25M



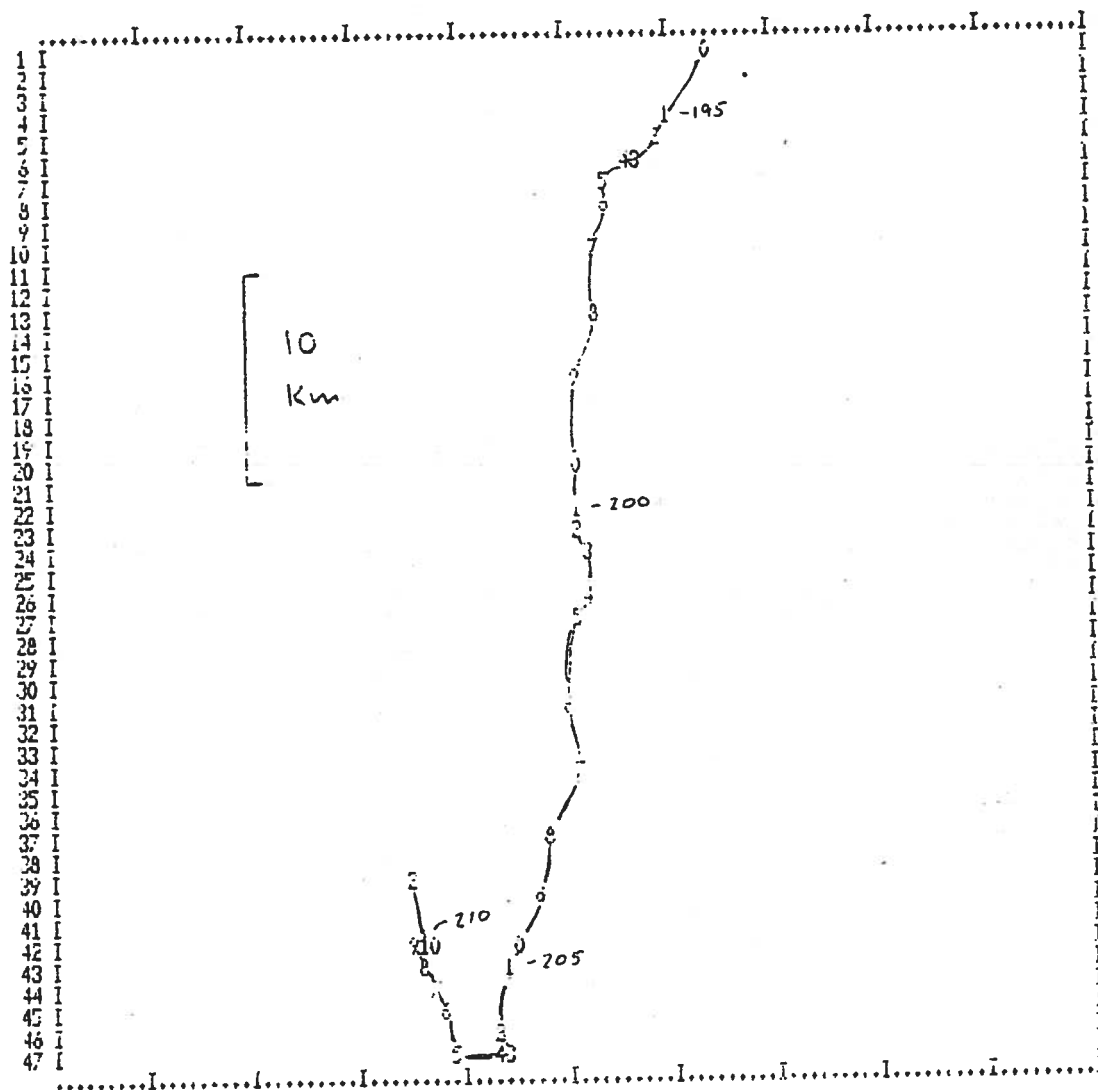
 ENCINA STA1 (INSIDE) - 2/27 -> 4/4/86 - 12.5/25M



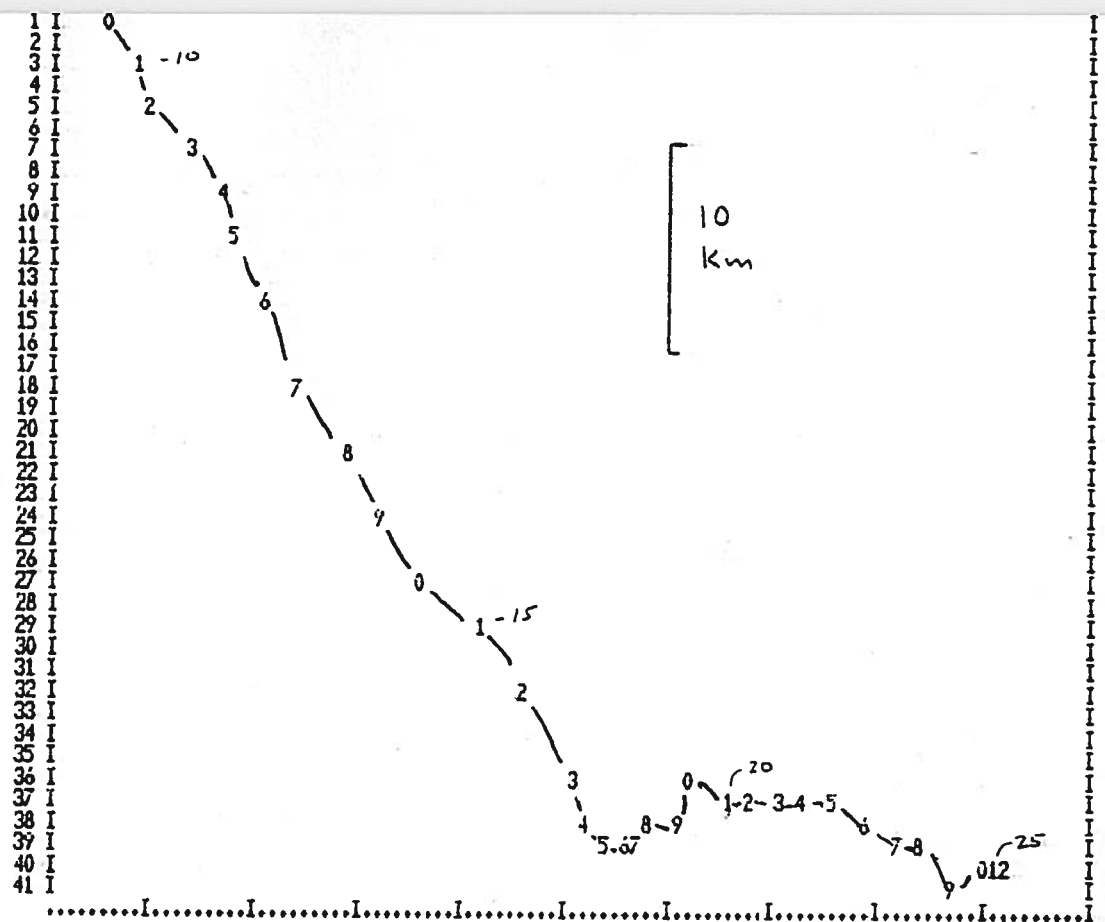
 ENCINA STA1 (INSIDE) - 2/27 -> 4/4/86 - 12.5/25M



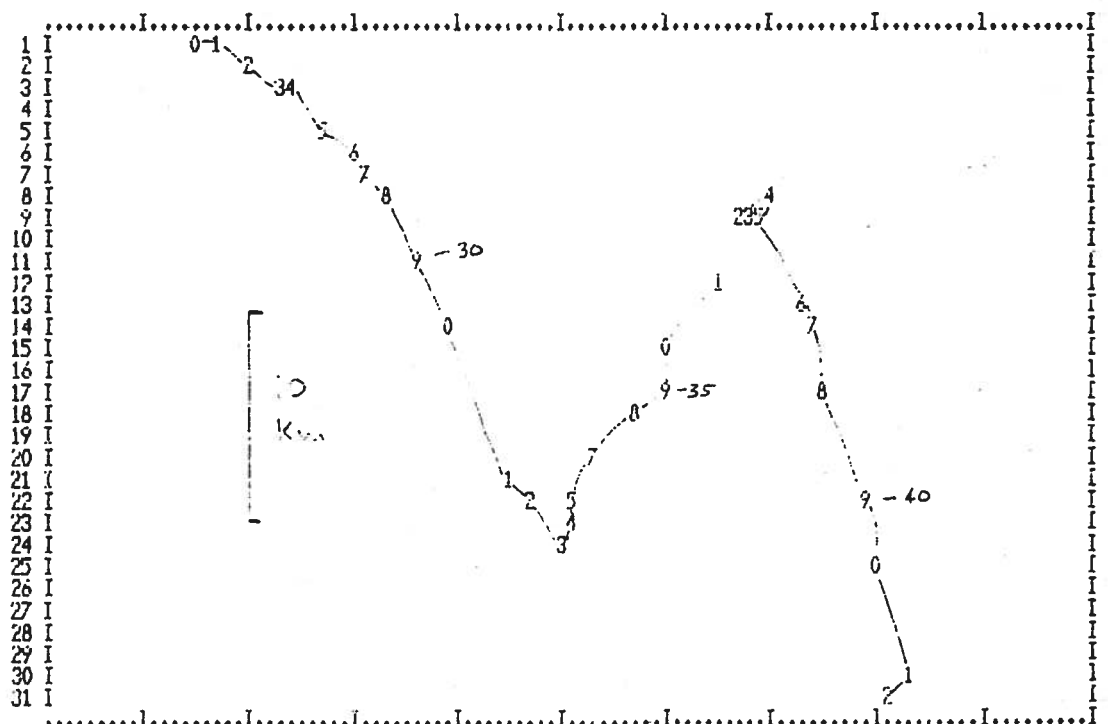
 ENCINA (STA1 INSHORE) - 7/13-28/15/86 - 12.5/25M #3004



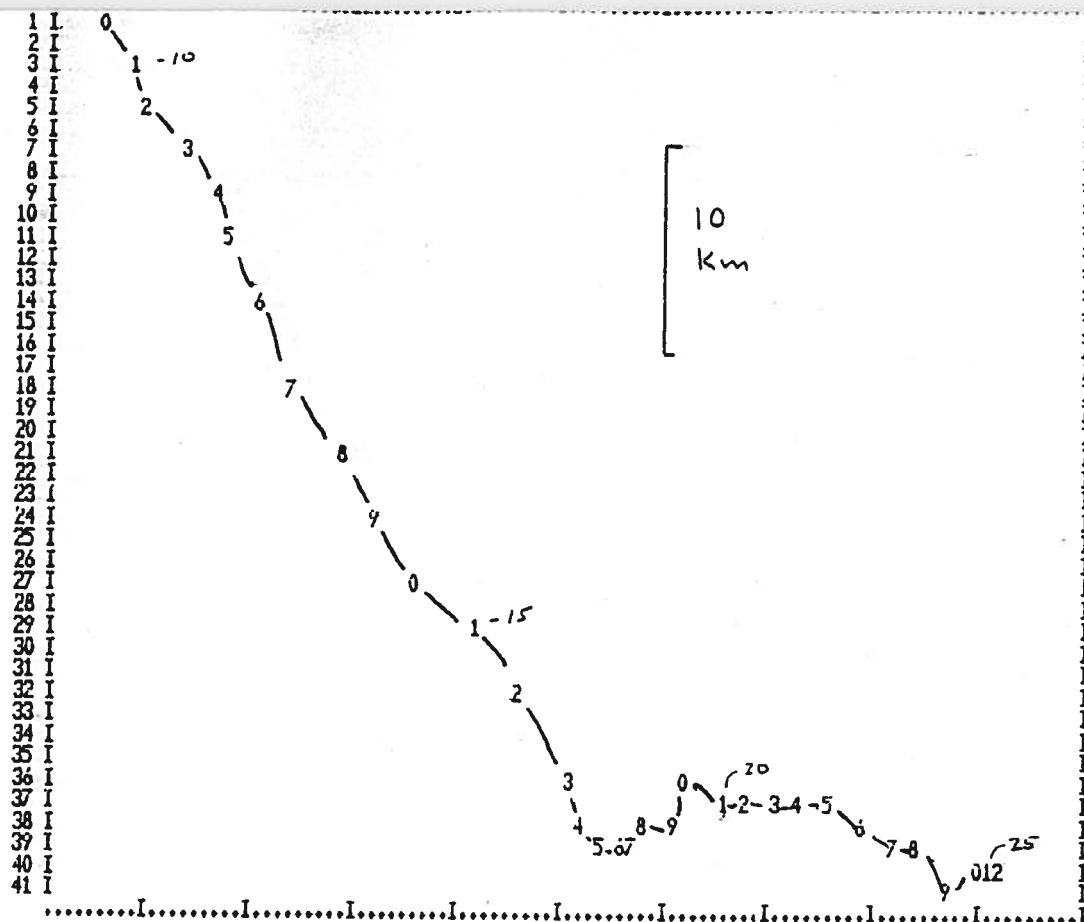
 ENCINA (STAI INSHORE) - 7/13-28/15/86 - 12.5/25M #8004



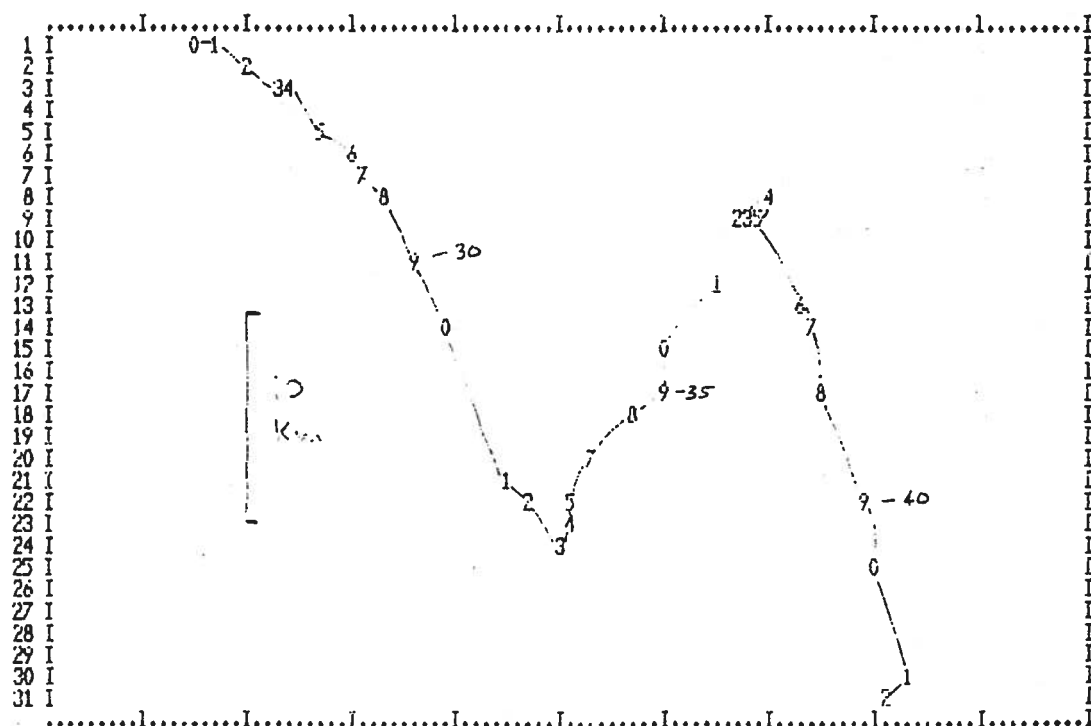
 ENCINA STA#1 (INSHORE) - 1/9->2/10/86 - +2/25M



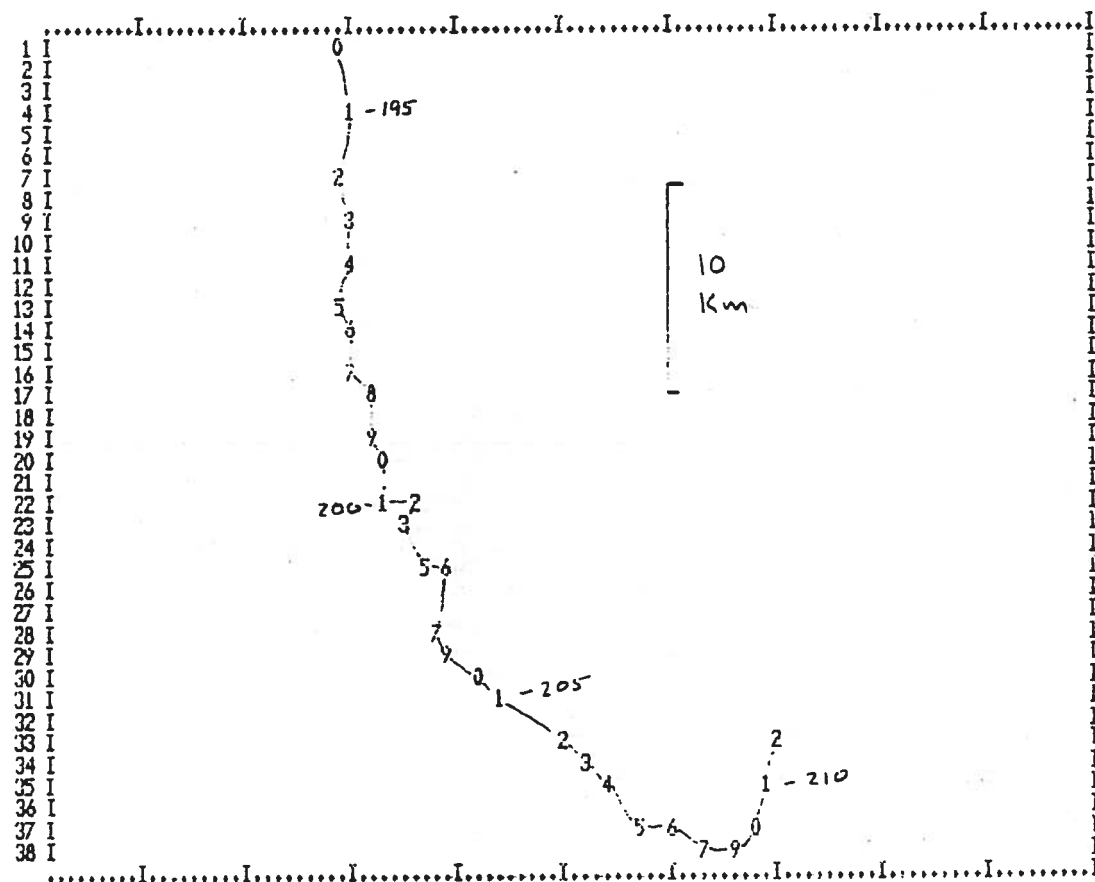
 ENCINA STA#1 (INSHORE) - 1/9->2/10/86 - +2/25M



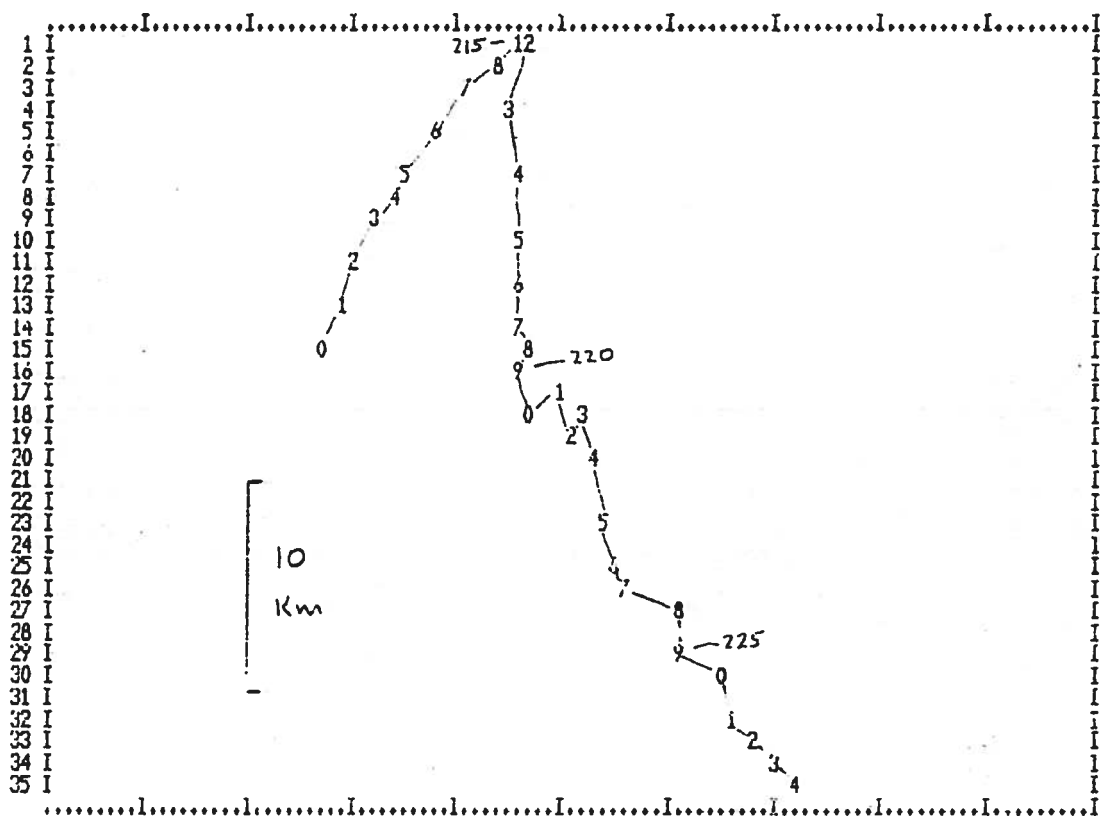
 ENCINA STA#1 (INSHORE) - 1/9->2/10/86 - +2/25M



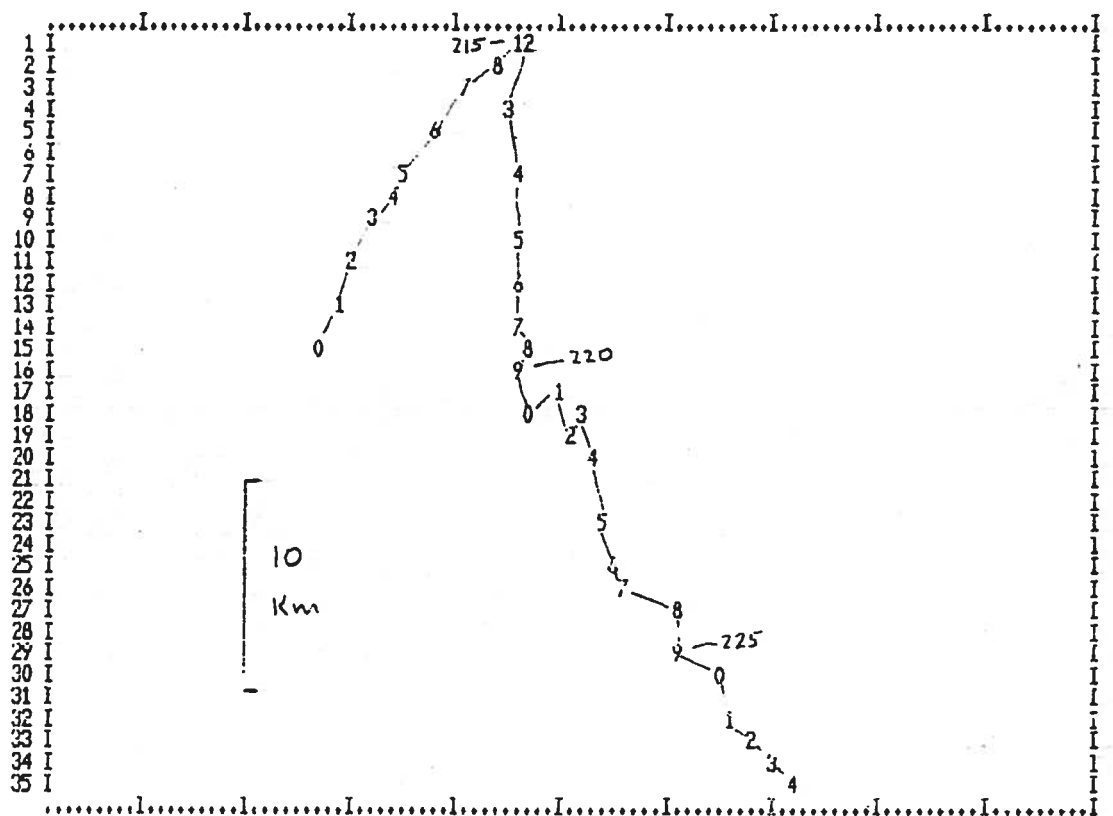
 ENCINA STA#1 (INSHORE) - 1/4->2/10/86 - +2/25M



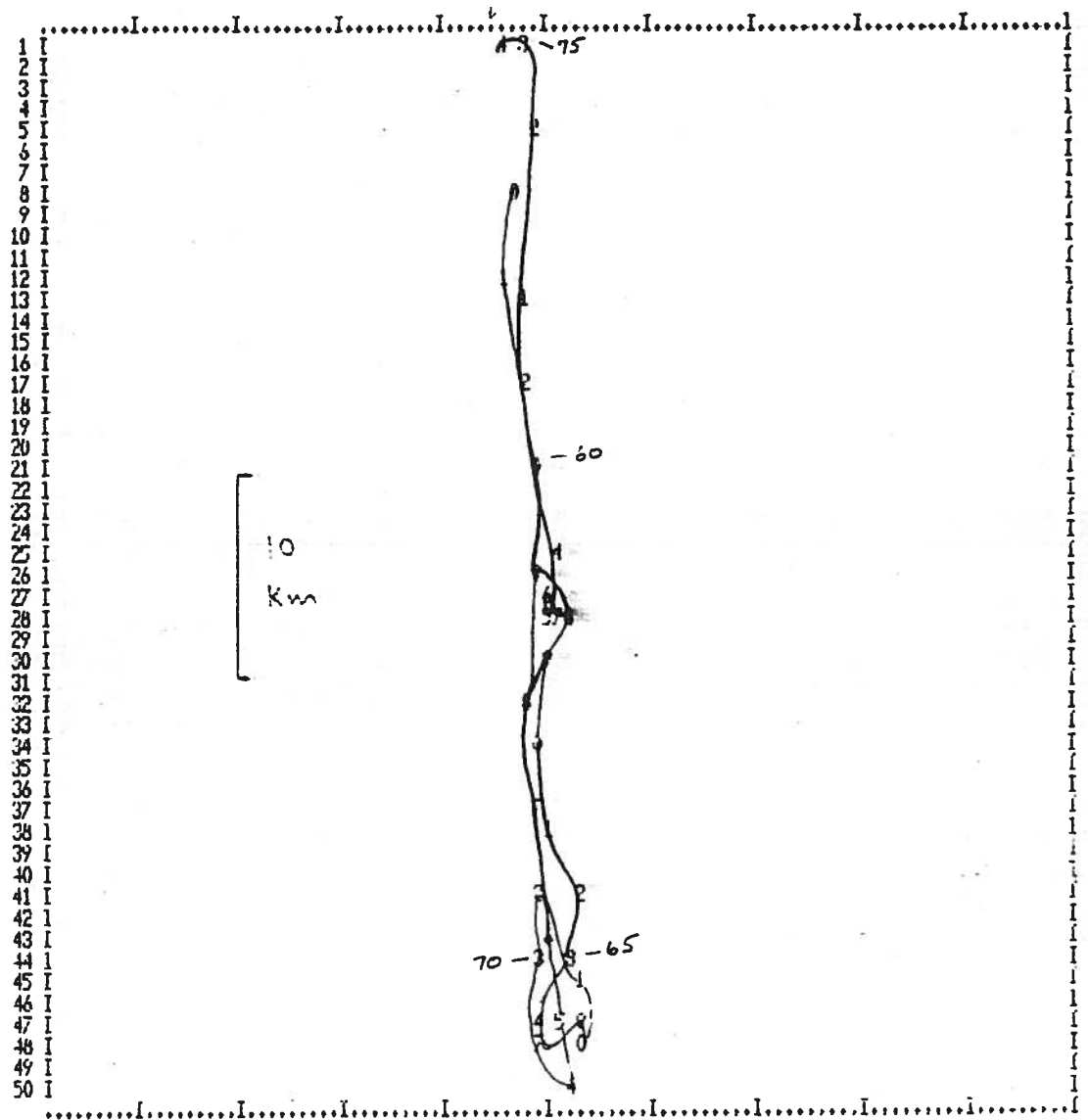
 ENCINA (STA1 INSHORE) - 7/13->8/15/86 - 23/25M #8404



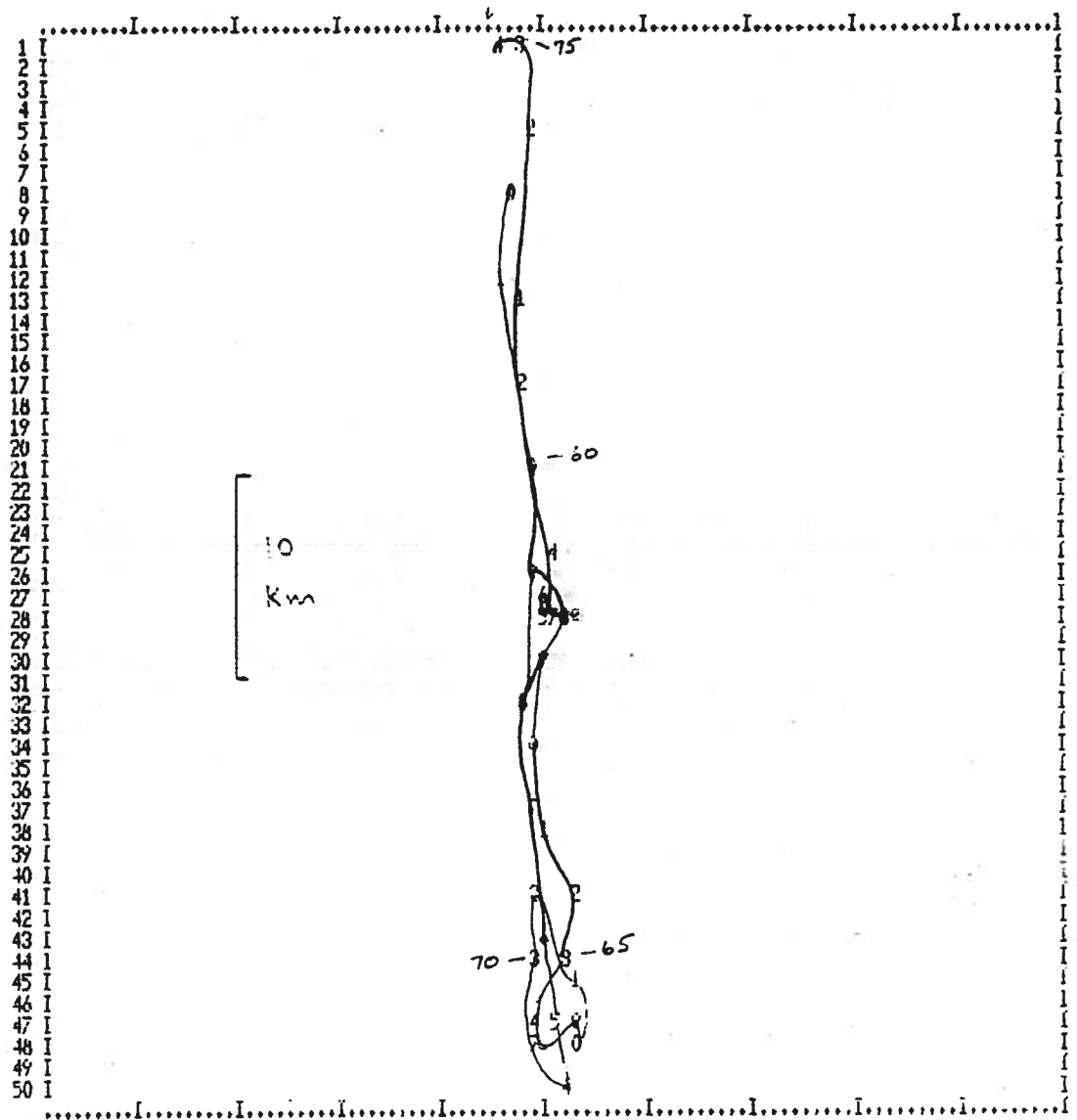
 ENCINA (STA1 INSHORE) - 7/13-8/15/86 - 23/25M #8404



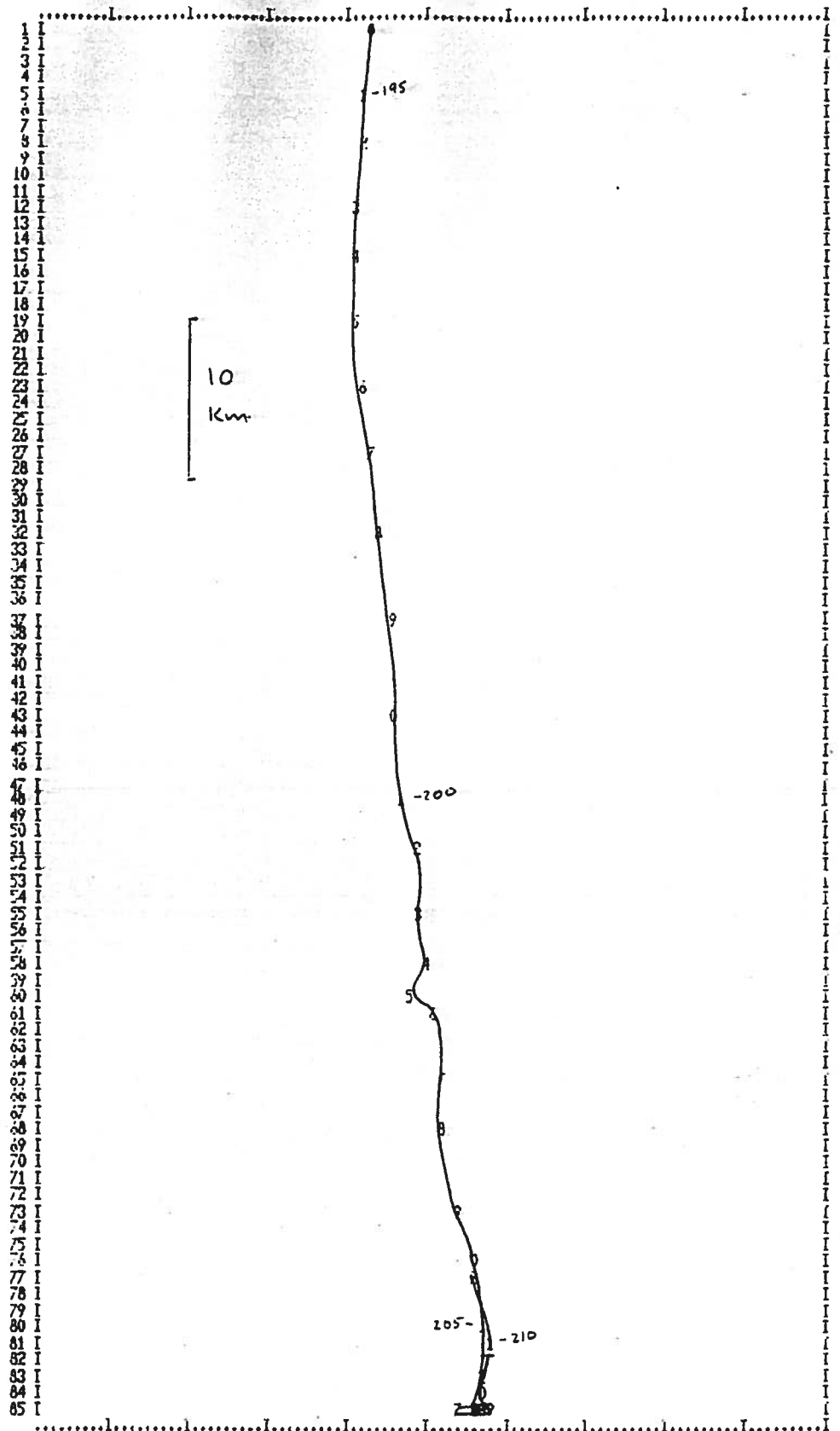
 ENCINA (STA1 INSHORE) - 7/13-8/15/86 - 23/25M #8404



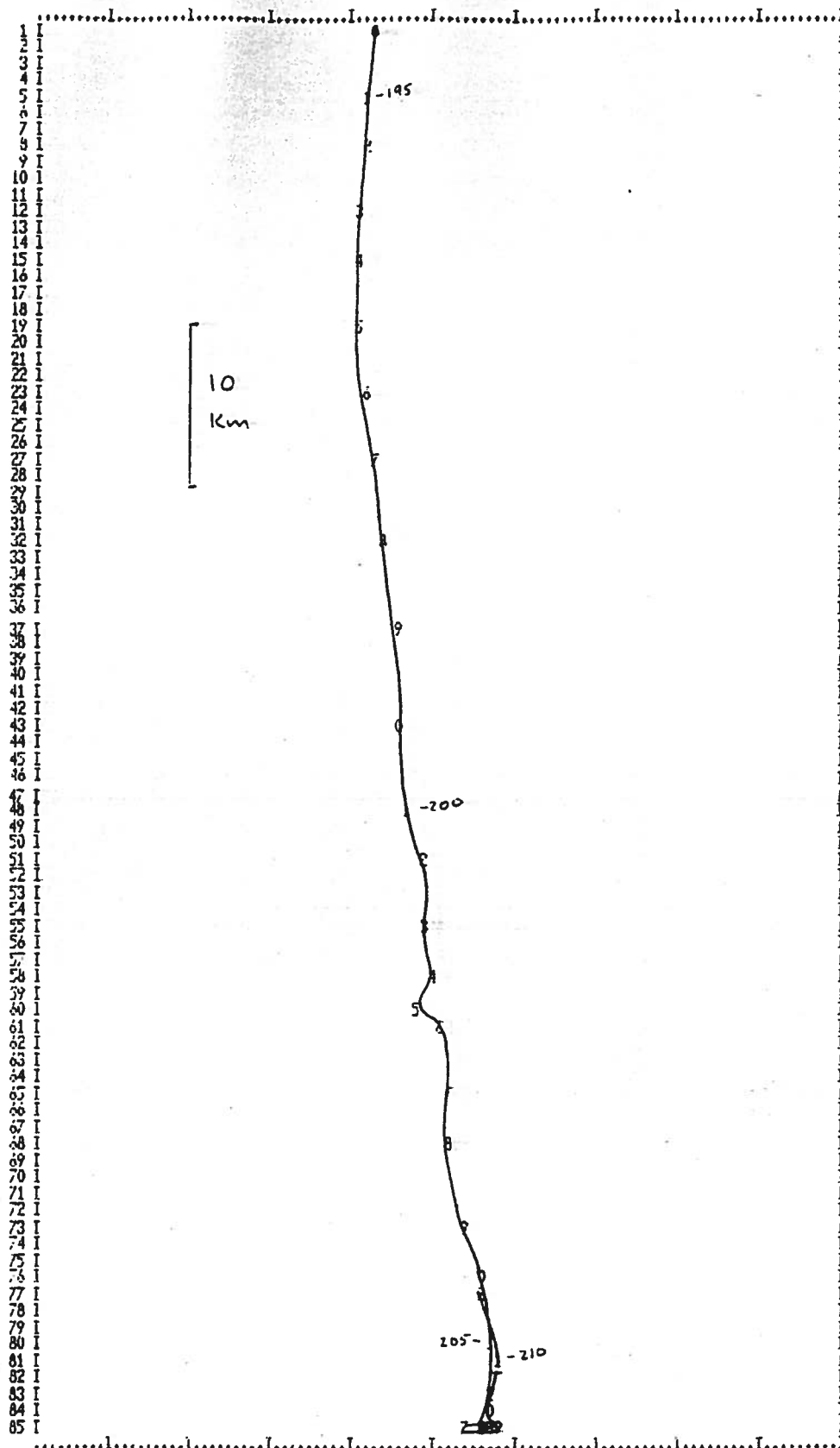
ENCINA STA2 (OUTFALL) - 2/27 -> 4/4/86 - 20/46M



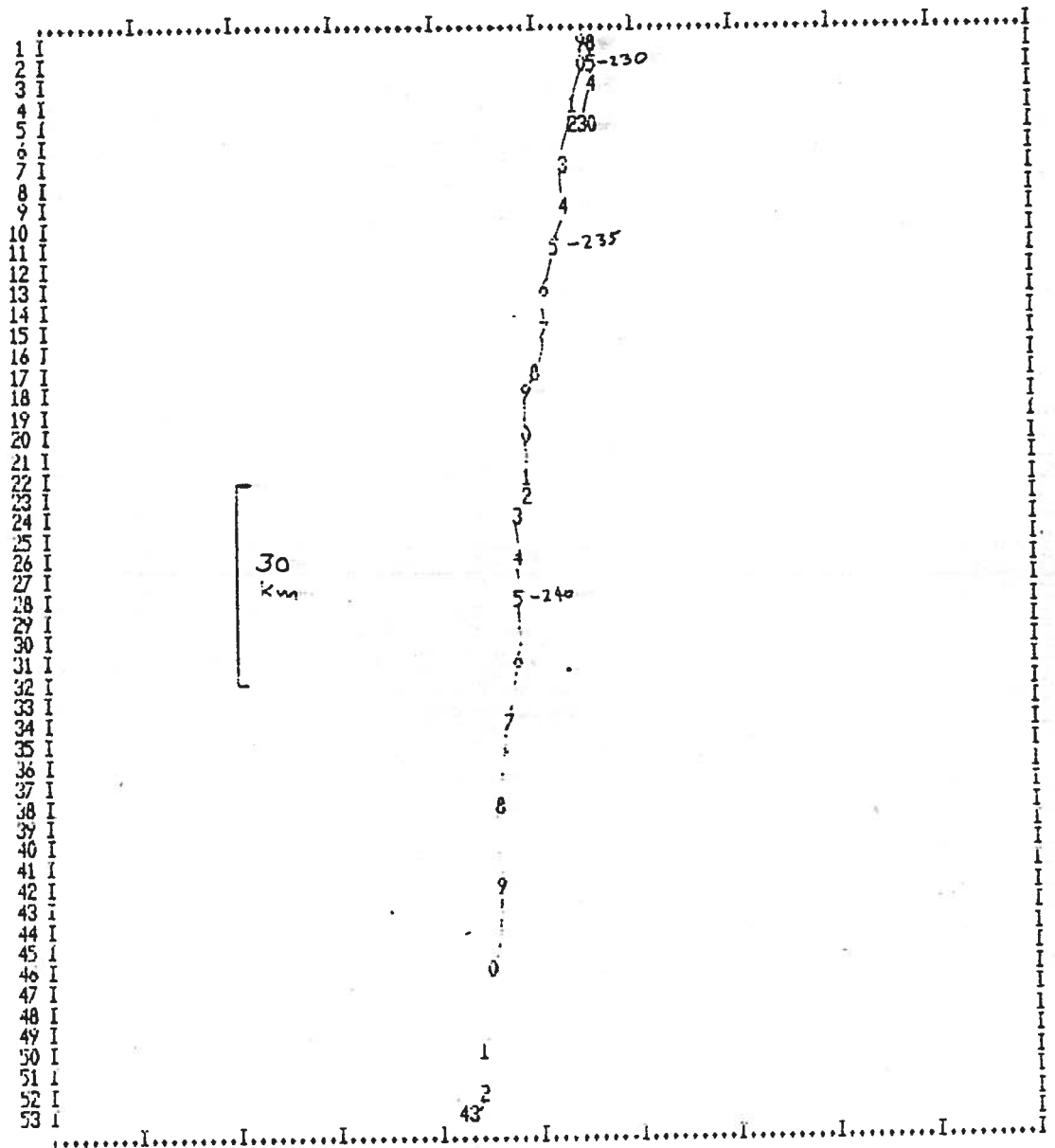
 ENCINA STA2 (OUTFALL) - 2/27 -> 4/4/86 - 20/46M



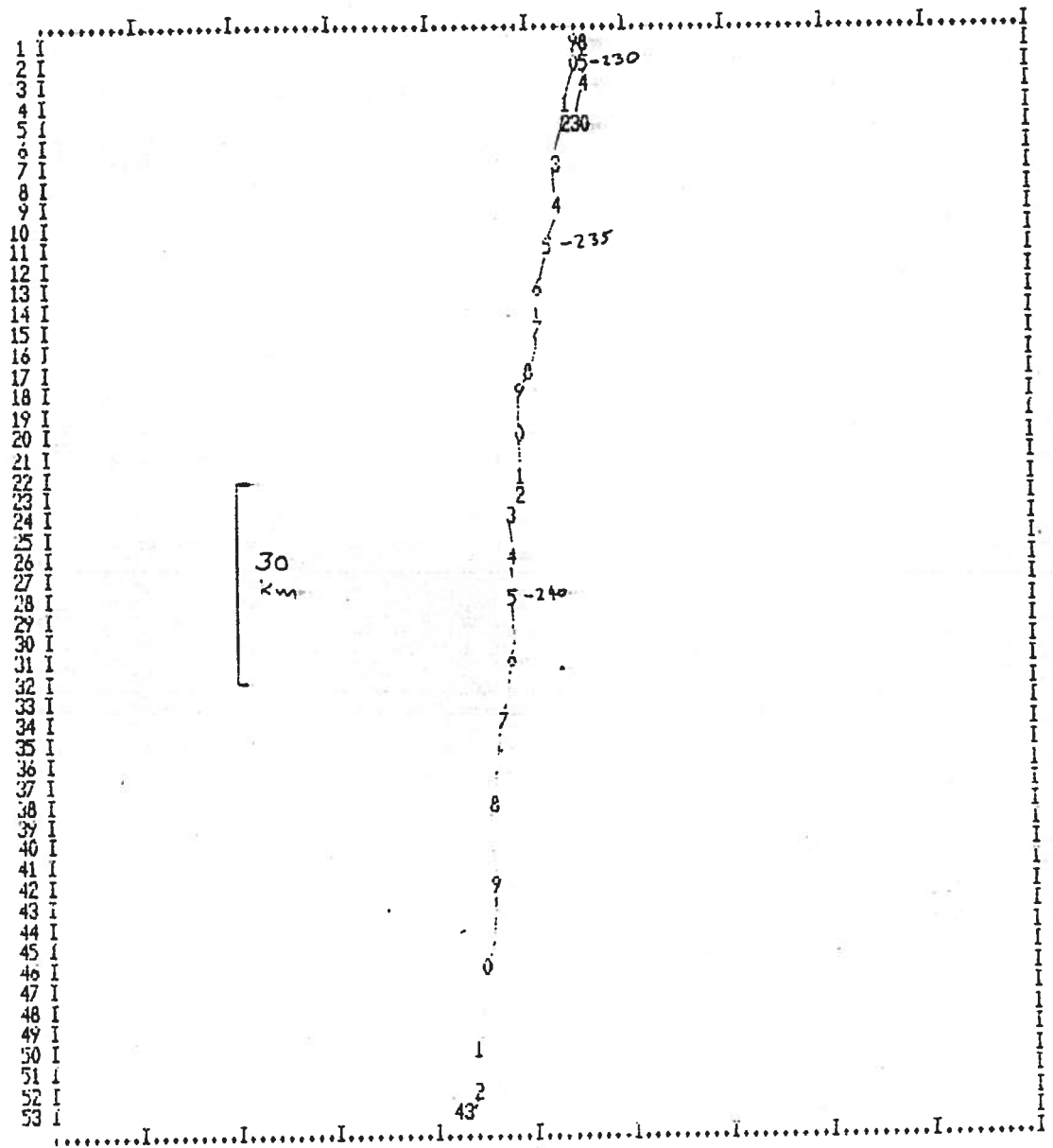
 ENCINA (STA2 OUTFALL) - 7/13-78/15/82 - 16/46M #8001



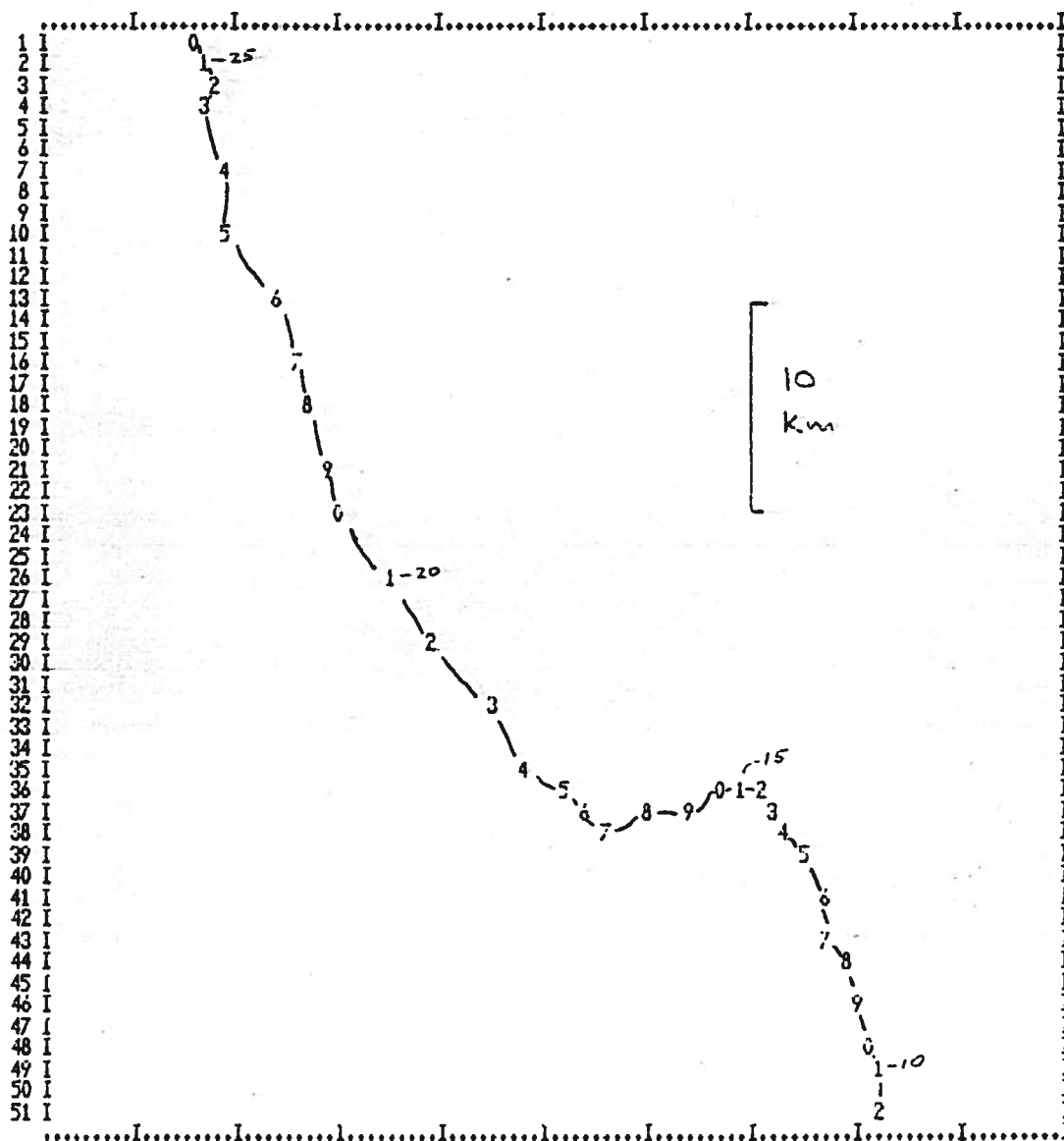
 ENCINA (STAZ OUTFALL) - 7/13-78/15/82 - 16/46M #8001



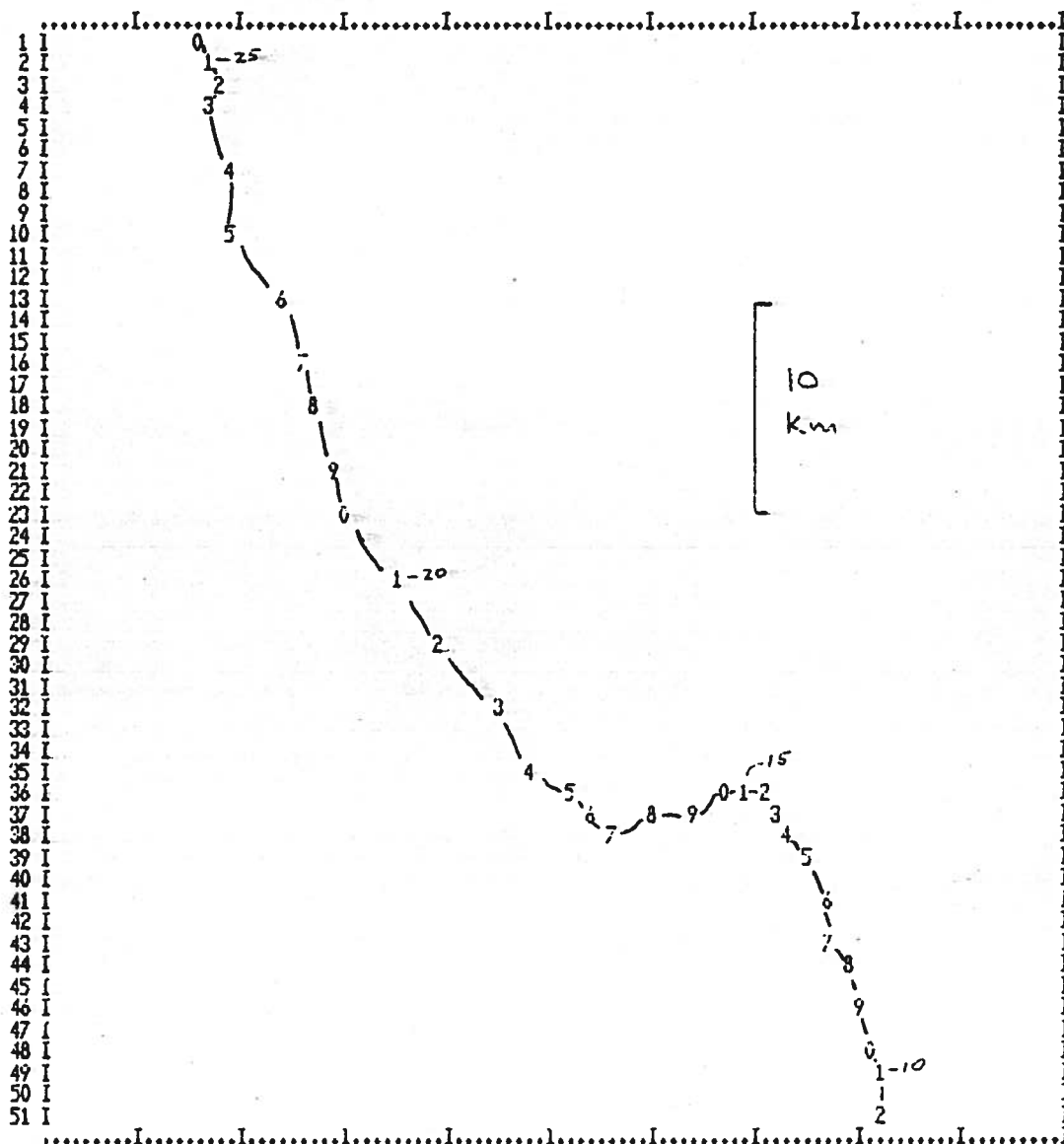
 ENCINA STAZ (OUTFALL) - 8/15->9/18/86 - 16/46M, #8001



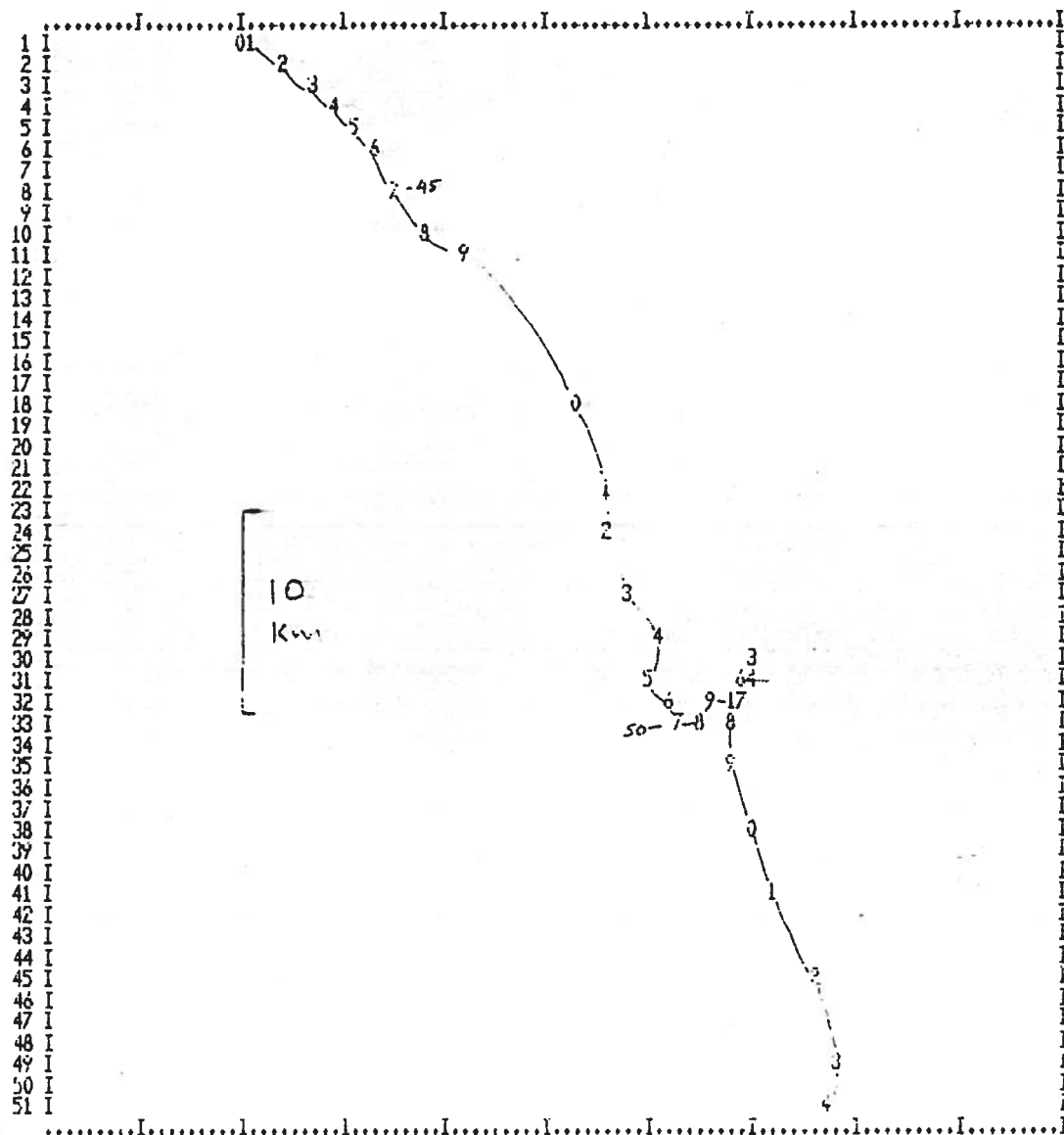
ENCINA STA2 (OUTFALL) - 8/15->9/18/86 - 16/46M, #8001



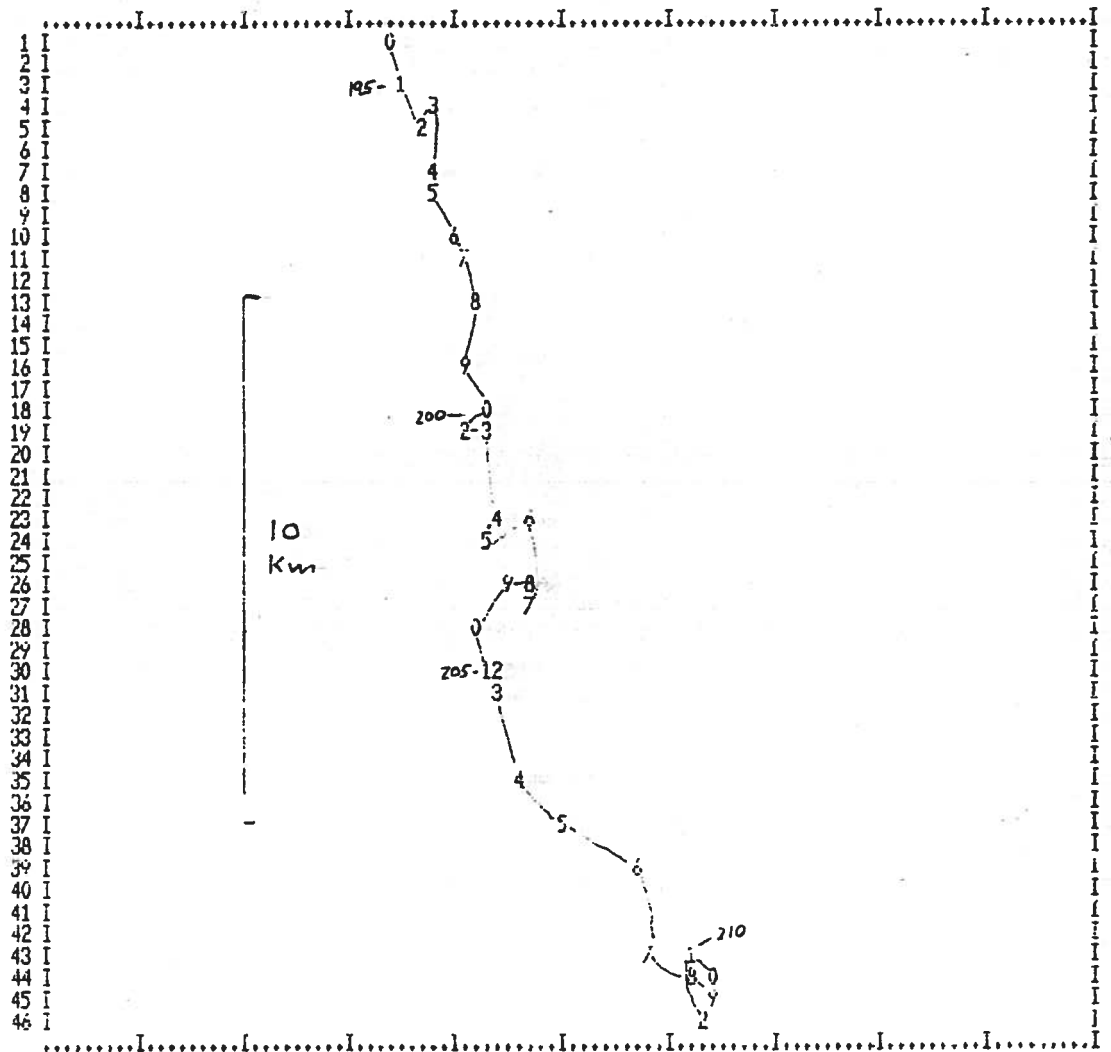
 ENCINA STA#2(OUTFALL) - 1/9->2/10/86 - +2/46M



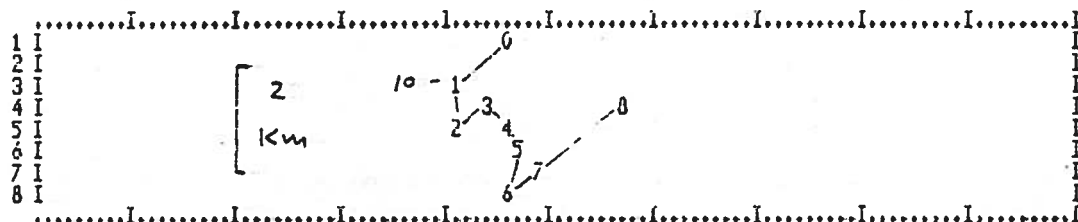
 ENCINA STA#2(OUTFALL) - 1/9->2/10/86 - +2/46M



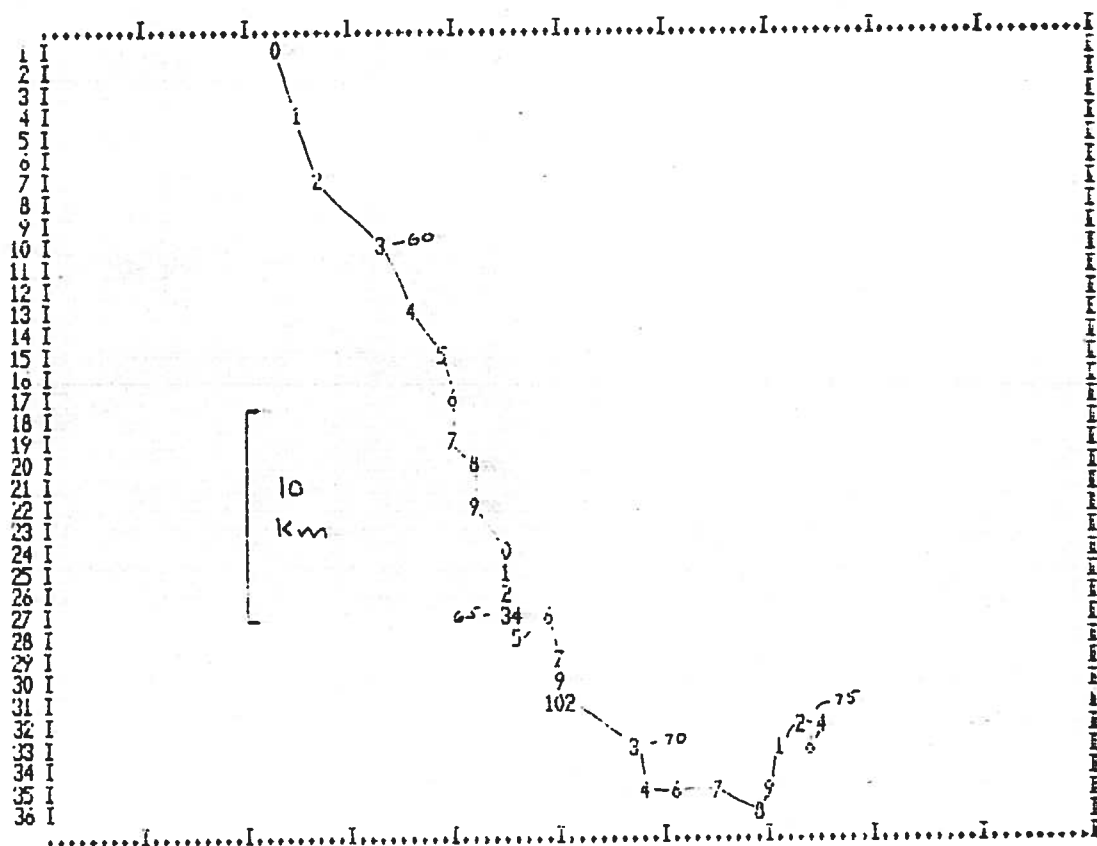
 ENCINA (STA2-OUTFALL) - 2/10->2/27/86 - +2/46M



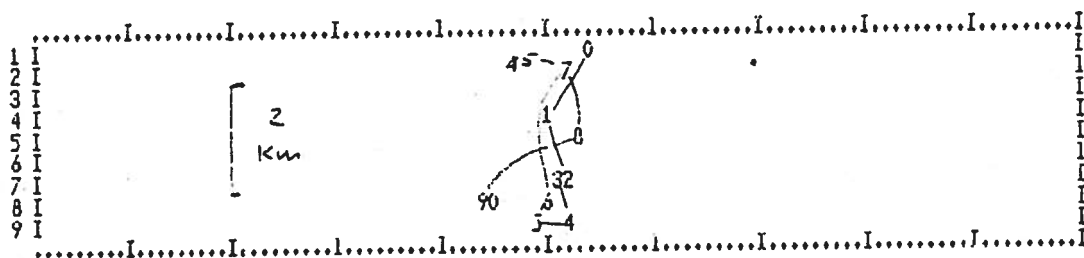
 ENCINA (STA2-OUTFALL) - 7/13->8/15/85 - +2/45M #8403



 ENCINA STA#4 (CANYON) - 1/9->1/13/86 - 20/46M



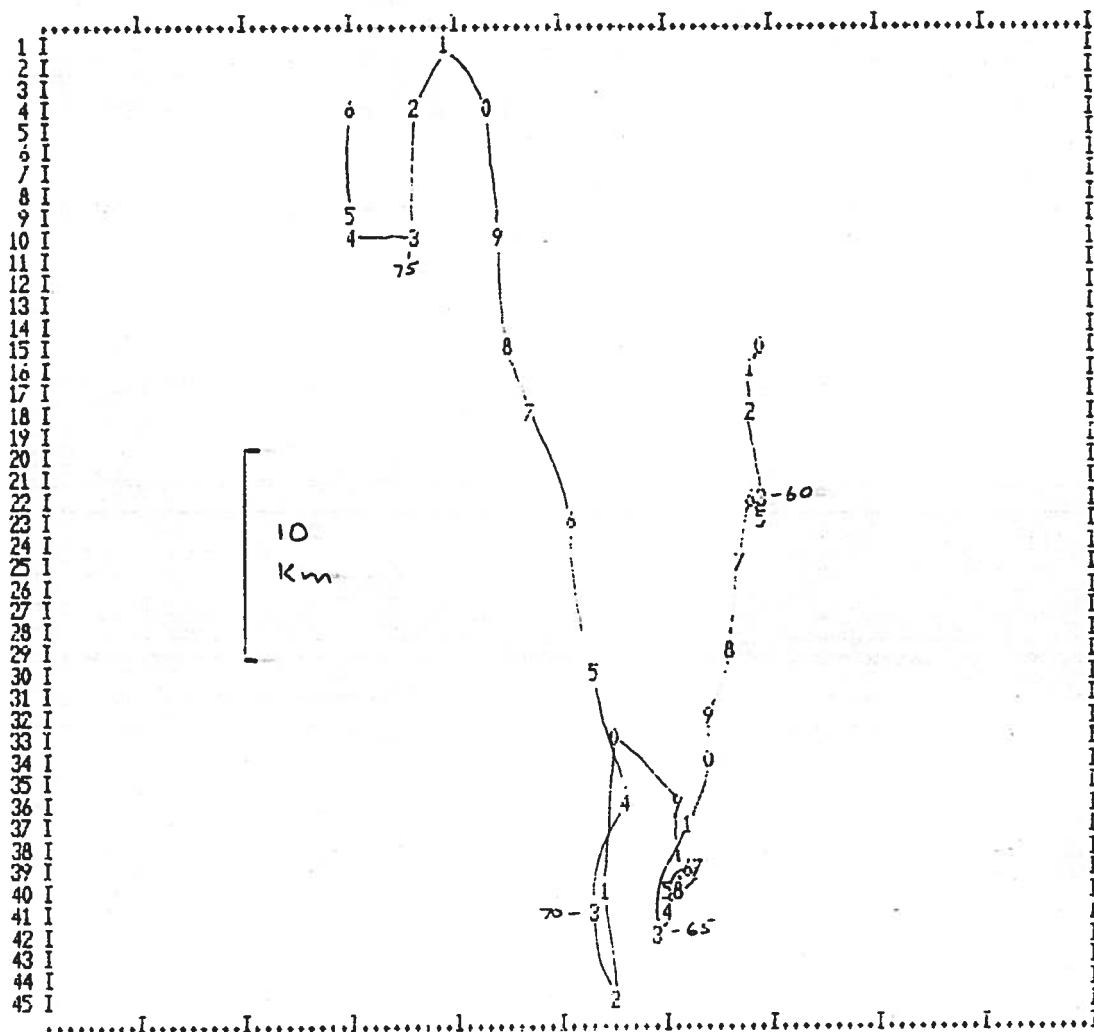
 ENCINA STA2 (OUTFALL) - 2/27 -> 4/4/96 - +2/46M



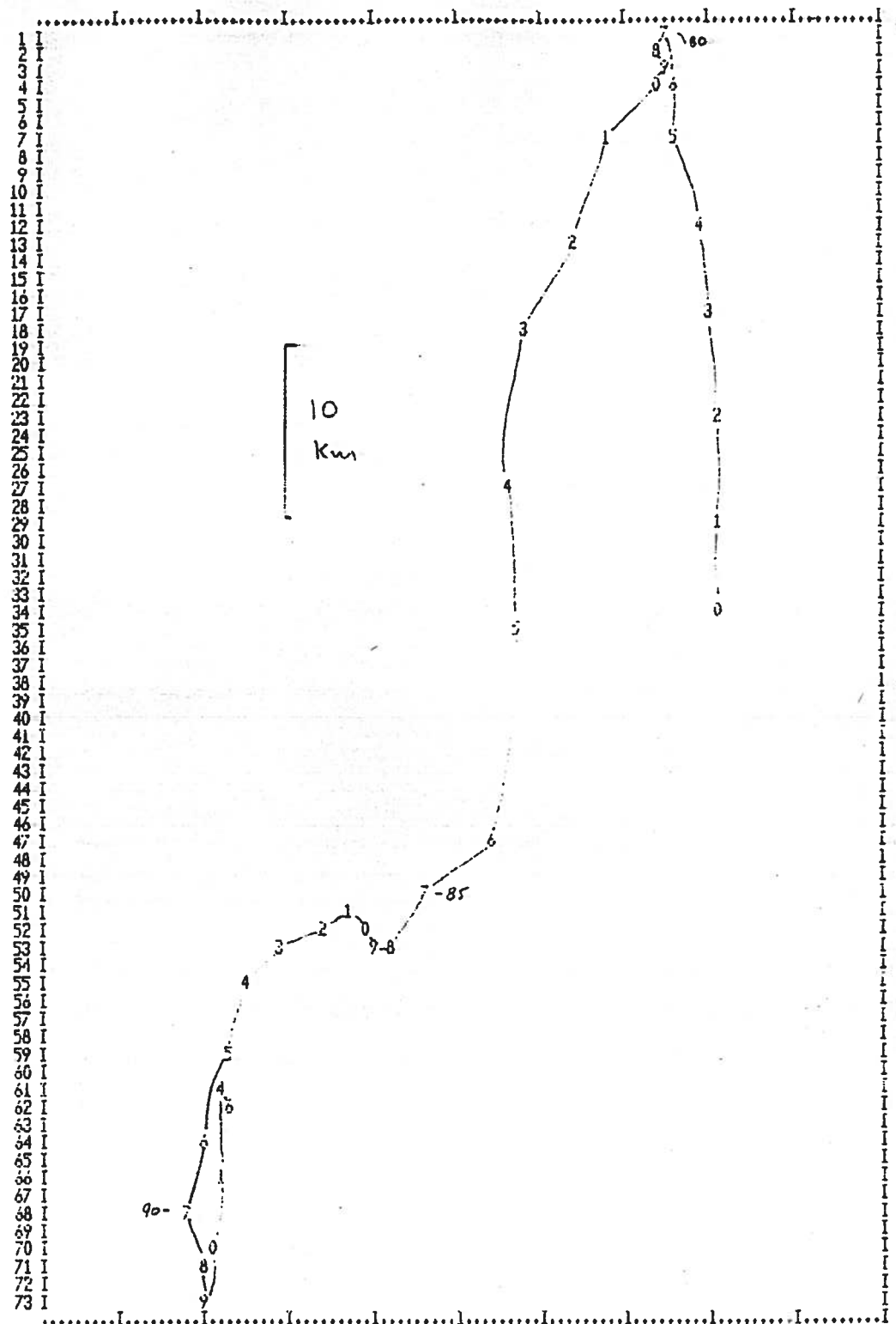
 ENCINA (STA4-CANYON) - 2/10->2/15/86 - 20/46M #8003



 ENCINA (STA4-CANYON) - 2/10->2/15/86 - 20/46M #8003

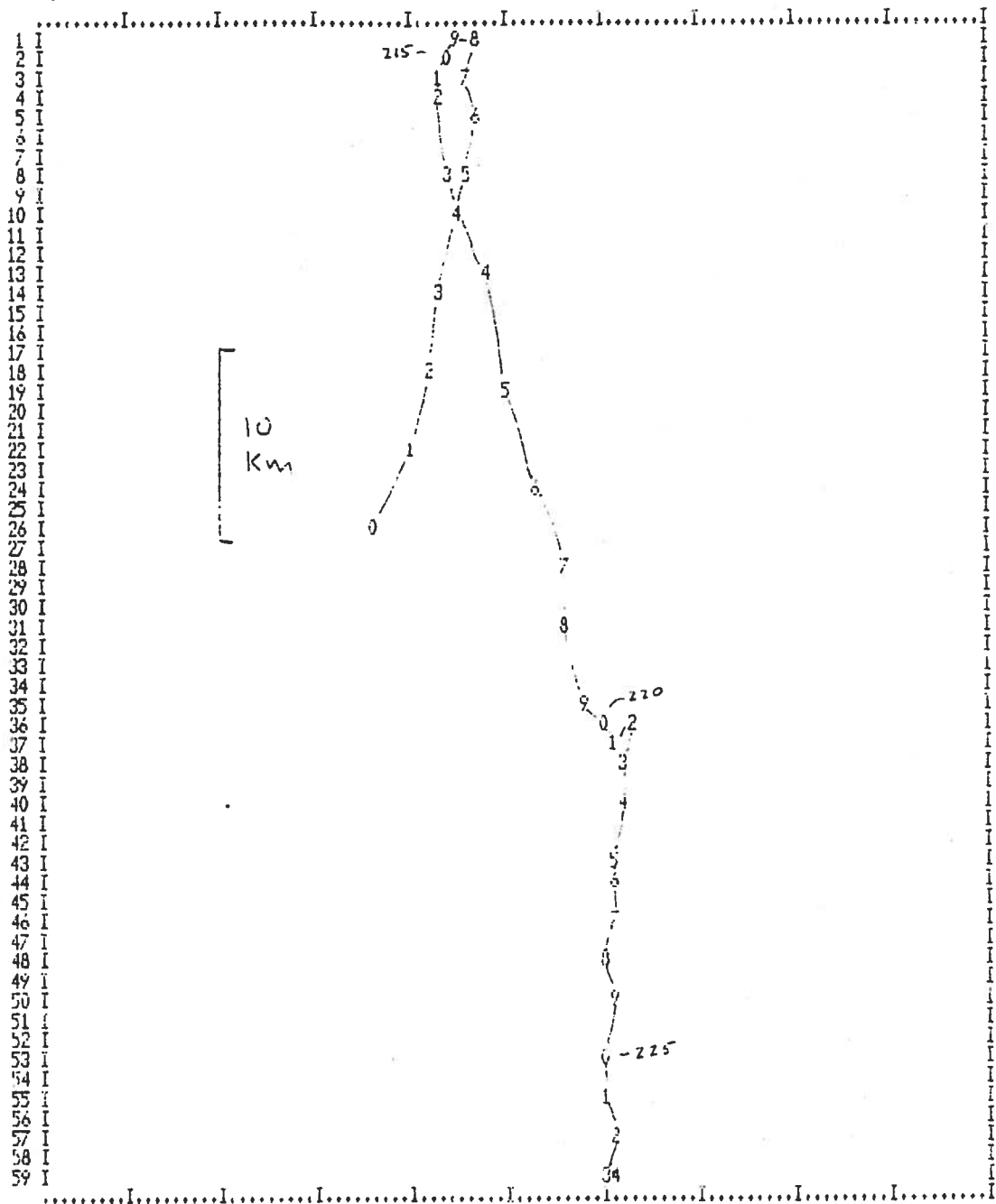


 ENCINA (STA 4-CANYON) - 2/27->4/3/86 20/40M #8401

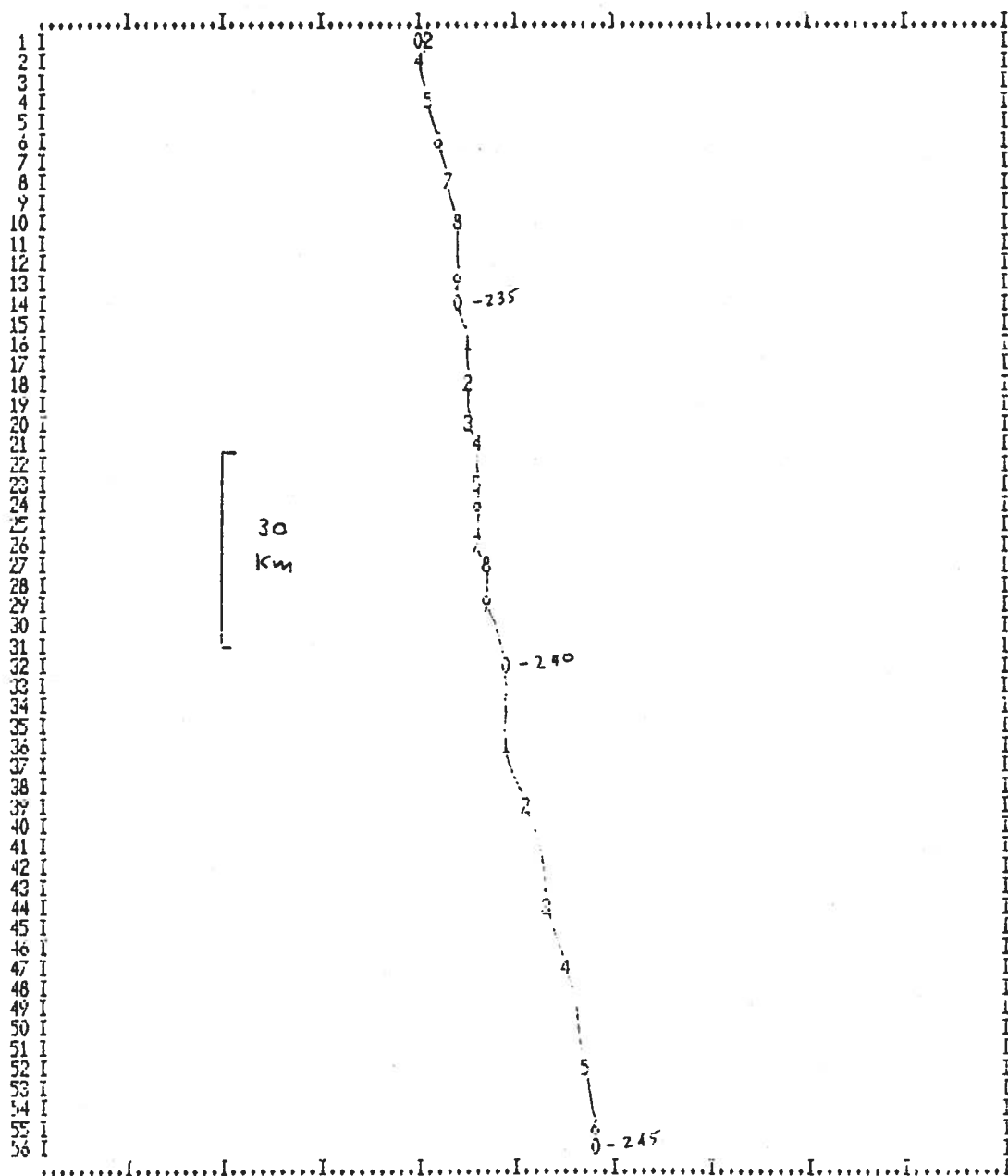


 ENCINA (STA 4-CANYON) - 2/27->4/3/86 20/40M #8401

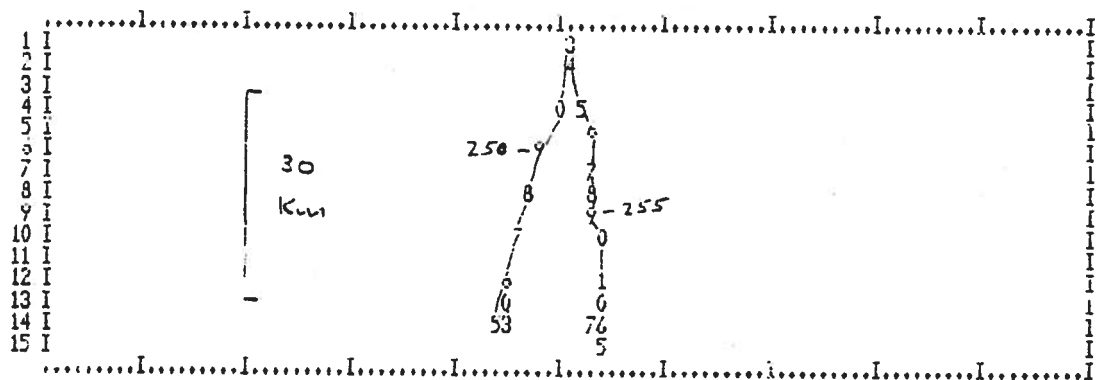
ENCINA (STA4-CANYON) - 7/13-78/15/86 - 16/46M #8201



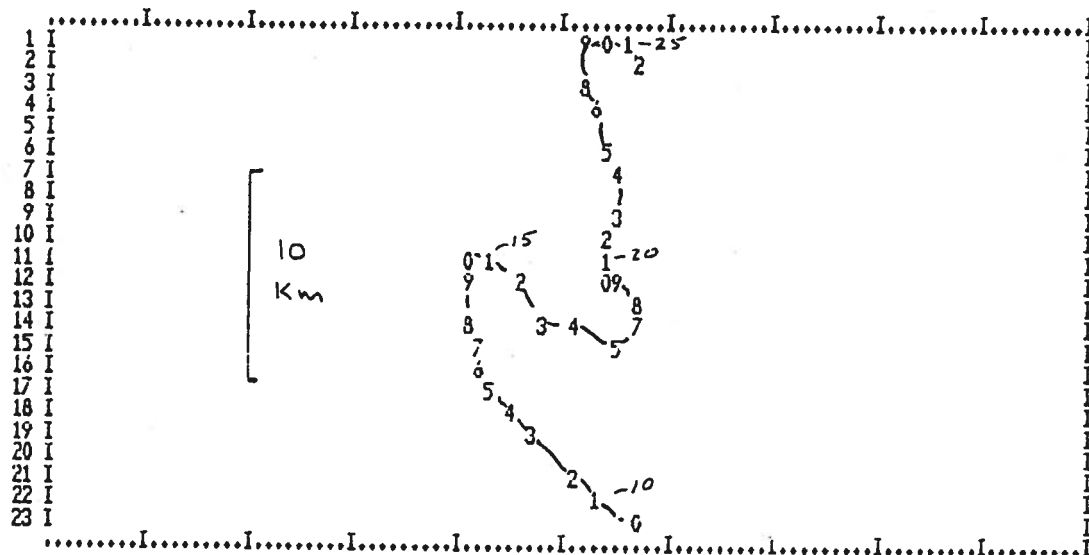
 ENCINA (STA4-CANYON) - 7/13-8/15/86 - 16/46M #8201



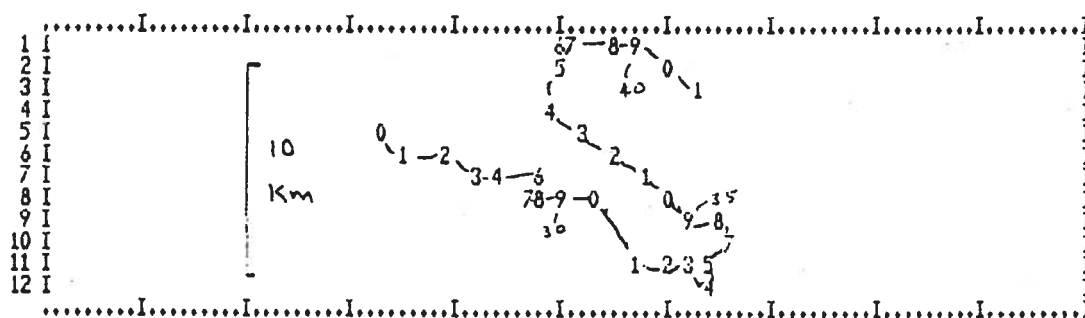
 ENCINA STA 4 (CANYON) - 8/18->9/16/86 - 16/46M



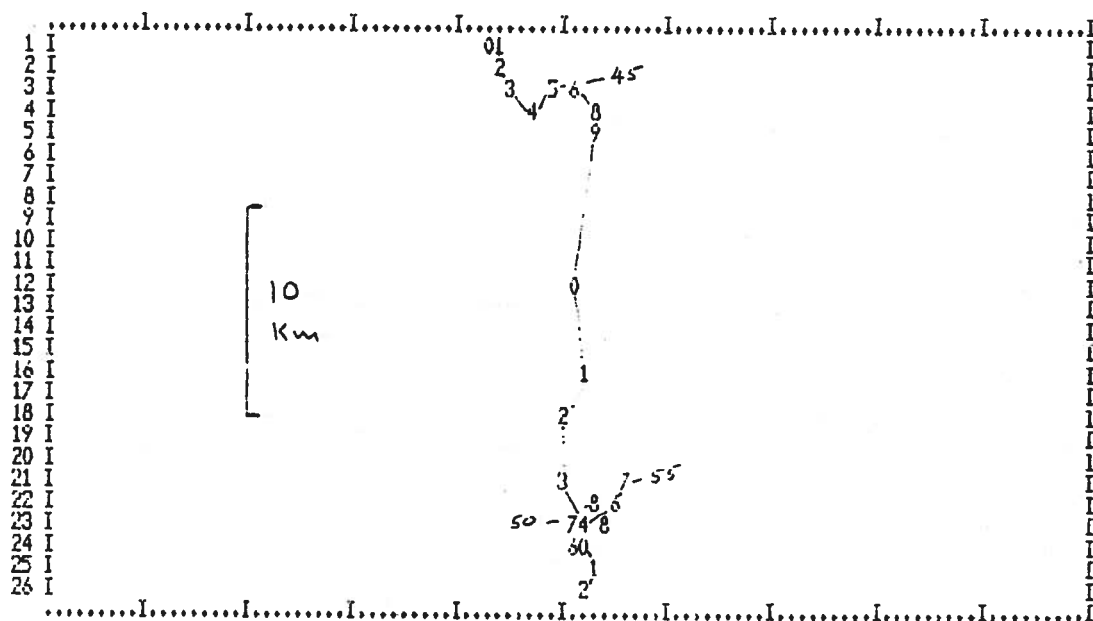
 ENCINA STA 4 (CANYON) - 8/18->9/16/86 - 16/46M



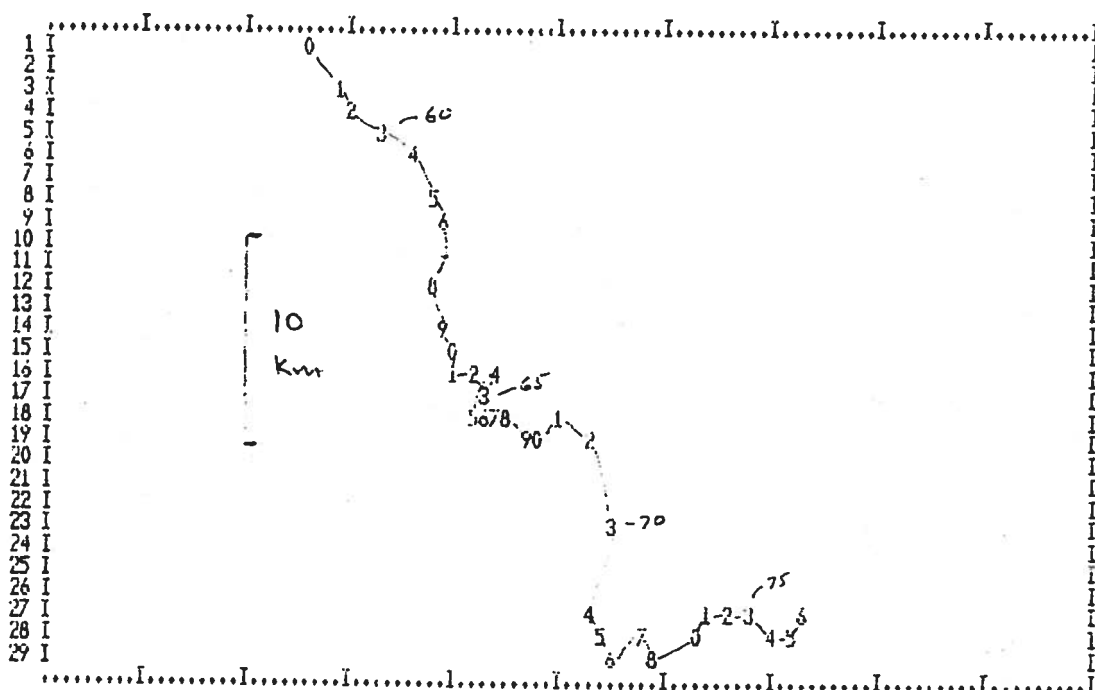
 ENCINA STA#4(CANYON) - 1/9->2/10/86 - +2/46M



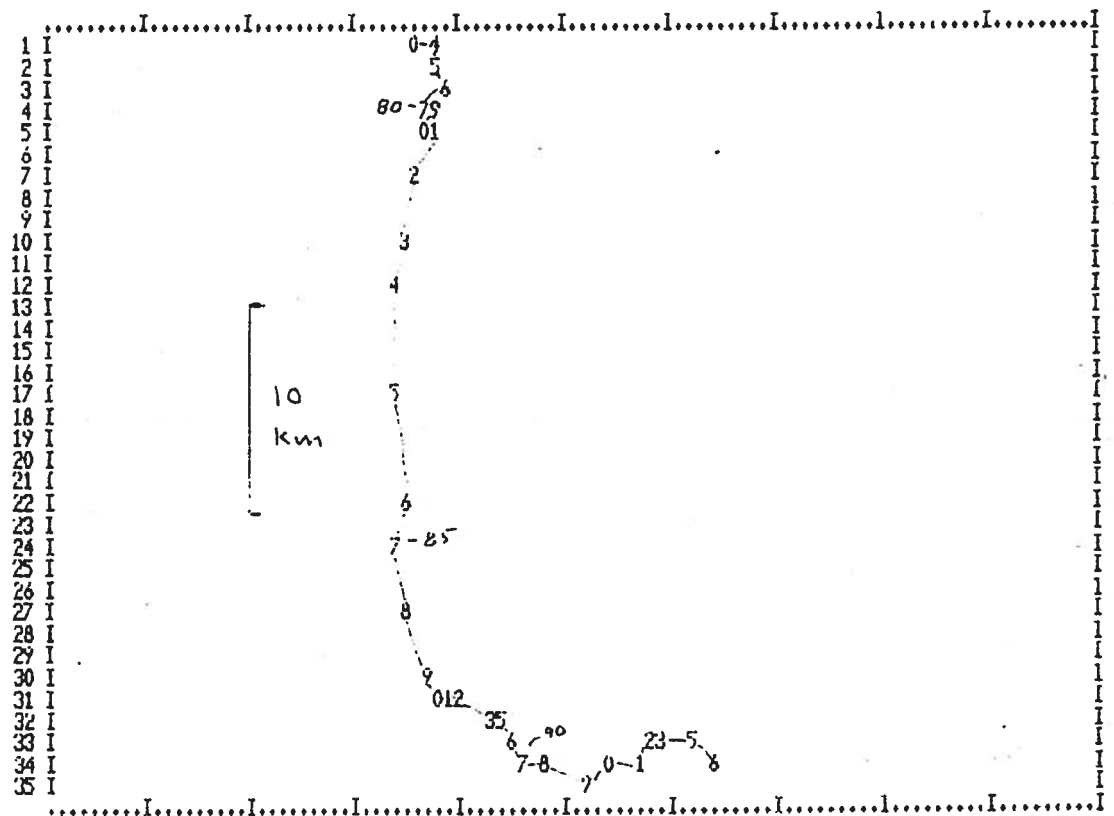
 ENCINA STA#4(CANYON) - 1/9->2/10/86 - +2/46M



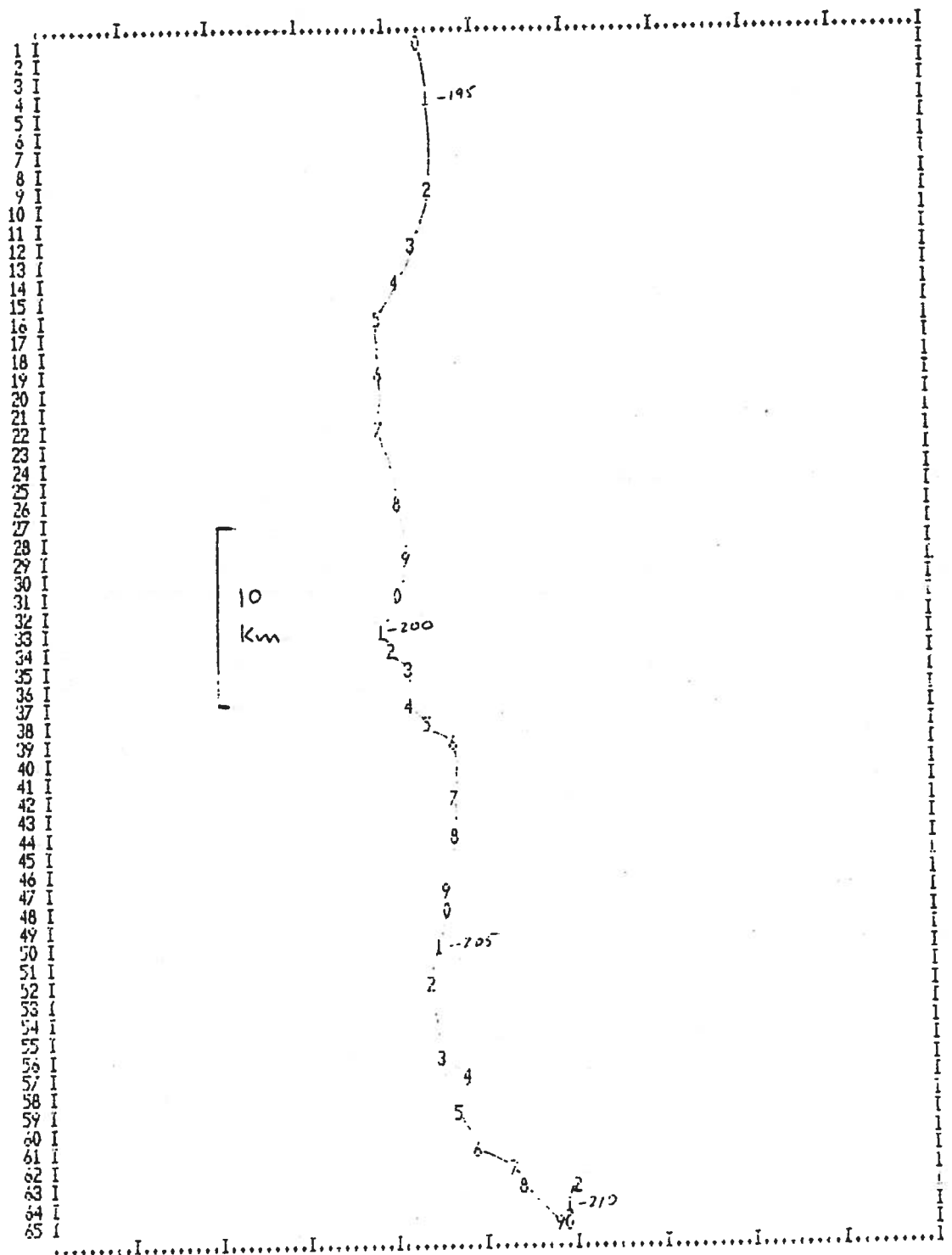
 ENCINA (STA4 CANYON) - 2/10->2/27/86 - +2/46M



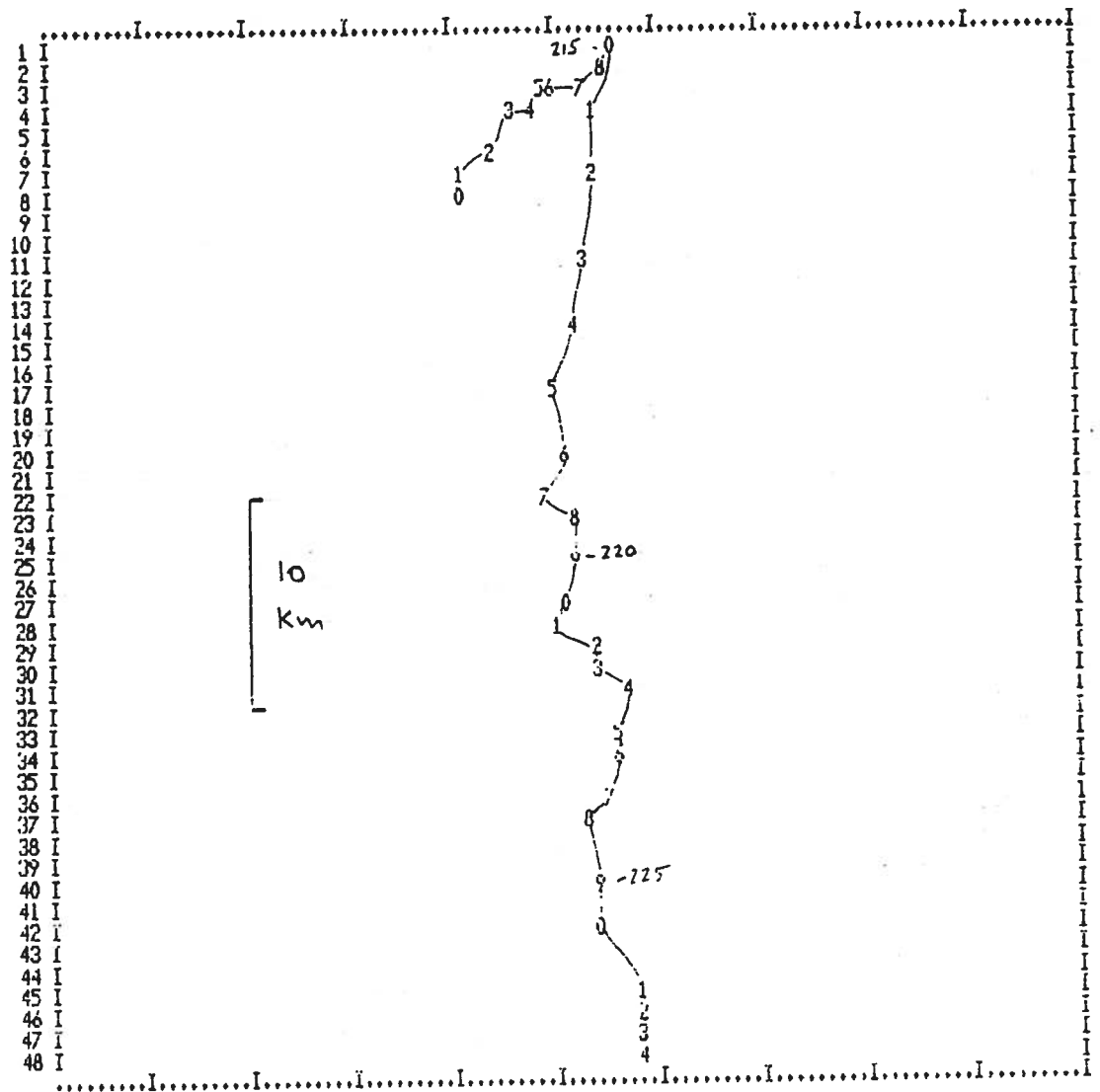
 ENCINA STA4 (CANYON) - 2/27 -> 4/4/86 - +2/46M



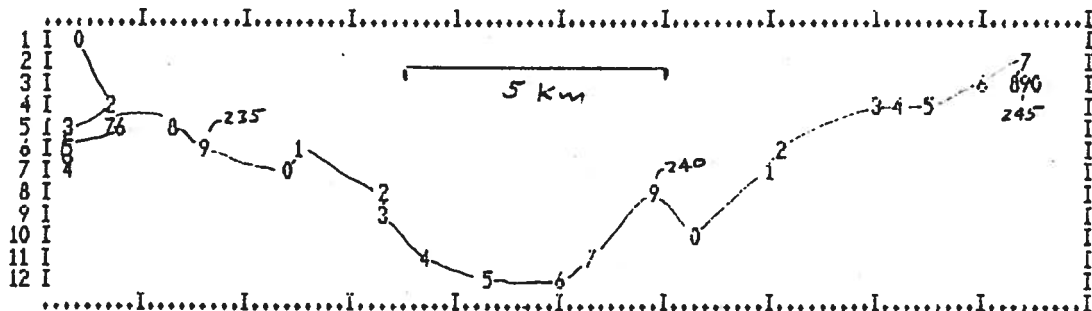
ENCINA STA4 (CANYON) - 2/27 -> 4/4/86 - +2/46M



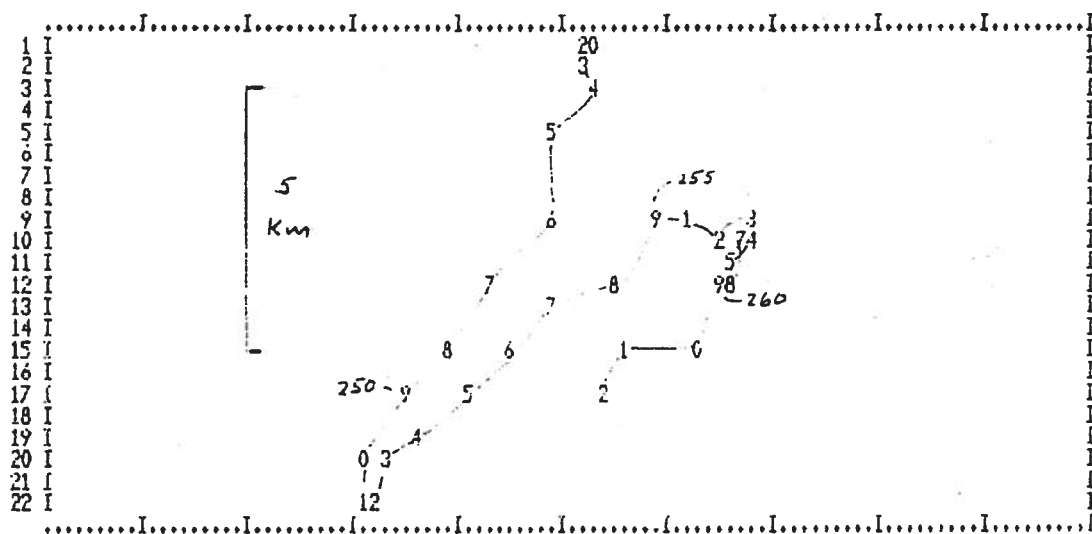
 ENCINA (STA4-CANYON) - 7/13-8/15/86 - +2/46M #8301



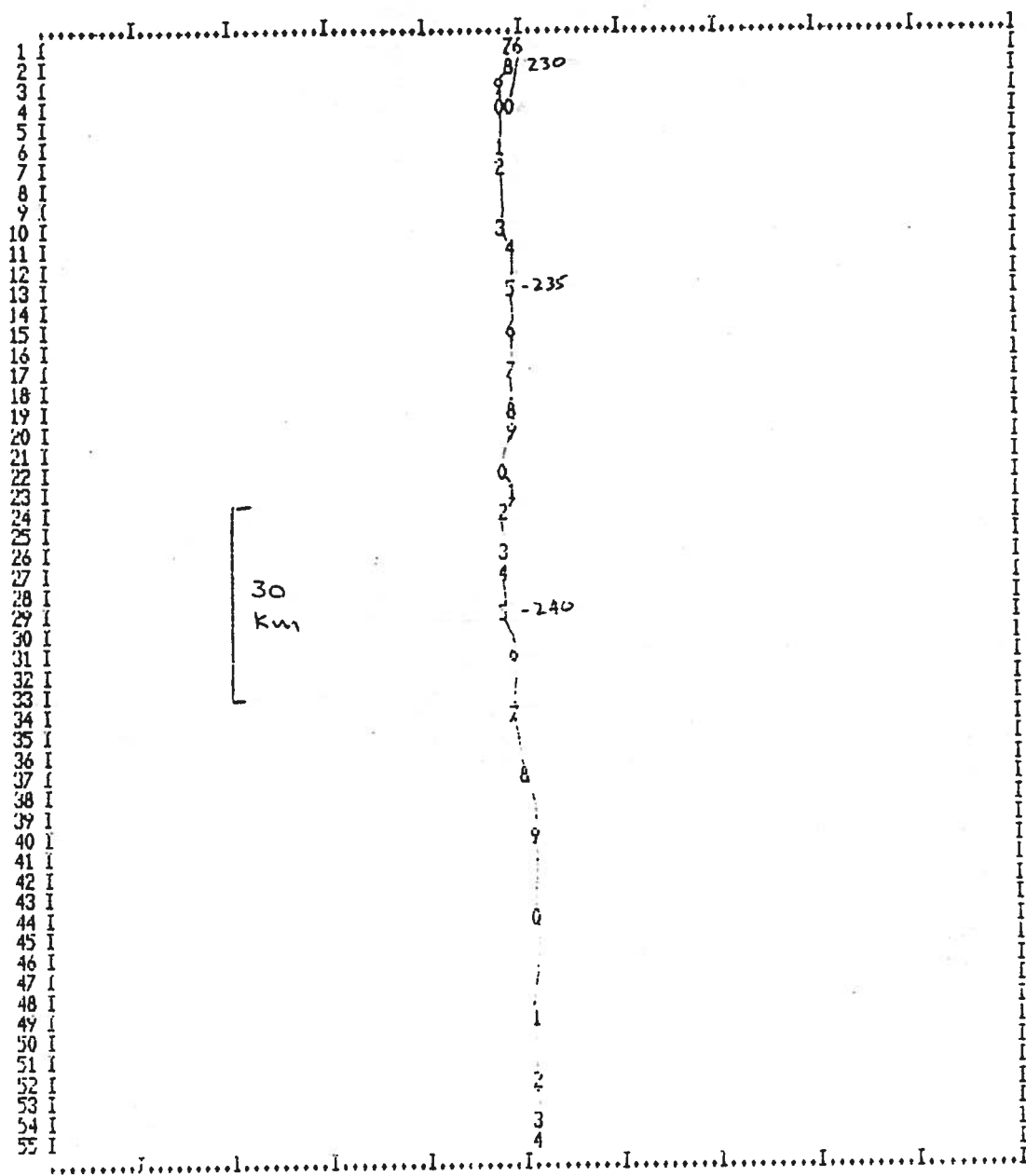
 ENCINA (STA4-CANYON) - 7/13->8/15/86 - +2/46M #8301



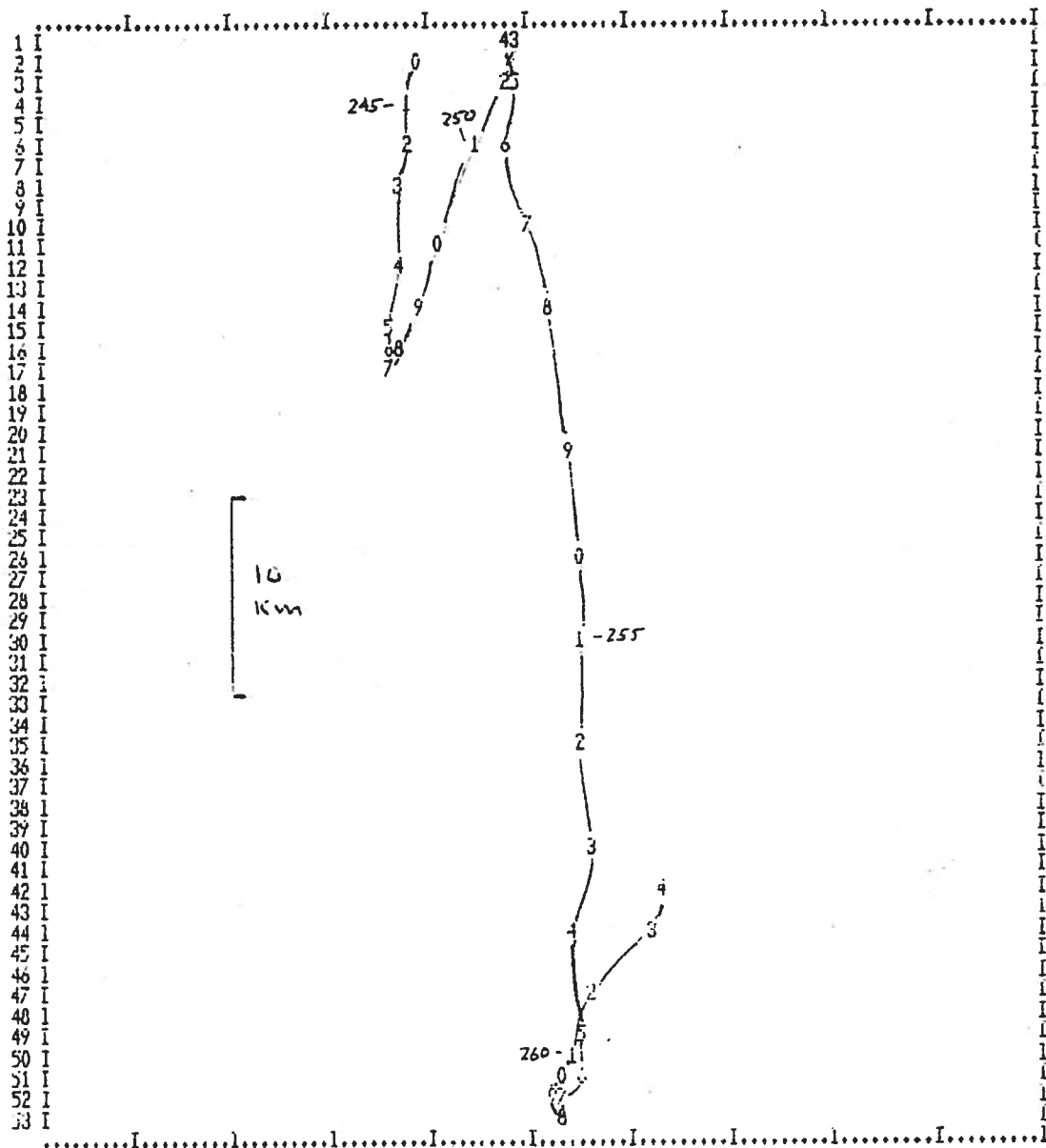
 ENCINA STA 4 (CANYON) - 8/18->9/18/86 - +2/46M



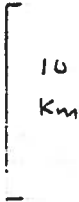
 ENCINA STA 4 (CANYON) - 8/18->9/18/86 - +2/46M



 ENCINA STA 5 (UPCOAST) - 8/15-29/18/86 - 16/46M



 ENCINA STA 5 (UPCOAST) - 8/15-29/18/86 - 16/46M



ENCINA STA 5 (UPCOAST) - 8/15-29/18/86 - 44/46M